NUMERICAL INVESTIGATION OF NATURAL CONVECTION FROM VERTICAL PLATE FINNED HEAT SINKS

A THESIS SUBMITTED TO
THE GRADUATE SCHOOL OF NATURAL AND APPLIED SCIENCES
OF
MIDDLE EAST TECHNICAL UNIVERSITY

BY

KAMİL MERT ÇAKAR

IN PARTIAL FULFILLMENT OF THE REQUIREMENTS
FOR
THE DEGREE OF MASTER OF SCIENCE
IN
MECHANICAL ENGINEERING

JUNE 2009

Approval of the thesis:

NUMERICAL INVESTIGATION OF NATURAL CONVECTION FROM VERTICAL PLATE FINNED HEAT SINKS

submitted by **KAMİL MERT ÇAKAR** in partial fulfillment of the requirements for the degree of **Master of Science in Mechanical Engineering Department, Middle East Technical University** by,

Prof. Dr. Canan Özgen _____
Dean, Graduate School of **Natural and Applied Sciences**

Prof. Dr. Süha Oral _____
Head of Department, **Mechanical Engineering**

Prof. Dr. Kahraman Albayrak _____
Supervisor, **Mechanical Engineering Dept., METU**

Asst. Prof. Dr. İlker Tarı _____
Co-supervisor, **Mechanical Engineering Dept., METU**

Examining Committee Members:

Prof. Dr. M. Haluk Aksel _____
Mechanical Engineering Dept., METU

Prof. Dr. Kahraman Albayrak _____
Mechanical Engineering Dept., METU

Asst. Prof. Dr. İlker Tarı _____
Mechanical Engineering Dept., METU

Asst. Prof. Dr. Almıla Güvenç Yazıcıoğlu _____
Mechanical Engineering Dept., METU

Asst. Prof. Dr. Ali İbrahim Atılgan _____
Mechanical Engineering Dept., GAZI UNV.

Date: _____

I hereby declare that all information in this document has been obtained and presented in accordance with academic rules and ethical conduct. I also declare that, as required by these rules and conduct, I have fully cited and referenced all material and results that are not original to this work.

Name, Last Name : KAMİL MERT ÇAKAR

Signature :

ABSTRACT

NUMERICAL INVESTIGATION OF NATURAL CONVECTION FROM VERTICAL PLATE FINNED HEAT SINKS

Çakar, Kamil Mert

M.Sc., Department of Mechanical Engineering

Supervisor: Prof. Dr. Kahraman Albayrak

Co-Supervisor: Asst. Prof. Dr. İlker Tarı

June 2009, 133 pages

The steady-state natural convection from vertically placed rectangular fins is investigated numerically by means of a commercial CFD program called ICEPAK. The effects of geometric parameters of fin arrays on the performance of heat dissipation from fin arrays are examined. In order to simulate the different fin configurations and compare the results with literature, two experimental studies from literature are selected. Optimum fin spacing for both studies are found numerically and compared with experimental studies.

The models are first verified by simulating natural convection on vertically placed flat plate and comparing the results with literature. After verification 30 different fin array configurations for the first experimental case study and 15 different fin array configurations for the second experimental case study from literature are analyzed.

It is observed that the present results agree very well with the optimum fin spacing results of the experimental studies. It is also observed that the

empirical correlations in the literature are conservative and the numerically obtained correlations predict higher heat transfer rates.

Keywords: Natural convection, vertical rectangular fins, optimum fin spacing

ÖZ

DİKEY PLAKA FİNLİ ISI DAĞITICILARINDAKİ DOĞAL KONVEKSİYONUN SAYISAL METODLARLA SİMULASYONU

Çakar, Kamil Mert

Yüksek Lisans, Makina Mühendisliği Bölümü

Tez Yöneticisi: Prof. Dr. Kahraman Albayrak

Ortak Tez Yöneticisi : Asst. Prof. Dr. İlker Tarı

Haziran 2009, 133 sayfa

Dikey olarak yerleştirilmiş finli ısı dağıtıcılarındaki kararlı durumdaki doğal konveksiyon ticari bir sayısal akışkanlar dinamiği yazılımı olan ICEPAK ile incelenmiştir. Fin yapılarının değişik geometrik parametrelerinin fin yapılarından atılan ısı miktarına olan etkileri araştırılmıştır. Literatürden iki deneysel çalışma seçilerek bu çalışmalarda kullanılan değişik fin yapıları simule edilmiş ve deney sonuçları ile sonuçlar karşılaştırılmıştır. Her iki deneysel çalışma için ideal fin aralıkları sayısal metodlarla bulunmuş ve deney sonuçları ile karşılaştırılmıştır.

Modeller önce dikey düz plaka üzerindeki doğal konveksiyonun incelenmesi ve literatür ile karşılaştırılması ile doğrulanmıştır. Modellemenin doğrulanmasından sonra ilk deneysel çalışma için 30, ikinci deneysel çalışma için ise 15 değişik fin yapısı çözümlenmiştir.

İdeal fin aralıkları için bulunan sonuçların deney sonuçlarıyla çok iyi bir şekilde uyuştuğu gözlenmiştir. Ayrıca finlerden atılan ısı transferi değerlerinin

literatürdeki emprik çıkarımlarda olması gerekenden daha az olduğu ve analiz sonuçlarında bu değerlerin çok daha yüksek olduğu gözlenmiştir.

Anahtar kelimeler: Doğal konveksiyon, dikey dikdörtgen finler, ideal fin aralığı

To My Family

ACKNOWLEDGMENTS

I would like to express my sincere gratitude to Prof. Dr. Kahraman Albayrak and Asst. Prof. Dr. İlker Tarı for their continuous guidance, encouragement, support, advice, and supervision throughout this study.

I would like to specially thank my colleague and friend Mustafa Ocak for his aid and support for this study. I also would like to express my appreciation to Cem Gözükara and Berkan Erdoğmuş for their guidance.

My special thanks go to my colleagues and friends Onur Doğan, Güvenç Canbaloğlu, Gökhan Cüylan, Murat Halisçelik, Berkan Büyükdağlıoğlu, Kaan Özsoy and Koray Atılgan for their support and encouragement.

I am also very grateful to Hüseyin Sabri Aliefendioğlu and Devrim Anıl for their endless support and understanding.

I also would like to thank TUBITAK for their financial support throughout this study.

Lastly I would like to express my endless gratitude to my family for their love, support and faith in me.

TABLE OF CONTENTS

LIST OF TABLES

TABLES

LIST OF FIGURES

FIGURES

LIST OF SYMBOLS

h	Convection heat transfer coefficient, W/(m^{2}K)
A	Area, m^2
Nu	Nusselt number
Nu_s	Nusselt number based on fin spacing
Gr	Grashof number
Gr_s	Grashof number based on fin spacing
Pr	Prandtl number
h_s	Average heat transfer coefficient based on fin spacing, W/(m^{2}K)
h_b	Vertical heat transfer coefficient, W/(m^{2}K)
S	Fin spacing
H	Fin height
N	Number of fins
L	Fin length
W	Fin width
t	Fin thickness
d	Base plate thickness
S_{opt}	Optimum fin spacing
Ra	Rayleigh number
Q_{in}	Power supplied to heater base plate, W
Q_c	Total convection heat transfer rate from fins, W
$(Q_0)_c$	Convection heat transfer rate when there are no fins, W
Q_{out}	Heat transfer rate from the bottom plate to upper plate, W

T_w	Average base plate temperature, ^{0}C
T_a	Ambient temperature, ^{0}C
T	Temperature, ^{0}C
ΔT	Base-to-ambient temperature difference, ^{0}C
T_f	Film temperature, ^{0}C
k	Thermal conductivity, W/(m K)
k_t	Thermal conductivity due to turbulent transport, W/(m K)
g	Gravitational acceleration, m/s^2
p	Pressure, Pa
μ	Dynamic viscosity, N s/m^2
I	Unit tensor
β	Volumetric thermal expansion coefficient, 1/K
σ	Stefan-Boltzmann constant, W/(m^{2}K^4)
ν	Kinematic viscosity, m^2/s
α	Thermal diffusivity, m^2/s
ε	Emissivity

CHAPTER 1

INTRODUCTION

Heat is generated as a by-product in many engineering applications. This usually unwanted by-product can decrease the performance of the systems since almost every engineering system is designed to work in a certain temperature limit. If these limits are exceeded by overheating, this may even lead to total system failure. Therefore many engineering systems try to avoid this overheating problem as much as possible by using different methods for dissipation of heat away from the system to surrounding.

Using fins is one of the cheapest and easiest ways to dissipate unwanted heat and it has been commonly used for many engineering applications successfully. Rectangular fins are the most popular fin type because of their low production costs and high effectiveness. Although rectangular fins can be used in two different orientations as vertical and horizontal, vertical orientation is used more widely since it is more effective than the horizontal one.

Convection and radiation heat transfers are two modes of heat transfer that takes place while dissipating heat from fins to surrounding. Since all of the considered fin configurations are made of aluminum alloys, which have low emissivity values, radiation heat transfer values are low. Therefore convection heat transfer is the dominant heat transfer mode while dissipating heat from fins.

Rate of heat dissipation from a fin configuration by convection heat transfer depends on the heat transfer coefficient and the surface area of the fins. It is possible to increase the heat transfer coefficient, h by forcing the fluid to flow over the fins by means of fans. But this option costs more and also requires more volume for the fans to operate. Therefore sometimes the designer has to rely on natural convection heat transfer for dissipating unwanted heat from the fins. The surface area of the fins can also be increased by adding more fins to the base material in order to increase the total heat transfer from the fins. But the number of the fins should be optimized because it should be noted that adding more fins also decreases the distance between the adjacent fins. This may cause resistance to air flow and boundary layer interference which in return decrease the heat transfer coefficient.

Although rectangular fin geometries and their thermal effectiveness are investigated extensively in literature, most of the studies are done for limited range of fin configurations. Moreover even though there are many experimental studies on performance of fin configurations, the amount of numerical studies is lacking. In this study, the heat transfer performances of wide range of vertical fin configurations are investigated by the help of a commercial CFD program, ICEPAK ®. In order to compare the results and further examine the performance of vertical fin arrays two experimental studies from the literature are selected for investigation. The first study is from Ref. [1] in which heat dissipation performance of 30 different fin configurations are examined. The second study is from Ref. [2] in which 15 different fin array configuration are investigated.

ICEPAK analyses are done using two different computer configurations. The two computer configurations are as follows:

- Intel ® Core ™ 2 Quad CPU Q9450 @2.66 GHz with 8 GB RAM
- Intel ® Core ™ 2 Duo CPU T7500 @2.20 GHz with 4 GB RAM

The runtimes of the analyses done on these computer configurations vary from one fin configuration to another. However the average run time is 25 minutes for the first computer configuration whereas 40 minutes for the second computer configuration.

The results are first checked with theoretical results of natural convection over vertical flat plate and then with experimental studies in order to guarantee the validity of the solution procedure. The main objective of this work is to demonstrate a convenient CFD based solution to determine the performance of different fin configurations. Since it is not possible to perform an experiment on every possible fin configuration, a CFD solution can be used to predict the effectiveness of different fin configurations. The governing equations solved by the help of ICEPAK are given below:

The mass conservation equation:

$$\frac{\partial \rho}{\partial t} + \nabla \cdot \left(\rho \vec{\upsilon} \right) = 0 \tag{1.1}$$

The conservation of momentum equations:

$$\frac{\partial}{\partial t}\left(\rho \vec{\upsilon} \right) + \nabla \cdot \left(\rho \vec{\upsilon} \vec{\upsilon} \right) = -\nabla p + \nabla \cdot \left(\bar{\bar{\tau}} \right) + \rho \vec{g} + \vec{F} \tag{1.2}$$

where $\vec{F}$ contains other source terms that may rise from resistances, sources and etc. and $\bar{\bar{\tau}}$ is the stress tensor and can be defined as:

$$\bar{\bar{\tau}} = \mu \left[\left(\nabla \vec{\upsilon} + \nabla \vec{\upsilon}^{T} \right) - \frac{2}{3} \nabla \cdot \vec{\upsilon} I \right] \tag{1.3}$$

The conservation of energy equation:

$$\frac{\partial}{\partial t}\left(\rho h \right) + \nabla \cdot \left(\rho h \vec{\upsilon} \right) = \nabla \cdot \left[\left(k + k_t \right) \nabla T \right] + S_h \tag{1.4}$$

where h is sensible enthalpy and S_h is the volumetric heat source.

The thesis is organized in 8 chapters with 4 appendices covering relevant details. In Chapter 2, previous studies regarding the various fin configurations are examined. In Chapter 3, modeling details of the fin configurations in ICEPAK is explained. In Chapter 4, models are checked and verified by investigating first natural convection on vertical flat plate and then following the same verification procedure done in Ref. [1] and Ref. [2]. In Chapter 5, results are given and compared with the experimental results. The flow visualization is presented in Chapter 6. The results are correlated and compared with literature in Chapter 7. Finally conclusion is given in Chapter 8.

CHAPTER 2

PREVIOUS STUDIES

Natural convection from finned surfaces has been investigated in literature extensively both theoretically and experimentally. Numerical studies were also done to find a convenient model for the phenomena. Furthermore in all of the previous studies, different geometries and configurations were studied to find the optimum fin structure for maximum heat transfer rate.

One of the earliest studies about natural convection heat transfer from fin arrays was conducted by Starner and McManus [5]. Four different fin array configurations with three base types were investigated and heat transfer coefficients were calculated. Flow patterns for each case were observed by using smoke filaments. It was concluded that fin height, fin spacing and base orientation have significant effect on rate of heat transfer from fin arrays.

Another experimental study regarding the natural convection heat transfer from both vertically and horizontally oriented fin arrays was done by Leung and Probert [6]. The effects of fin spacing and fin height were investigated for a limited number of fin array configurations. It was observed that optimum fin spacing was within 9.0 - 9.5 mm range for a fin array that has 150 mm length. It was also inferred from the study that fin height and base-to-ambient temperature difference have insignificant effect on optimum fin spacing.

Leung et al. [7] performed an experimental study on heat transfer from vertically placed fin arrays produced from an aluminum alloy. It was found that for different configurations the maximum heat transfer rate from the fin arrays was obtained at the fin spacing value of 10 mm.

Jonas and Smith [8] conducted an experimental study in order to find the optimum fin spacing for horizontally placed rectangular fin arrays. An interferometer was used to measure local temperature gradients. The measured temperature gradients were used to determine the corresponding heat transfer coefficients. It was inferred from the results that the fin spacing, S has a significant effect on the heat transfer coefficients. The following correlations were also obtained:

$$Nu_s = 6.7\times10^{-4}\times Gr_s\times Pr\times\left[1\text{-}\exp\left(\frac{7460}{Gr_s\times Pr}\right)^{0.44}\right]^{1.7} \quad \text{for } S < 2 \text{ inches} \tag{2.1}$$

$$Nu_s = 0.54\times\left(Gr_s\times Pr\right)^{0.25} \quad \text{for } S > 2 \text{ inches} \tag{2.2}$$

where Pr stands for Prandtl number, Nu_s stands for Nusselt number and Gr_s stands for Grashof number based on fin spacing.

Filtzroy [9] conducted a study in order to find the optimum fin spacing for the maximum rate of natural convection heat transfer from vertically placed fins in the laminar flow regime. The following correlation which relates the ratio of average heat transfer coefficient based on fin spacing to vertical heat transfer heat coefficient was suggested:

$$\frac{h_s}{h_b} = \frac{1.68}{24}\times\left[\frac{S}{H}\times\left(Gr_s\times Pr\right)^{0.25}\right]^3\times\left[1\text{-}\exp\left(\frac{-24}{1.68\times\left[\frac{S}{H}\times\left(Gr_s\times Pr\right)^{0.25}\right]^3}\right)\right] \tag{2.3}$$

where h_s stands for average heat transfer coefficient based on fin spacing and h_b stands for vertical heat transfer heat coefficient.

Yüncü and Anbar [10] conducted an experimental study of natural convection heat transfer from horizontally placed rectangular fin arrays. A set of 15 sets

of fin arrays with different fin spacing and fin heights were used. The base-to-ambient temperature was also varied by means of an electrical heater. This experimental study was done in order to show the separate effects of fin height, fin spacing and base-to-ambient temperature difference on the natural heat transfer. It was found that the natural heat transfer rate reaches to a maximum value as a function of fin height and fin spacing for a given base-to-ambient temperature. A correlation relating the ratio of natural convection heat transfer rate from fins to that of a simple base plate as a function of fin height, fin length and fin spacing was also presented as follows:

$$\frac{Q_{fc}}{Q_{pc}} = 0.923 \times \exp\left[1.336 \times \left(N^{-0.013N}\right) \times \frac{H}{s}\right] \tag{2.4}$$

where Q_{fc} is convection heat transfer rate while Q_{pc} is total heat transfer rate.

Yüncü and Mobedi [11] investigated the three dimensional steady state natural convection from horizontally placed longitudinally short rectangular fin arrays numerically. A finite difference code in Cartesian coordinate system based on vorticity-vector potential approach was used to solve the problem. Effects of different geometric parameters of fin arrays on flow configurations occurring in the channel of fin arrays were analyzed. As a result of observations two types of flow patterns were found. In the first one, for narrow fin spacing, it was observed that air can only enter into the channel from the end regions. On the other hand, if the fin spacing is large enough it was observed that air is free to enter the channel from the middle part of the fin. The effects of fin height, fin spacing and fin length on the heat transfer rate were also analyzed and it was concluded that the effects of these parameters were very much interconnected.

Güvenç [2] investigated natural convection heat transfer from vertically oriented rectangular fin arrays experimentally. 15 different fin configurations with varied fin height, fin spacing and base-to-ambient temperature were used

in the experiments. It was found that fin spacing is the most important variable for maximum natural heat transfer rate. Hence it was observed that the maximum natural heat transfer rate is reached for optimum fin spacing. The comparison of the experimental results with Ref. [10] showed that it can also be concluded that vertical fin arrays are more effective in dissipating heat from surfaces than horizontal fin arrays.

Harahap et al. [12] performed experiments on miniaturized vertical rectangular fin arrays in order to investigate the effect of miniaturizing on steady state rate of natural heat transfer. The base area of rectangular fin arrays was selected as 49x49 mm^2 and it was miniaturized to 25x25 mm^2 with varying intermediate areas in between. Two different fin spacing values of 3 mm and 11 mm were used. It was observed that regardless of the fin spacing heat dissipation rate per unit area increases with decrease in base area of fin arrays. This effect was more significant for square base plates. It was also found out that the rate of heat transfer was more for the fin spacing value of 11 mm. Furthermore it was observed that more heat was dissipated from the fin arrays when the width of the base plate is larger than the length of the base plate.

Vollaro et al. [13] analyzed natural convection from rectangular and vertical finned plates numerically in order to optimize the fin configuration. The maximum heat transfer rate from fin array was investigated for the optimum fins spacing as a function of parameters such as dimensions, thermal conductivity, fins absorption coefficient and fluid thermo-physical properties. Effects of the emissivity of the fin material and of the heat exchanged by the finless portion of the base plate on the optimum performance were also evaluated.

A numerical study was performed to investigate the natural convection from horizontally placed rectangular thick fin arrays with short lengths by Dialameh et al. [14]. Finite volume scheme was used to solve the three dimensional elliptic governing equations. The results showed the same two flow patterns as

given in Ref. [11]. It was observed that the free convection heat transfer coefficient increases with the increasing differences in temperature and fin spacing whereas decreases with increase in fin length. Furthermore it was found out that effect of fin thickness and height on the heat transfer is negligible. Optimum fin spacing value was found to be 7 mm for maximum heat transfer from fin arrays with channel aspect ratio H/L $\leq$0.24.

Kundu and Das [15] performed an analytical study to investigate performance and optimum design analysis of four fin array types. In this regard, longitudinal rectangular fin array, annular rectangular fin array, longitudinal trapezoidal fin array and annular trapezoidal fin array under convective cooling conditions are investigated. Considerable effect of the conduction through the supporting structure and the convection from the interfin spacing was observed. A method was also developed for optimizing the fin dimensions when the total fin volume and the interfin spacing are given.

Leung and Probert [16] performed an experimental study in order to find the effect of the gap width between two consecutive fin arrays arranged one above the other upon the steady state natural heat transfer from the fin arrays. Two identical rectangular fin arrays which have their bases aligned in the same vertical plane were used. It was observed that 18 mm gap width slightly increases the rate of heat transfer by means of natural convection. It was also concluded that a slight improvement in heat dissipation can be achieved when consecutive short fins are used instead of long fins. On the other hand, it was found that heat dissipation rate decreases if the gap width between two consecutive fin arrays is less than 12 mm.

Mobedi and Sunden [17] investigated the steady state conjugate conduction-convection on vertically placed fin arrays with small heat source inside. A computer code was written by using finite difference method in order to solve the governing equations. It was observed that heat transfer rate does not vary with the location of the heat source for a small conduction-convection

parameter. Nevertheless it was noticed that the location of the heat source affects the heat transfer rate if the conduction-convection parameter is large. Therefore it was concluded that a best location for the heat source exists in order to maximize the heat transfer rate from fin array.

An experimental study was performed by Nada [18] in order to investigate the free convection heat transfer and flow characteristics of heated rectangular fin arrays in enclosures. Effects of fin length and fin spacing were observed for wide range of Rayleigh numbers. In this regard, an optimization in fin array geometry was suggested. It was also reported that for high range of Ra, fin effectiveness decreases and Nusselt number increases with an increase in Ra, however for low range of Ra and large fin spacing, Nusselt number and fin effectiveness increases with Ra. It was also observed that fin effectiveness and Nusselt number increases with a decrease in fin spacing until a certain value is reached. It iwas reported that this certain value was reached where fin spacing to fin height ratio, S/H=1. After this value the Nusselt number and fin effectiveness decreases with the decrease in fin spacing.

A numerical analysis on natural convection heat transfer from horizontally placed rectangular shrouded fin arrays were performed by Yalcin et al. [19] Commercially available CFD package PHOENICS was used to solve the governing three dimensional elliptic governing equations. The effects of size and configuration of fins, the clearance gap between fin tips and shroud, and the base and fin temperatures on the rate of heat transfer was observed. According to the obtained results, an optimum fin configuration and clearance gap was suggested.

Yazıcıoğlu [1] performed an experimental study on steady state natural convection heat transfer from vertical rectangular fins made of aluminum. Thirty different fin configurations were used to investigate the effect of fin spacing, fin height, fin length on the performance of heat dissipation from the fin arrays. While fin spacing was varied from 5.75 mm to 85.5 mm, fin height

was varied from 5 mm to 25 mm. Two different fin lengths, 250 mm and 340 mm were used. Moreover five different power inputs varying from 25W to 125W were supplied to fin arrays in order to observe the heat transfer from fins for different base-to-ambient temperature differences. It was found that the rate of heat transfer from fin arrays depends on the geometric parameters and the base-to-ambient temperature differences. Furthermore it was observed that for a given base-to-ambient temperature difference there was an optimum fin spacing value which maximizes the rate of convective heat transfer from fin arrays for all of the fin configurations. In order to predict the order of magnitude of optimum fin spacing at a given fin length and base-to-ambient temperature difference, a scale analysis was done. From this scale analysis the following correlations were derived:

$$\frac{S_{opt}}{L}=3.94\times Ra_L^{-1/4} \tag{2.5}$$

$$Q_{cmax}=(Q_0)_c+0.125\times Ra_L^{1/2}\times k\times H\times \Delta T\times\left(\frac{W}{L}\right) \tag{2.6}$$

where Q_{cmax} is total convection heat transfer rate and $(Q_0)_c$ is the convection heat transfer rate when there are no fins.

CHAPTER 3

ICEPAK MODEL

Two experimental studies from literature for vertical fin heat sink case in Ref. [1] and Ref. [2] are investigated using ICEPAK 4.4.8. For the first experimental study (Case Study 1) two different configuration sets consisting of 30 different large fin configurations are modeled in this study. For the second experimental study (Case Study 2) 15 different smaller fin configurations are analyzed. In this chapter the method used in modeling of these configurations and solution settings are given.

3.1 Case Study 1

3.1.1 Modeling

Two different set-up configurations according to explanations and given dimensions are modeled in Ref. [1]. Although in the experimental set-up there were more components, a simplified model is created since the exact details of the components used in set-up were not given in Ref. [1]. Consequently, in the present study model, the models consist of an aerated concrete block, a base plate for heat generation and fin array configurations. The views of the modeled set-up are given Figure 3.1.1.1 and Figure 3.1.1.2.

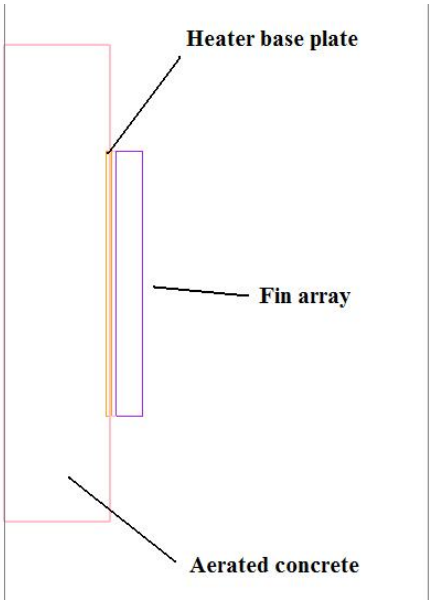

Figure 3.1.1.1 The side view of modeled set-up for Case Study 1

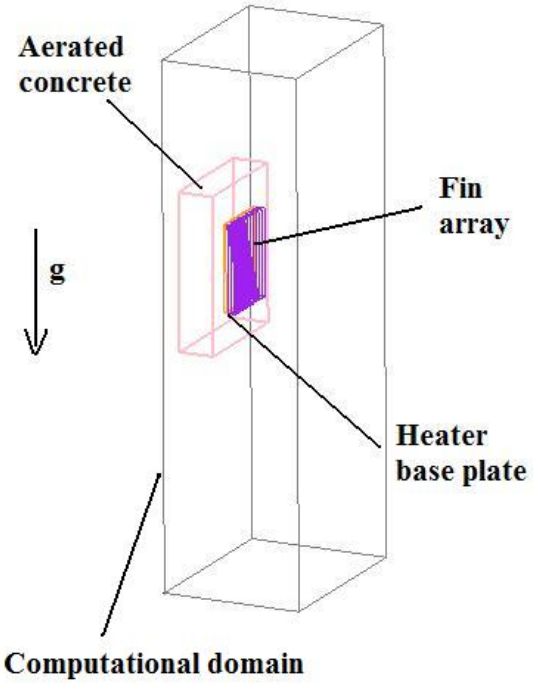

Figure 3.1.1.2 The 3D view of modeled set-up for Case Study 1

Since the dimensions of the aerated concrete block were not given in Ref. [1] an estimation of the dimensions is used to create the model. Therefore in the models a 340x450x100 mm block is used as the concrete block that fin models are mounted. Moreover an aluminum base plate is modeled as the heat generation source of the system. The dimensions of this heater base plate are taken as 180x250x5 mm for the first set-up with 250 mm heat sink length and 180x340x5 mm for the second set-up with 340 mm heat sink length. In both set-ups this heater base plate was buried 4 mm into the aerated concrete block to simulate the case in Ref. [1]. All the fin configurations are then mounted directly onto these heater base plates. Two different size domains are modeled to simulate the surroundings of the fin models. The dimensions of the surrounding air are taken as 540x1500x400 mm for the first set-up and 540x2040x400 mm for the second set-up. The dimensions of the models are given in Table 3.1.1.1.

Table 3.1.1.1 Dimensions of the components for Case Study 1

Dimensions (mm)		
Component	Set-up 1	Set-up 2
Heater base plate	180x250x5	180x340x5
Aerated concrete	340x450x100	340x450x100
Computational domain	540x1500x400	540x2040x400

In both set-up models all of the walls of the computational domain except the one on which concrete block is mounted, is chosen as open to surroundings. The one surface of the domain on which the concrete block is mounted, is taken as an adiabatic wall. The height of the domain is taken as 6 times of the

length of the fin array in order to simulate a large room. The fin array is placed 3 times the length of itself away from the bottom of the domain to allow more room for flow to develop. The effect of the domain size on the results is investigated in Appendix A.

Fin array configurations are taken exactly from the Ref. [1]. The fin array geometry is shown in Figure 3.1.1.3 and the dimensions of the fin configurations are shown in Table 3.1.1.2.

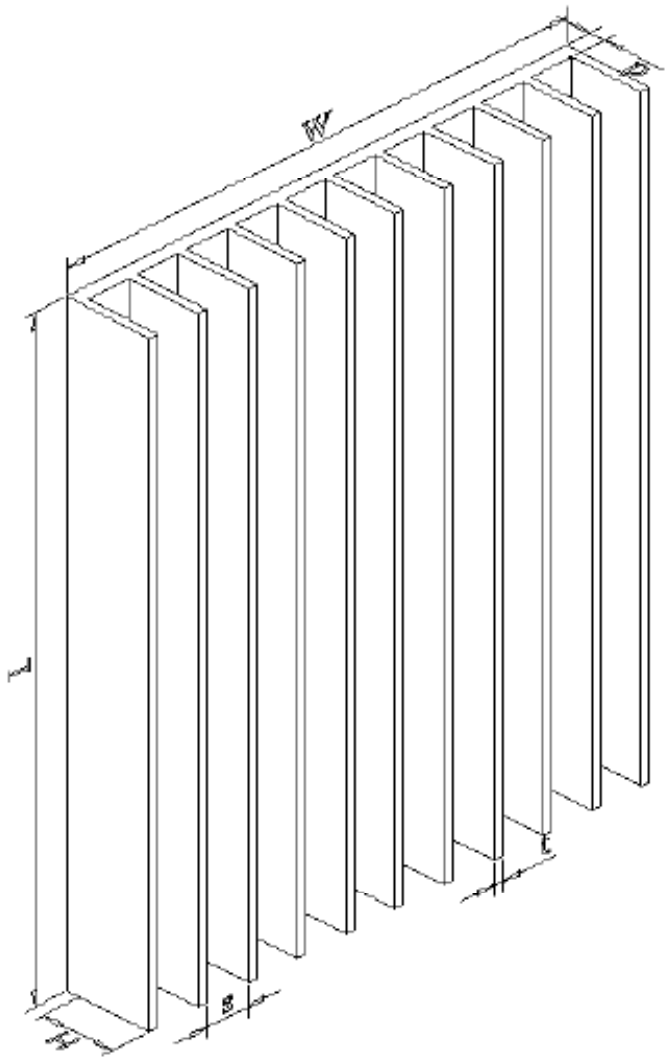

Figure 3.1.1.3 The 3D view of fin array for Case Study 1 (from Ref. [1])

Table 3.1.1.2 Dimensions of fin array configurations for Case Study 1

Fin Length L(mm)	Fin Width W(mm)	Fin Thickness t(mm)	Base Thickness d(mm)
250, 340	180	3	5
Set No.	Fin Height H(mm)	Fin Spacing s(mm)	Number of Fins n
1	25	85.5	3
2	25	32.4	6
3	25	14.7	11
4	25	8.8	16
5	25	5.85	21
6	15	85.5	3
7	15	32.4	6
8	15	14.7	11
9	15	8.8	16
10	15	5.85	21
11	5	85.5	3
12	5	32.4	6
13	5	14.7	11
14	5	8.8	16
15	5	5.85	21

Material types of the models are taken as they are given in Ref. [1]. The material properties used in the model are given in Table 3.1.1.3.

Table 3.1.1.3 Material properties of the components for Case Study 1

Component	Material Type	Specific Heat (J/kg C)	Conductivity (W/mK)	Emissivity	Roughness (mm)
Concrete Block	Aerated Concrete	1000	0.15	0.9	2
Heater Base Plate	Aluminum	900	130	0.2	0.02
Fin Array	Aluminum	900	130	0.2	0.02

Temperature readings from the fin array configurations are obtained from the thermocouple locations in Ref. [1]: 6 points are created on the fin array models to read local temperatures. The locations of the six points are shown in Figure 3.1.1.4.

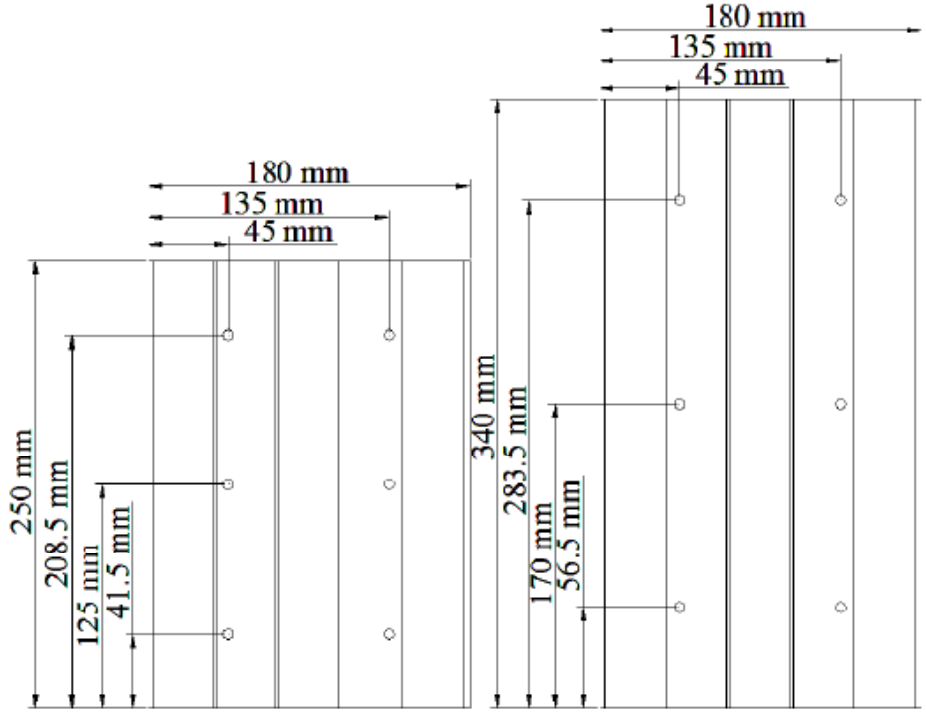

Figure 3.1.1.4 The locations of the six temperature reading points for Case Study 1 (from Ref. [1])

3.1.2 Basic Parameters and Assumptions

The analyses are done using the following basic parameters of the ANSYS ICEPAK software and assumptions.

- Radiation is on. View factor solution is used instead of discrete ordinates radiation method.
- Flow Regime is assumed as turbulent. Zero equation turbulence model is used as the turbulence model.

- Gravity vector is checked and the value of the gravitational acceleration is taken as -9.80665 m/s^2 in y direction.
- Default fluid is taken as air and air is stagnant.
- Ambient temperature and radiation temperature is taken as 20 ^oC.
- Steady state solution is selected.
- Initial conditions of velocities are taken as 0 m/s whereas the initial condition of temperature is taken as ambient temperature (20 ^oC).
- Ideal gas option is checked and the operational pressure is taken as 101325 N/m^2.
- No-slip boundary condition for surfaces.
- No contact resistances.

3.1.3 Solution Settings

The analyses are done using the following solution settings of the ANSYS ICEPAK software.

- Number of iterations is taken as 250.
- Convergence criterion of flow is taken as 10^{-4} whereas convergence criterion of energy is taken as 10^{-9}. Convergence of the results is investigated in Appendix B.
- Standard discretization scheme is selected for pressure whereas first order discretization scheme is selected for momentum and temperature. Effects of the second order discretization scheme on the results are investigated in Appendix C.
- Under-relaxation factors are taken as follows:
    - Pressure: 0.3
    - Momentum: 0.7
    - Temperature: 1.0
    - Viscosity: 1.0
    - Body Forces: 1.0
- Double Precision is selected.

3.1.4 Meshing

All of the components of the model (concrete block, heater base plate and fin array model) are modeled inside of an assembly volume. By the help of this separate volume, it would be possible create different mesh sizes inside and outside of the assembly. Therefore finer meshes are used to model the flow near the fin array more precisely whereas coarser meshes are used outside this assembly volume to decrease the mesh size. The parameters used to create the assembly volume are given in Figure 3.1.4.1.

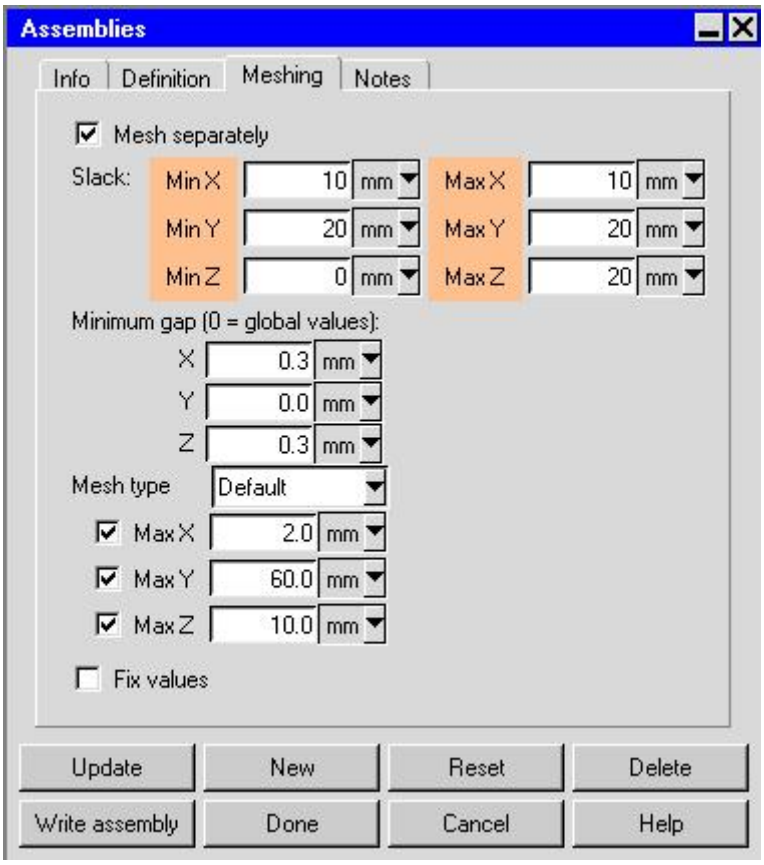

Figure 3.1.4.1 Assembly parameters used for creating a separate assembly volume

The general mesh size properties outside the assembly volume are shown in Figure 3.1.4.2.

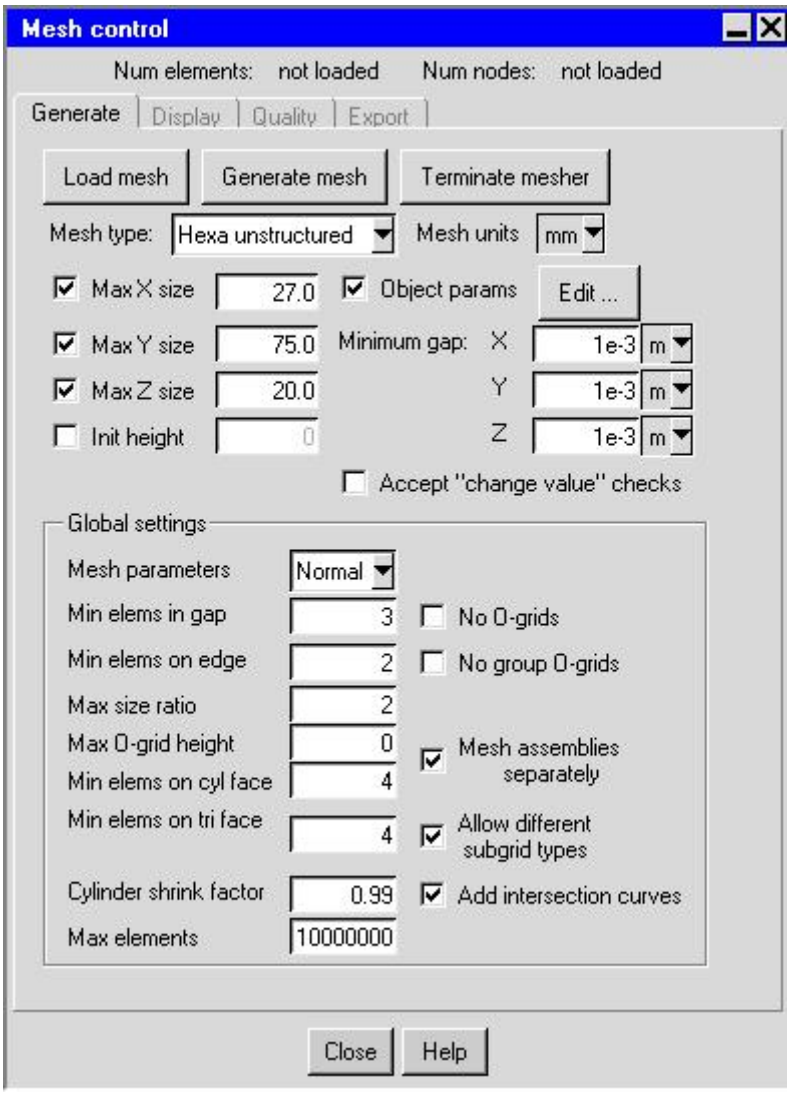

Figure 3.1.4.2 The general mesh size control parameters

The mesh size properties used inside the assembly volume for fin array is shown in Figure 3.1.4.3 and the non-conformal mesh structure of the model is shown in Figure 3.1.4.4.

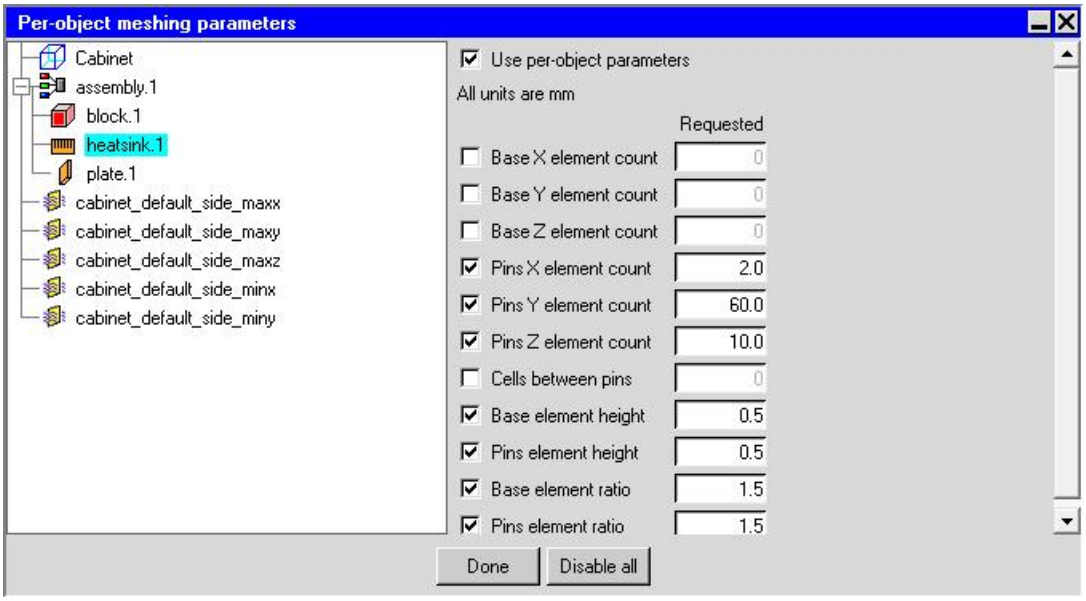

Figure 3.1.4.3 The mesh size parameters for fin arrays

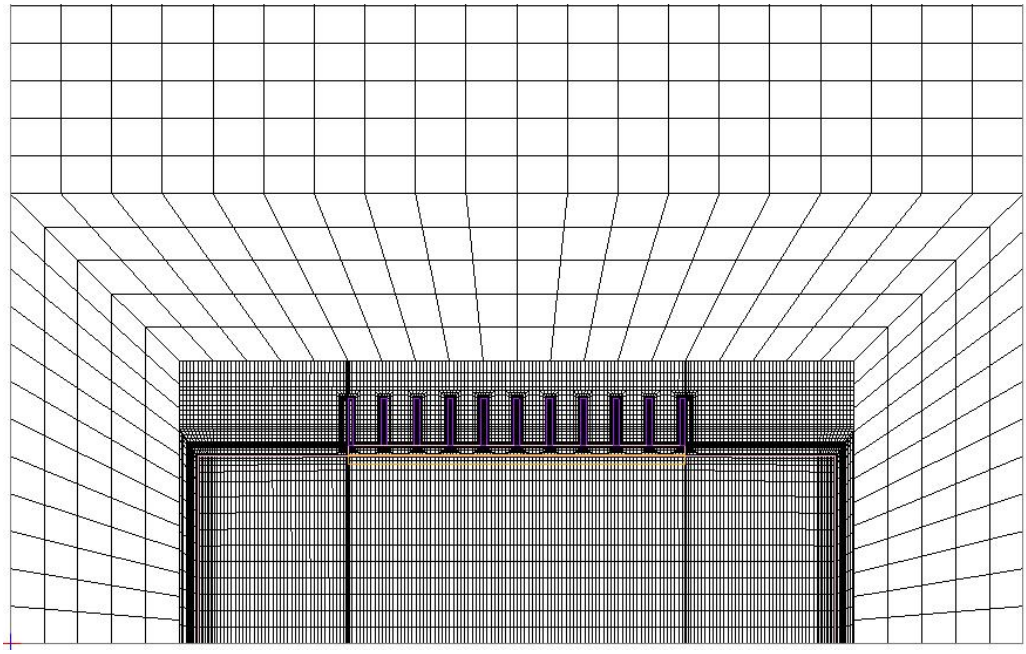

Figure 3.1.4.4 Top view of non-conformal mesh structure for Case Study 1

The finer mesh near to the fin array structure can be seen in Figure 3.1.4.5.

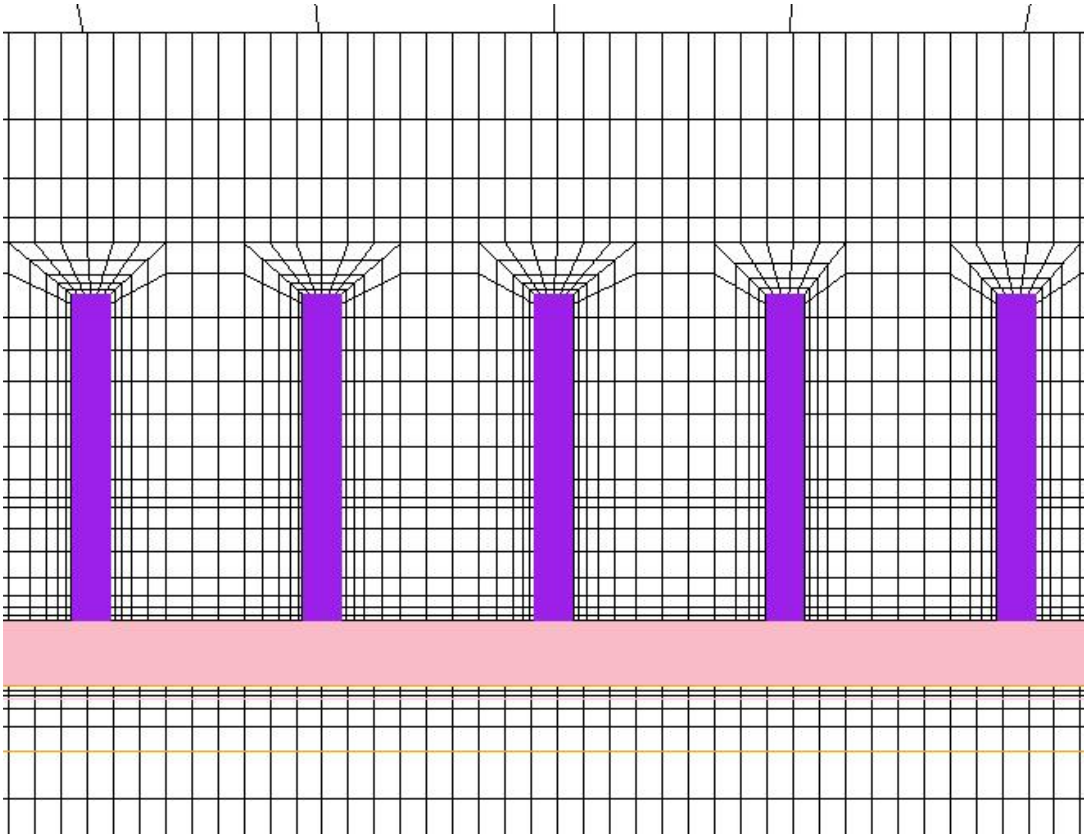

Figure 3.1.4.5 Fine meshes near to the fins for Case Study 1

Effects of different mesh sizes on the results and the reason behind the selection of the mesh size are presented in Appendix D.

3.2 Case Study 2

3.2.1 Modeling

Similar to Case Study 1, a simplified model is used to simulate the experimental study explained in Ref. [2], since the exact details of the model were not given. The model of Case Study 2 consists of an insulation block, a base plate for heat generation and fin array configurations. The views of the created model are given in Figure 3.2.1.1 and Figure 3.2.1.2.

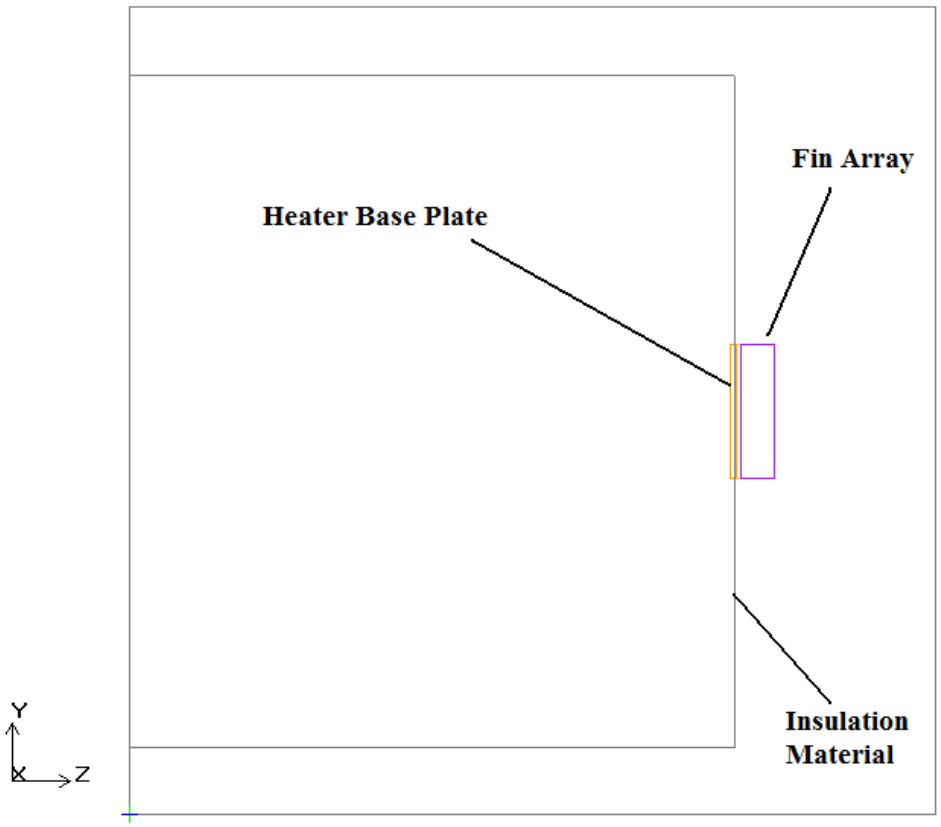

Figure 3.2.1.1 Side view of the model for Case Study 2

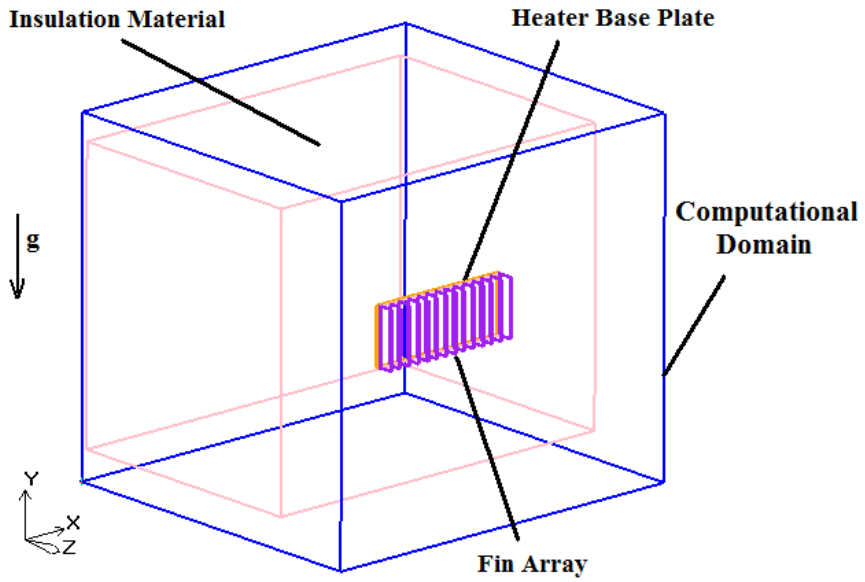

Figure 3.2.1.2 The 3D view of the model for Case Study 2

A block model is used to simulate the insulation material on which heater base plate and fin array are mounted. The heater base plate modeled as a 2 mm thick copper plate and it is buried to the insulation material block to simulate the case in experiment. All of the fin configurations are mounted directly onto this heater plate without considering the contact resistance. The dimensions of the components of the model are taken directly from Ref. [2] and they are shown in Table 3.2.1.1.

Table 3.2.1.1 Dimensions of the components for Case Study 2

Component	Dimensions (mm)
Heater base plate	250x100x2
Insulation Material	650x500x450
Computational domain	670x600x400

In a similar fashion, as explained for Case Study 1 all of the walls of the domain except the one on which insulating material is mounted is chosen as open to surroundings. The one surface of the domain on which the insulating material is mounted, is taken as an adiabatic wall. Once more, the height of the domain is selected as 6 times of the length of the fin array in order to simulate large room condition. The fin array is again mounted 3 times the length of itself away from the bottom surface of the domain in order to allow more room for flow to develop due to temperature difference.

Fin array configurations are taken exactly from the Ref. [2]. The fin array geometry is shown in Figure 3.2.1.3 and the dimensions of the different fin configurations are shown in Table 3.2.1.2.

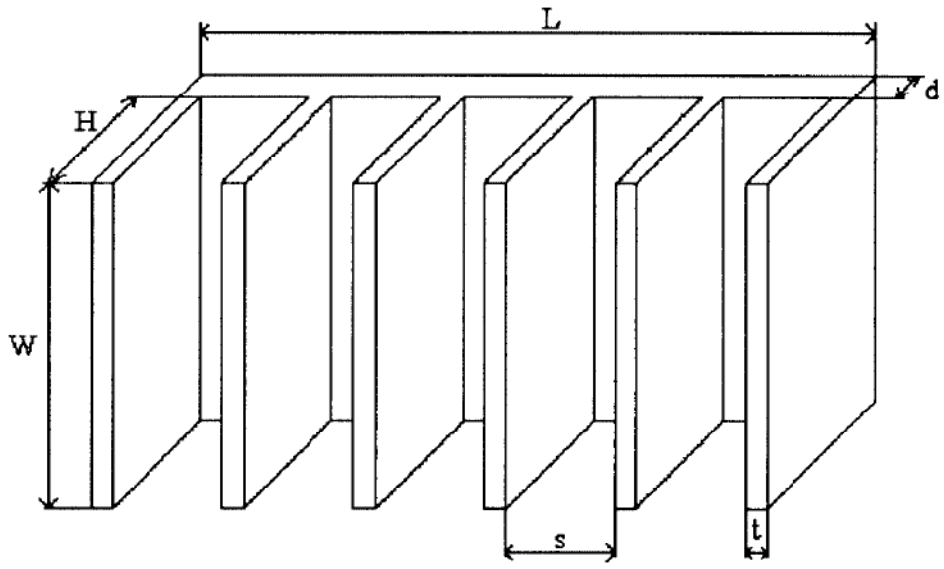

Figure 3.2.1.3 The 3D view of fin array for Case Study 2 (from Ref. [2])

Table 3.2.1.2 Dimensions of fin array configurations for Case Study 2

Set No.	Fin Height H(mm)	Fin Spacing s (mm)	Number of Fins N
1	25	58.75	5
2	25	32.3	8
3	25	16	14
4	25	7.3	25
5	25	4.5	34
6	15	58.75	5
7	15	32.3	8
8	15	16	14
9	15	7.3	25
10	15	4.5	34
11	5	58.75	5
12	5	32.3	8
13	5	16	14
14	5	7.3	25
15	5	4.5	34

Material types of the models are taken as they are given in Ref. [2] except for the insulating material. Since the exact details of the mounting of the fin array to insulating material is not known, the material properties of the insulating material block is found using trial and error method in verification of the model. The material properties are given in Table 3.2.1.3.

Table 3.2.1.3 Material properties of the components for Case Study 2

Component	Material Type	Specific Heat (J/kg C)	Conductivity (W/mK)	Emissivity	Roughness (mm)
Insulating Material	Fiberboard	835	0.22	0.85	0.5
Heater Base Plate	Copper	385	380	0.15	0.02
Fin Array	Aluminum	900	130	0.2	0.02

Temperature readings from the fin array configurations are taken similar to it was done in Ref. [2]: 6 points are created on the fin array models to read the local temperatures. The locations of the six points are shown in Figure 3.2.1.4.

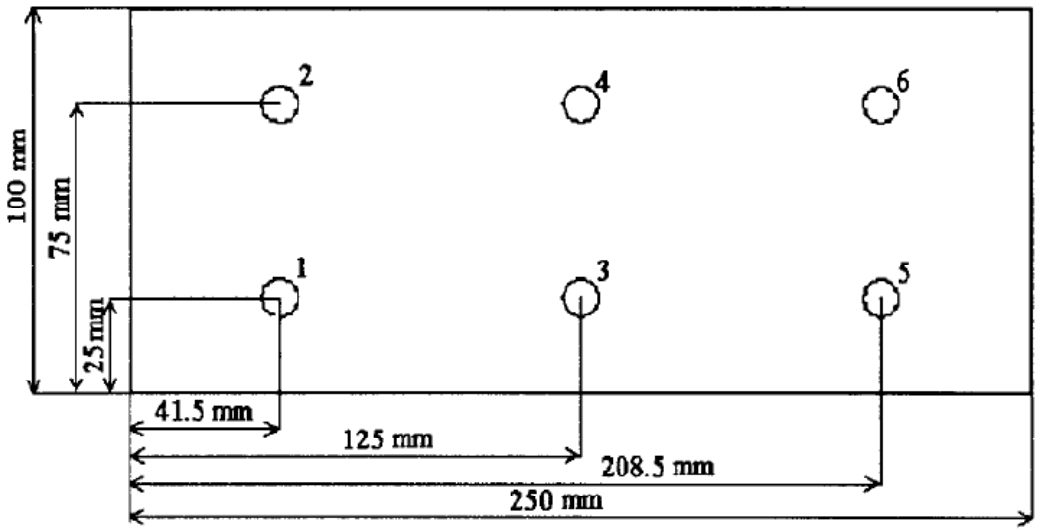

Figure 3.2.1.4 The locations of the six temperature reading points for Case Study 2

3.2.2 Basic Parameters and Assumptions

The same parameters and assumptions that are used for Case Study 1 except the flow regime parameter are also used for this case study in all of the runs. The flow regime in this study is assumed as laminar.

3.2.3 Solution Settings

The same solution settings that are used for Case Study 1 are also used for this case study in all of the runs.

3.2.4 Meshing

Unlike Case Study 1, the heater base plate and the fin array are modeled inside of an assembly volume. Since the dimensions of the insulating material are very large, it is not taken into the assembly volume in order to reduce the mesh size. Again, by the help of a separate assembly volume, it would be possible to create finer meshes near the fin array whereas coarser meshes outside the volume. The mesh size controls are taken exactly the same as they are in Case Study 1. The non conformal mesh structure of the model is shown in Figure 3.2.4.1 and Figure 3.2.4.2.

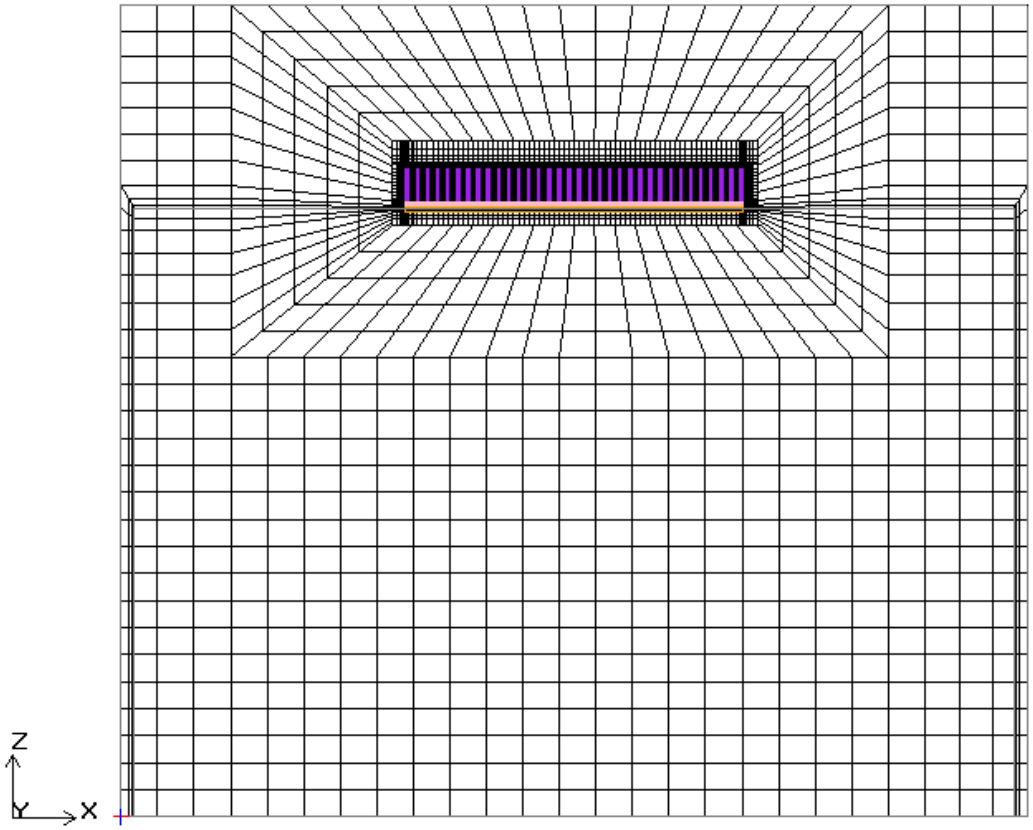

Figure 3.2.4.1 Top view of non-conformal mesh structure for Case Study 2

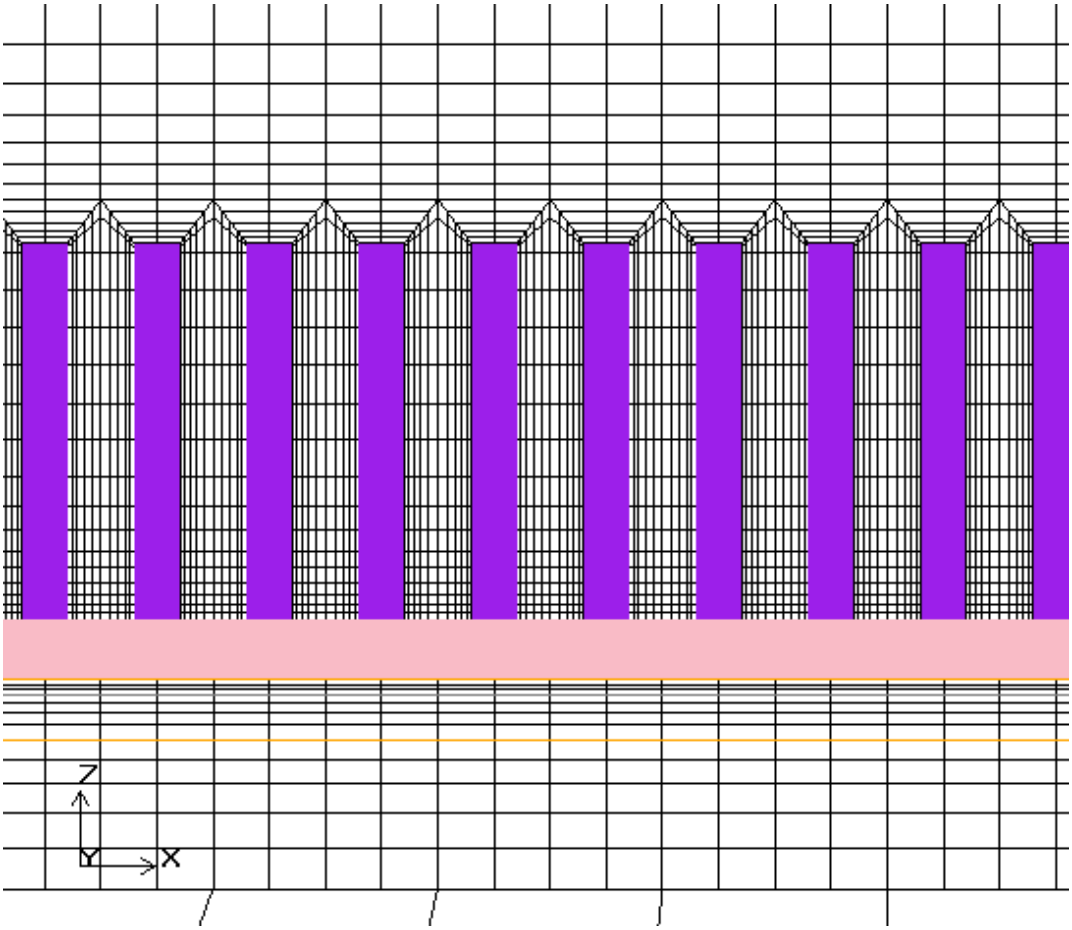

Figure 3.2.4.2 Fine meshes near to the fins for Case Study 2

CHAPTER 4

MODEL VERIFICATION

In order to verify the model and the solution parameters, two different verification methods are used for both of the case studies investigated from literature [1][2]. In the first method, natural convection over a vertical flat plate is investigated and the results obtained from the analyses are compared with the results from correlations that are available in literature. In the second method, two parallel plates placed very close to each other are used as explained in both Ref. [1] and Ref. [2].

4.1 Verification of Case Study 1

4.1.1 Vertical Flat Plate

In this case, heater base plate mentioned in Chapter 3 is used as the vertical flat plate. The dimensions of the plate are 250x180x5 mm. The view of the model is shown in Figure 4.1.1.1 and mesh structure of the model is shown in Figure 4.1.1.2.

.

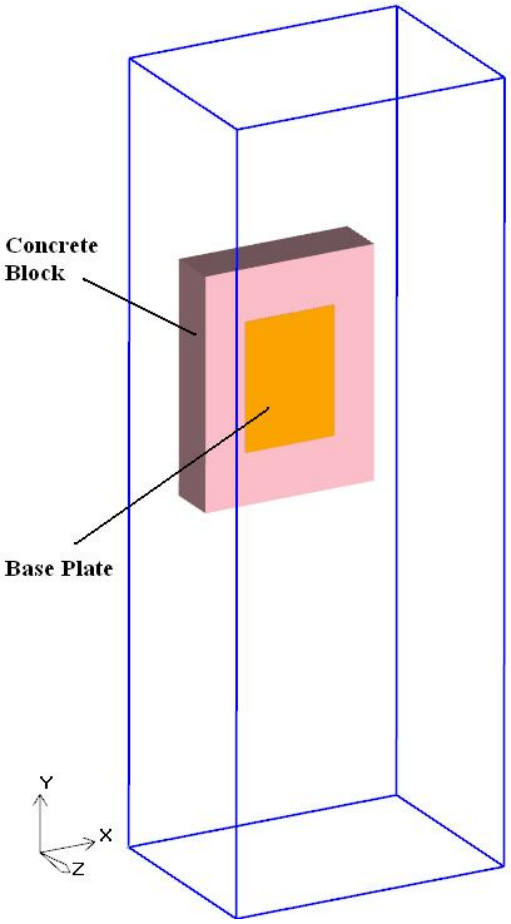

Figure 4.1.1.1 3D view of the model

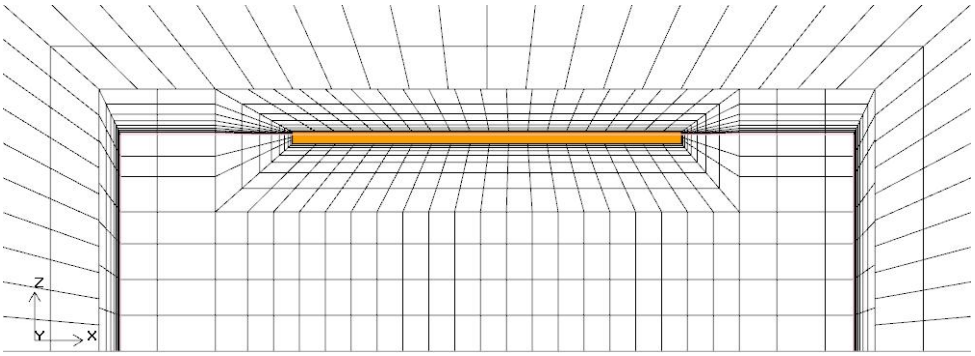

Figure 4.1.1.2 Mesh structure of flat plate

Different power inputs (Q_{in}) ranging from 20W to 140W are generated inside the plate in order to produce heat. The average temperature of the plate (T_w) and the convection heat transfer rate (Q_c) are obtained for each different power input to the plate (Q_{in}). The tabulated results are given in Table 4.1.1.1.

Table 4.1.1.1 Average surface temperature of the plate and convection heat transfer values

Qin(W)	Tw(^{o}C)	Qc(W)
20	62.6	9.8
30	79.0	15.3
40	96.8	20.4
50	110.5	24.9
60	124.8	29.7
70	137.2	34.0
80	151.3	39.1
90	168.1	45.2
100	178.6	49.1
110	191.9	54.1
120	205.0	59.0
130	215.8	63.2
140	226.4	67.2

In order to compare the results obtained from analyses with theoretical studies, Rayleigh and Nusselt numbers must be calculated. A sample showing how to calculate Rayleigh and Nusselt numbers for the heat input of 60W is given below.

The obtained results from the CFD simulations are:

$Q_{in} = 60W \qquad T_w = 124.8^oC \qquad Q_c = 29.7W$

Constant parameters are:

$A = 0.045 m^2$ $L = 0.25 m$ $\varepsilon = 0.2$ $T_a = 20\,^{o}C$

$g = 9.81 m/s^2$ $\sigma = 5.67 \times 10^{-8} W/m^2 \times K^4$

In order to find Nu and Ra, the flow properties must be obtained. Therefore the film temperature is required.

$$T_f = \frac{T_w + T_a}{2} = 72.4\,^{o}C$$

Then flow properties are as follows:

$$\beta = \frac{1}{T_f} = \frac{1}{72.4+273} = 0.002895(1/K)$$ $k = 2.97 \times 10^{-2} W/m \times K$

$\nu = 2.05 \times 10^{-5} m^2/s$ $\alpha = 2.92 \times 10^{-5} m^2/s$ $Pr = 0.701$

Since all of the flow properties are known, Ra and Nu can be found as follows:

$$Ra = \frac{g \times \beta \times L^3 \times (T_w - T_a)}{\nu \times \alpha} = 77812433$$

Since Ra<1x10^9 flow is laminar.

$$h = \frac{Q_c}{A \times (T_w - T_a)} = 6.29(W/m^2 \times K)$$

$$Nu = \frac{h \times L}{k} = 53.05$$

where L is the characteristic length (length of the plate)

The correlation results for Nusselt numbers can be calculated as follows:

- McAdam's correlation [21]:

$$\mathrm{Nu} = 0.59 \times \mathrm{Ra}^{1/4} = 55.41$$

- Churchill and Usagi's correlation [21]:

$$\mathrm{Nu} = \frac{0.67 \times \mathrm{Ra}^{1/4}}{\left[1 + \left(\frac{0.492}{\mathrm{Pr}}\right)^{9/16}\right]^{4/9}} = 48.23$$

- Churchill and Chu's first correlation [21]:

$$\mathrm{Nu} = \left[0.825 + \frac{0.387 \times \mathrm{Ra}^{1/6}}{\left[1 + \left(\frac{0.492}{\mathrm{Pr}}\right)^{9/16}\right]^{8/27}}\right]^2 = 56.57$$

- Churchill and Chu's second correlation [21]:

$$\mathrm{Nu} = 0.68 + \frac{0.67 \times \mathrm{Ra}^{1/4}}{\left[1 + \left(\frac{0.492}{\mathrm{Pr}}\right)^{9/16}\right]^{4/9}} = 48.91$$

The obtained data from analyses is used in order to calculate Nusselts and Rayleigh numbers as explained above. Tabulated results of the analysis and the comparison of Nusselt numbers are given in Table 4.1.1.2.

Table 4.1.1.2 Comparison of Nusselt numbers

Ra	Nu				
	Present Study	Churchill and Chu's first relation	Churchill and Chu's second relation	McAdam's relation	Churchill and Usagi's relation
48576725	46.96	49.26	43.58	49.26	42.90
60842614	49.67	52.63	46.05	52.11	45.37
68545985	51.46	54.51	47.42	53.68	46.74
73641262	52.44	55.67	48.25	54.66	47.57
77812433	53.05	56.57	48.91	55.41	48.23
80123273	53.51	57.06	49.25	55.82	48.57
81679041	53.93	57.37	49.48	56.09	48.80
82662917	54.12	57.55	49.61	56.26	48.93
82894394	54.28	57.59	49.63	56.30	48.95
82847484	54.25	57.57	49.62	56.29	48.94
82500621	54.17	57.48	49.56	56.23	48.88
82029315	54.14	57.37	49.48	56.15	48.80
81434240	53.97	57.23	49.38	56.05	48.70

As it can be seen from Table 4.1.1.2, the results obtained from analyses are close to theoretical results.

4.1.2 Vertical Two Parallel Flat Plates

Heat generated in the heater base plate is dissipated to the surroundings by means of natural convection and radiation from fin arrays and conduction through the concrete block. In Ref. [1], in order to find heat loss by conduction, two parallel plates are used. These two parallel plates shown in Figure 4.1.2.1, are placed very close to each other and it is assumed that the heat is transferred only by conduction and radiation between these two plates. The heat transfer between the parallel plates can be calculated by simple conduction and radiation equations. Since the power input to the heater base plate is known,

the heat loss to the environment by means of conduction can be calculated by subtracting the heat transfer rate between plates from the total power input.

In Ref. [1], the results obtained from two parallel plates were used for calibration purpose. Since the conduction loss to the surrounding is not known, these two parallel plates were used to obtain this information. In order to verify the model and show that the model matches the experiment, a similar two parallel plate model is created. As it is also stated in Chapter 3, the dimensions of the concrete block are estimated since the dimension values are not given in Ref. [1]. Therefore by comparing the results obtained from the model and the experiment, the dimensions of the concrete block is also checked for consistency with the experimental set-ups. Dimensions of two parallel plates used in verification of the model are shown in Figure 4.1.2.1.

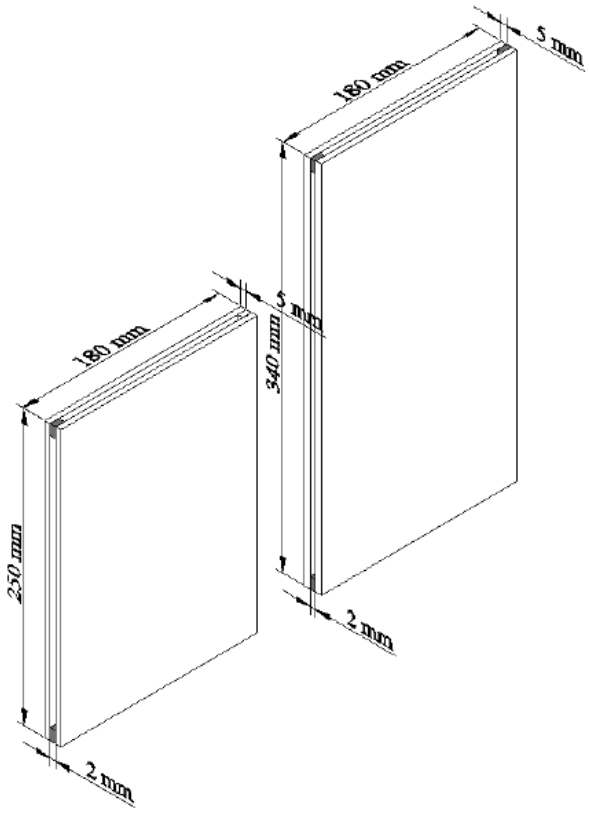

Figure 4.1.2.1 Dimensions of the two parallel plates (from Ref. [1])

The 3D view of the modeled two parallel plates mounted on the concrete block is shown in Figure 4.1.2.2.

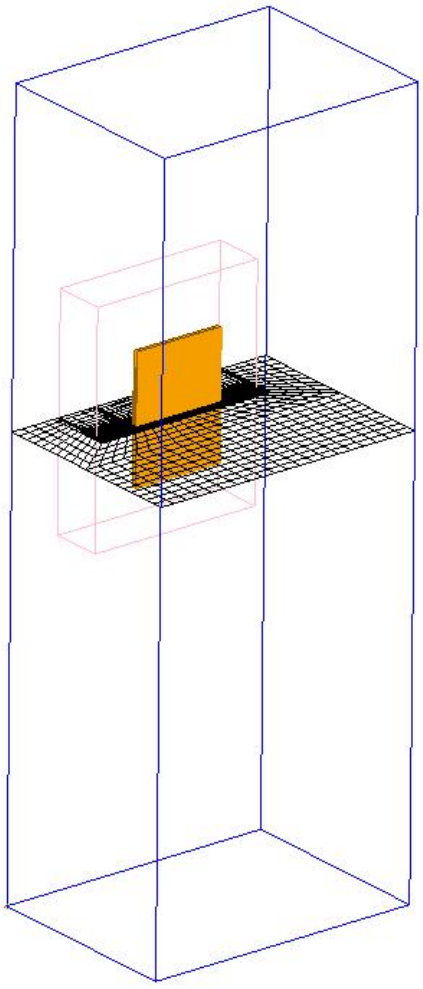

Figure 4.1.2.2 3D view of two parallel plate models

Exactly the same basic parameters and the solution settings described in Chapter 3 are used for this model. Once more the assembly volume is used to form a non-conformal mesh. The mesh structure of the model is shown in Figure 4.1.2.3.

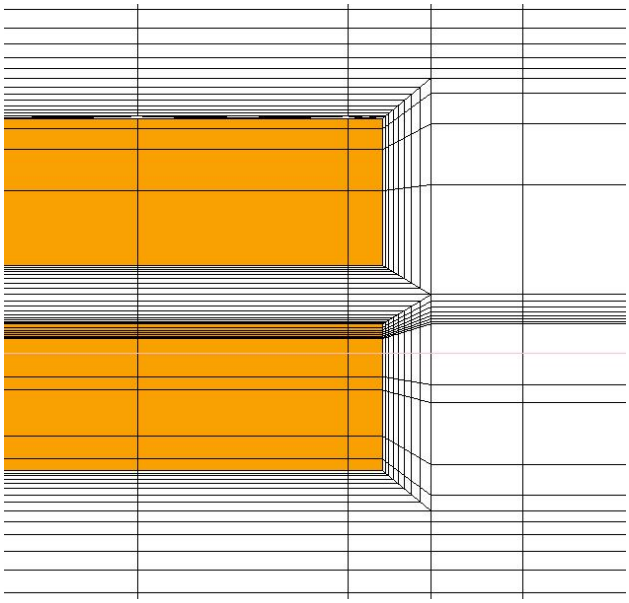

Figure 4.1.2.3 Mesh structure between the two parallel plates

Similar to Ref. [1], two cases are investigated. In the first case, two parallel plates with the length of 250 mm; whereas in the second case, two parallel plates with the length of 340 mm are used. In order to simulate the experiment, 13 different power inputs ranging from 20W to 140W are generated in the bottom plate. The temperatures of both plates and the heat flow from the bottom plate to the top plate are obtained from the analyses. The temperature of the bottom plate is denoted as T_1, temperature of the upper plate is denoted as T_2, and the heat flow from the bottom plate to the upper plate is denoted as Q_{out}.

The results for the two plates with the length of 250 mm are acquired from the analyses and the comparison of these results is shown in Figure 4.1.2.4 to Figure 4.1.2.6.

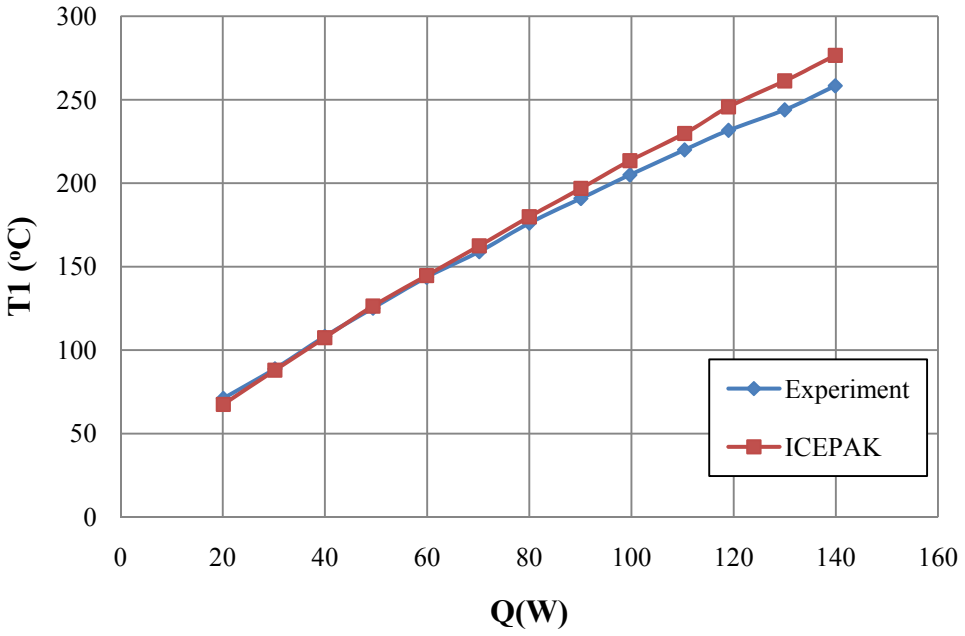

Figure 4.1.2.4 Variation of the bottom plate temperature (T_1) with power input to the bottom plate for L=250 mm

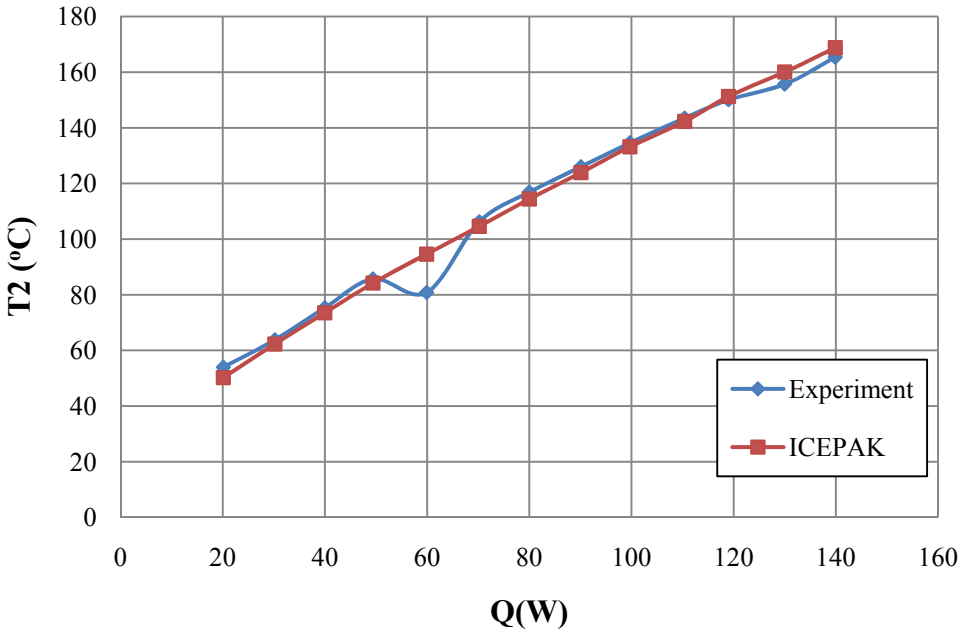

Figure 4.1.2.5 Variation of the upper plate temperature (T_2) with power input to the bottom plate for L=250 mm

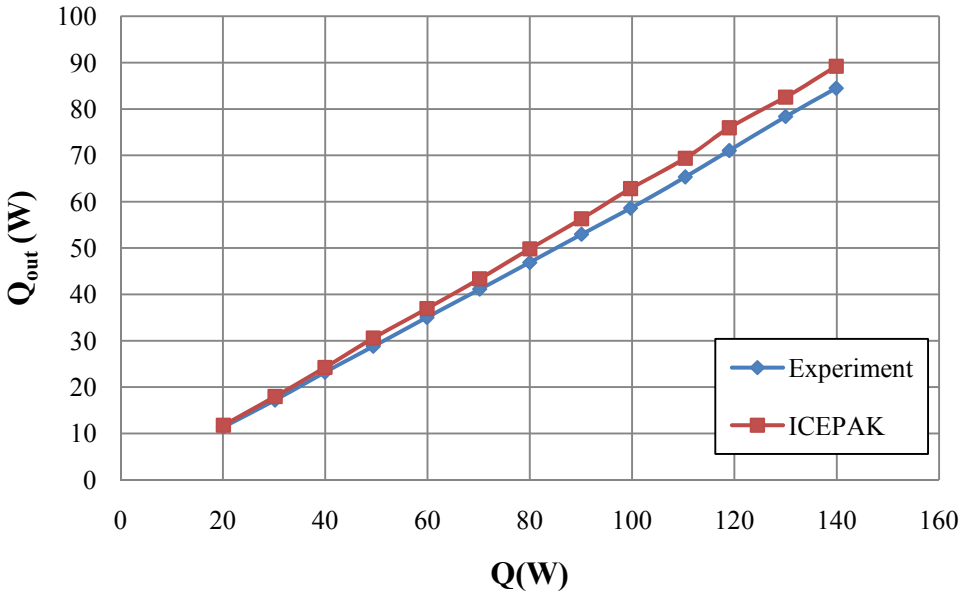

Figure 4.1.2.6 Variation of heat transfer from bottom plate to upper plate (Q_{out}) with power input to the bottom plate for L=250 mm

The plots show that for the plate length L = 250 mm, while the average the temperature of bottom plate (T_1) begins to deviate from experiment result for high power inputs, the average temperature of the upper plate (T_2) is similar for all power inputs. Besides, the value of heat transfer rate from the bottom plate to the upper plate (Q_{out}) also deviates from the experiment results for high power inputs. It can be observed that both deviations for the average temperature of the upper plate (T_2) and heat transfer rate from the bottom plate to upper plate are not very significant. Therefore it can be concluded that the model for the plate length L = 250 mm is verified with the experiment.

The results for the two plates with the length of 340 mm are acquired from the analyses and the comparison of these results is shown in Figure 4.1.2.7 to Figure 4.1.2.9.

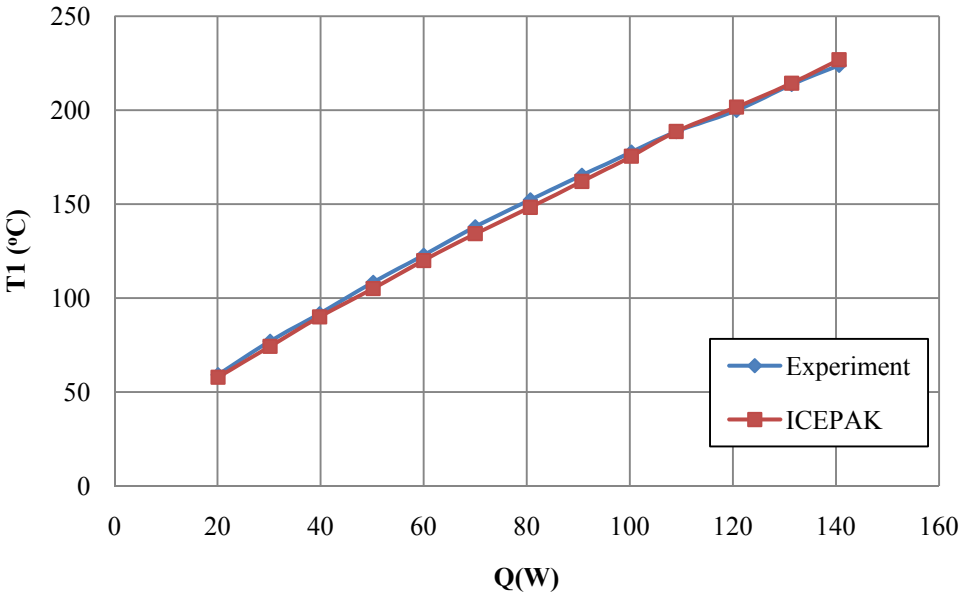

Figure 4.1.2.7 Variation of bottom plate temperature (T_1) with power input to the bottom plate for L=340 mm

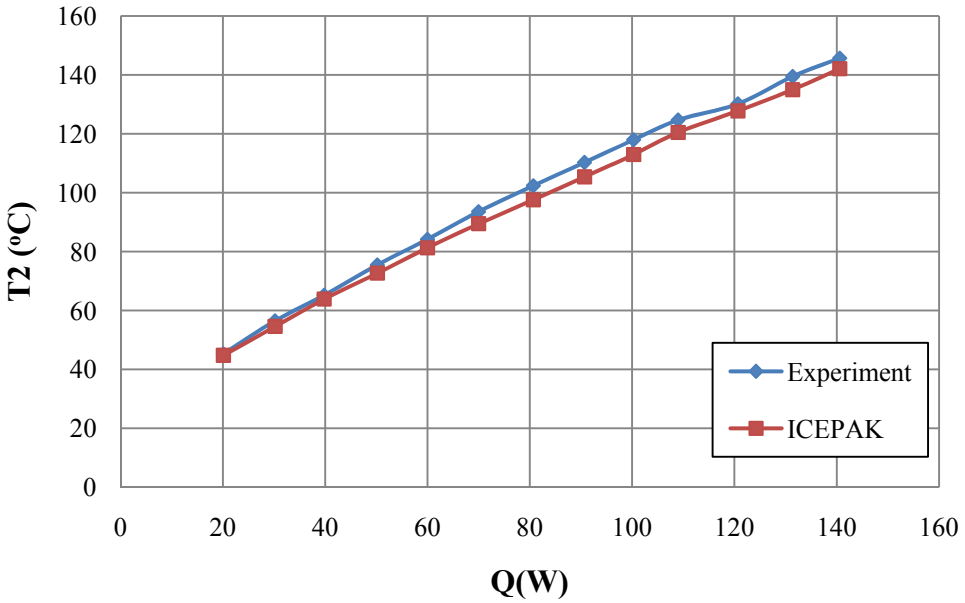

Figure 4.1.2.8 Variation of upper plate temperature (T_2) with power input to the bottom plate for L=340 mm

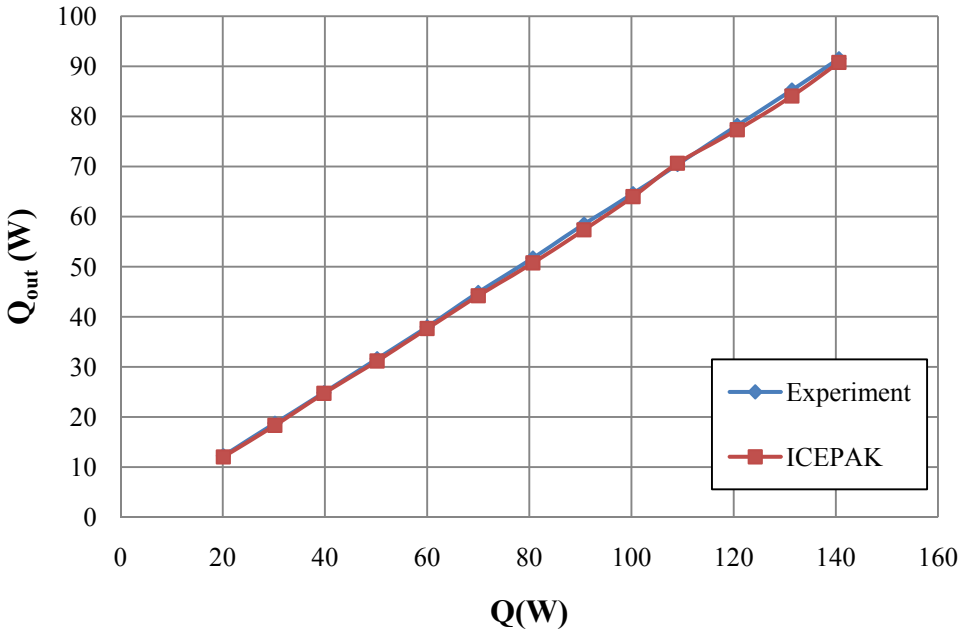

Figure 4.1.2.9 Variation of heat transfer rate from bottom plate to upper plate (Q_{out}) with power input to the bottom plate for L=340 mm

As it can be seen from figures, present study results for average temperature of the bottom plate T_1 and heat transfer rate from the bottom plate to the upper plate (Q_{out}) match with the experiment results. However the average temperature of the upper plate (T2) deviated from the experiment results slightly for high power inputs. Since this deviation is very small, it can again be concluded that the model of two parallel plates with length L = 340 matches with the experiment conducted in Ref. [1].

For both plate lengths, the results match with the experiment results. However, since the fin arrays are mounted on the bottom plate by mechanical means, it is not possible to obtain an exactly similar model. It is quite possible that there was an imperfect contact between the bottom plate and the fin array. Consequently, the contact resistance between the bottom plate and the fin array may cause different heat output results. Since it is not possible to model this

contact resistance precisely, in present study models it is assumed that the fin array mounted on the bottom plate with no contact resistance at all.

4.2 Verification of Case Study 2

4.2.1 Vertical Flat Plate

The heater base plate mentioned in Chapter 3 for Case Study 2 is used as the vertical flat plate here, again. The dimensions of the flat plate are taken as 250x100x2 mm. The flat plate is mounted on the insulating material block as explained in Chapter 3. The same basic parameters and the solution settings are used as explained in Chapter 3. The insulating material block is not taken into the assembly block because of its large volume in order to decrease the mesh size. The 3D view and the mesh structure of the model of the verification model is shown in Figure 4.2.1.1 and Figure 4.2.1.2.

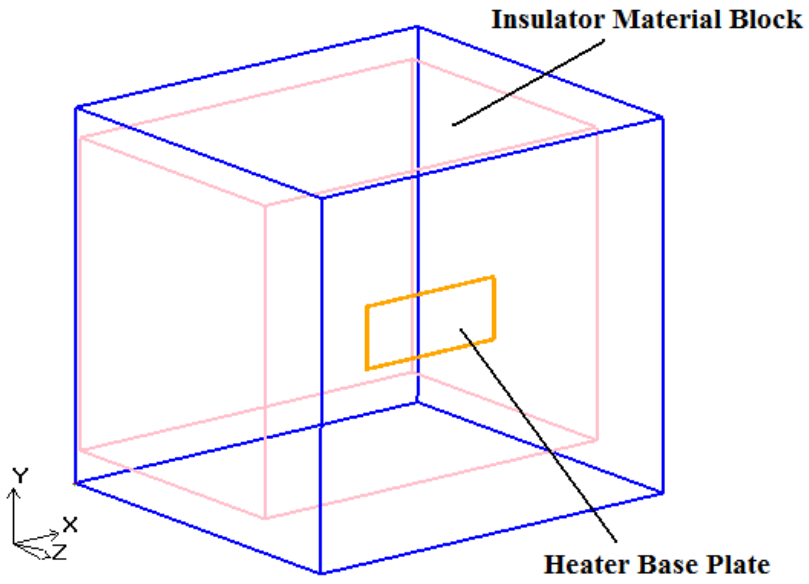

Figure 4.2.1.1 3D view of the model

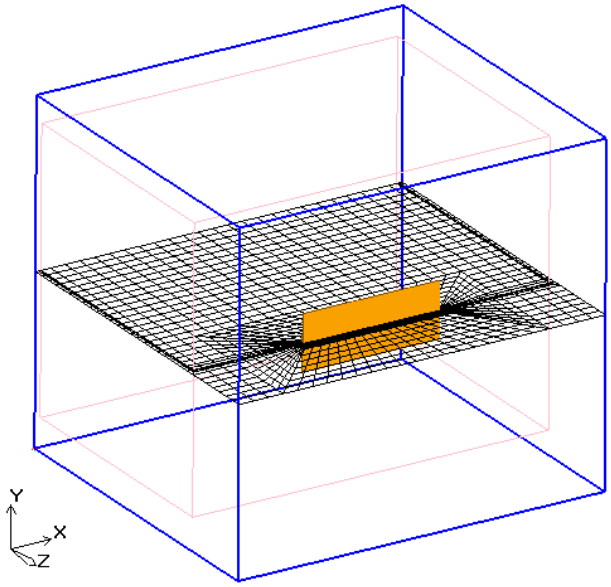

Figure 4.2.1.2 Mesh structure

Different power inputs ranging from 3 W to 48.3 W are supplied to the heater base plate in order to produce heat. The average temperature of the plate and the convection heat transfer from the plate are found from the analyses. It is not possible to obtain convection heat transfer rate directly from analyses. However it is possible to obtain it by subtracting the radiation heat transfer rate value from the total heat transfer rate which are both available from ICEPAK. The tabulated results are given in Table 4.2.1.1. The power input to the base plate is denoted as Q_{in}, average temperature of the plate as T_w and the convection heat transfer as Q_c.

Table 4.2.1.1 Average surface temperature of the plate and convection heat transfer values

Qin(W)	Tw(^{o}C)	Qc(W)
3	28.64	0.9
5	34.10	1.7
6.7	38.73	2.3
8	41.42	2.8
10	46.46	3.6
15	58.16	5.7
20	69.46	7.9
24.7	79.62	9.9
29.7	90.22	12.1
34.7	99.84	14.3
40.6	111.70	17.0
45.6	120.15	18.9
48.3	126.84	20.5

The results obtained from analyses are again compared with the theoretical studies, in order to verify the solution. The required Rayleigh and Nusselt numbers are calculated in a similar way explained in Section 4.1.1. The tabulated results and the comparison of the Nusselt numbers are given in Table 4.2.1.2.

Table 4.2.1.2 Comparison of Nusselt numbers

Ra	Nu				
	Present Study	Churchill and Chu's first relation	Churchill and Chu's second relation	McAdam's relation	Churchill and Usagi's relation
823563	16.40	15.72	16.17	17.77	15.49
1285759	17.89	17.70	17.99	19.87	17.31
1644982	18.66	18.91	19.09	21.13	18.41
1841468	19.87	19.50	19.61	21.73	18.93
2191073	20.56	20.44	20.45	22.70	19.77
2880841	22.06	22.02	21.85	24.31	21.17
3431589	23.02	23.11	22.79	25.39	22.11
3842336	23.75	23.84	23.43	26.12	22.75
4198482	24.31	24.43	23.93	26.71	23.25
4466840	24.99	24.85	24.29	27.12	23.61
4737195	25.36	25.26	24.64	27.53	23.96
4894500	25.64	25.48	24.83	27.75	24.15
5000748	25.74	25.64	24.96	27.90	24.28

It can be inferred from the Table 4.2.1.2 that the results obtained from analyses are consistent with the results obtained from theoretical correlations.

4.2.2 Vertical Two Parallel Flat Plates

Similar to the situation in Case Study 1, the power input to the heater plate is dissipated by means of convection and radiation from fin arrays to the surroundings and by conduction from the base plate to the insulator material. The conduction loss to the insulator material is not known beforehand; therefore once more two parallel flat plates were used in Ref. [2]. Since these two parallel flat plates are placed very close to each other, it is again assumed that heat transfer between them can be calculated by conduction and radiation heat transfer equations. By subtracting this heat transfer between two plates from the total power input to the system, it is possible to find the conduction loss.

In order to verify the model and show that the model matches the experiment, again a similar two parallel plate model is created. Furthermore as it is explained in Chapter 3, in order to simulate the real experiment trial and error method is used to find the conductivity of insulator material. This is needed because the exact mounting of the base plate to insulator material is needed to fully simulate the real experiment. However this information was not presented in Ref. [2].

Dimensions of two parallel plate used in this verification is shown in Figure 4.2.2.1

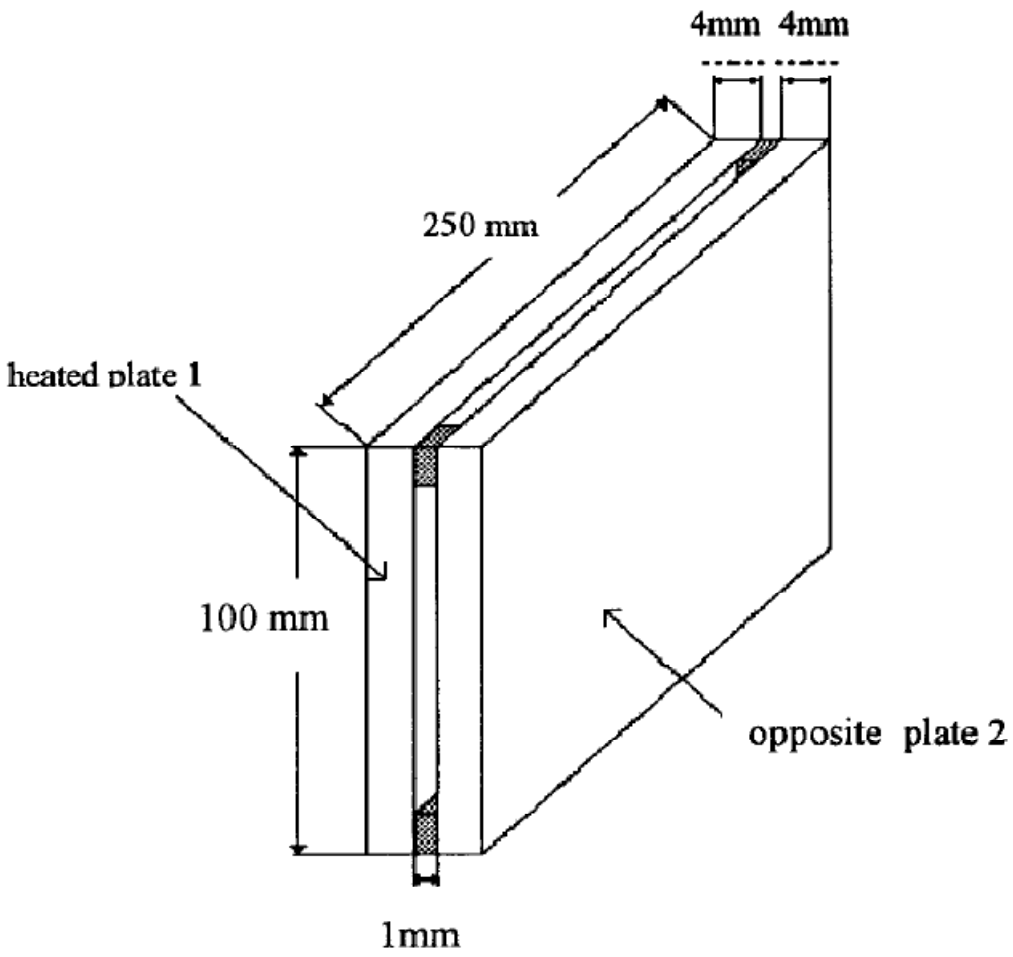

Figure 4.2.2.1 Dimensions of the two parallel plates (from Ref. [2])

The 3D view of the model created for verification is shown Figure 4.2.2.2.

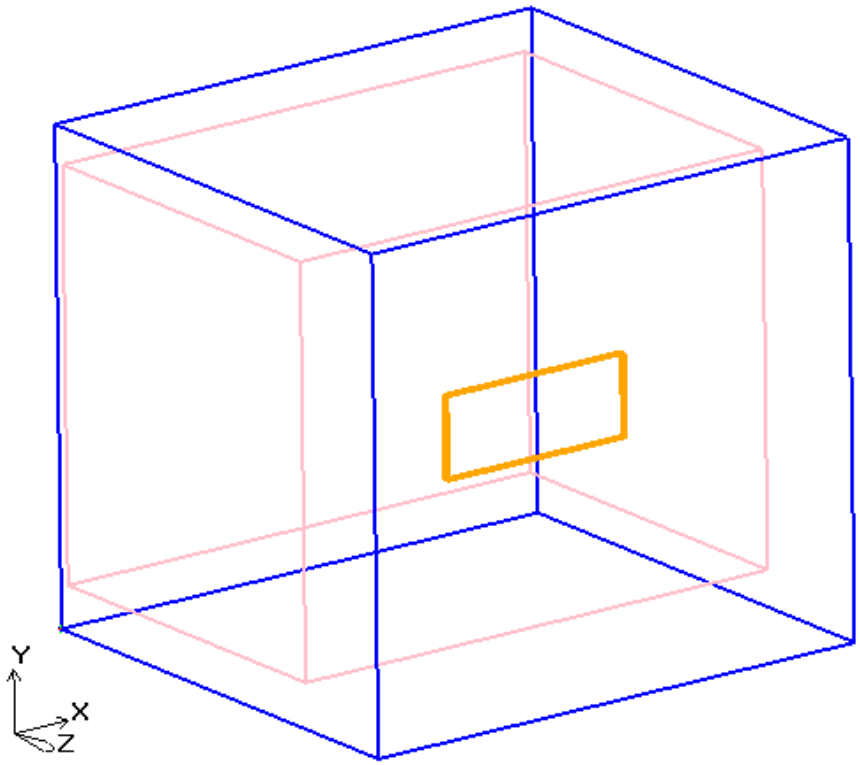

Figure 4.2.2.2 3D View of the model of two parallel plates

The same basic parameters and solution settings explained in Chapter 3 are used for this model. A separate assembly volume is again used to create finer meshes near the plates. Due to its large volume the insulator block is not taken into the assembly volume in order to decrease the mesh size. The mesh structure of the model is shown in Figure 4.2.2.3.

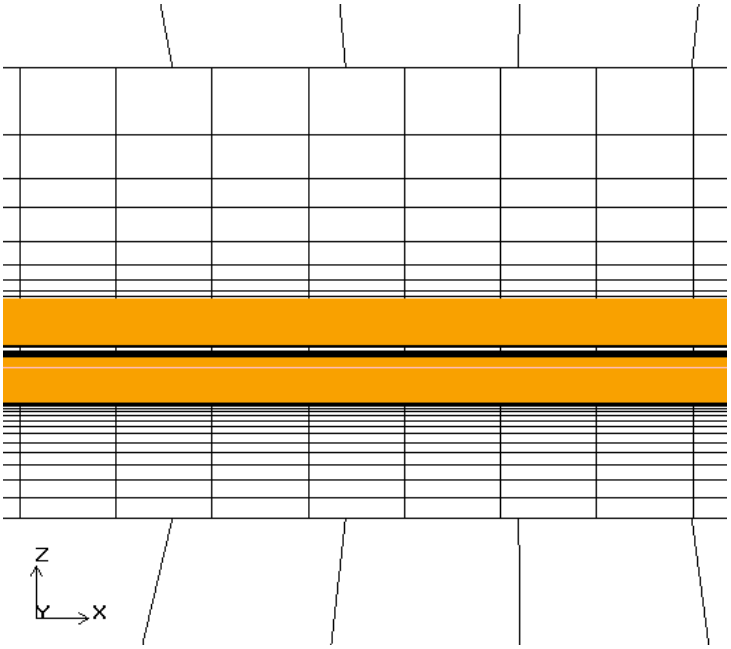

Figure 4.2.2.3 Mesh structure

In order to simulate the experiment setup, 8 different power inputs ranging from 15.1 W to 47.1 W are given to the base plate. The average temperatures of the both plates and the heat transfer rate between two plates are obtained from analyses. The temperature of the bottom plate is denoted as T_1, temperature of the upper plate is denoted as T_2, and the heat flow from the bottom plate to the upper plate is denoted as Q_{out}. The comparison of the ICEPAK results with experiment results is given in Figure 4.2.2.4 to Figure 4.2.2.6.

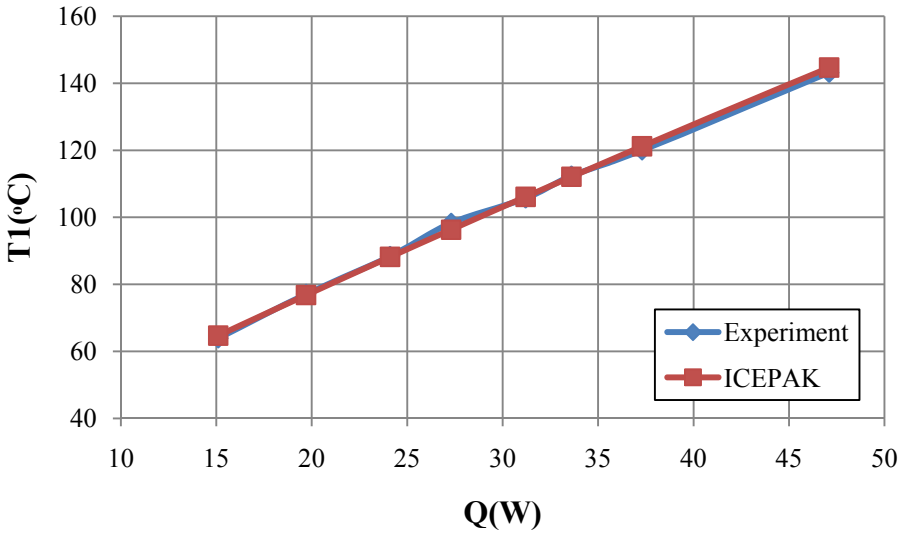

Figure 4.2.2.4 Variation of bottom plate temperature (T_1) with power input to the bottom plate

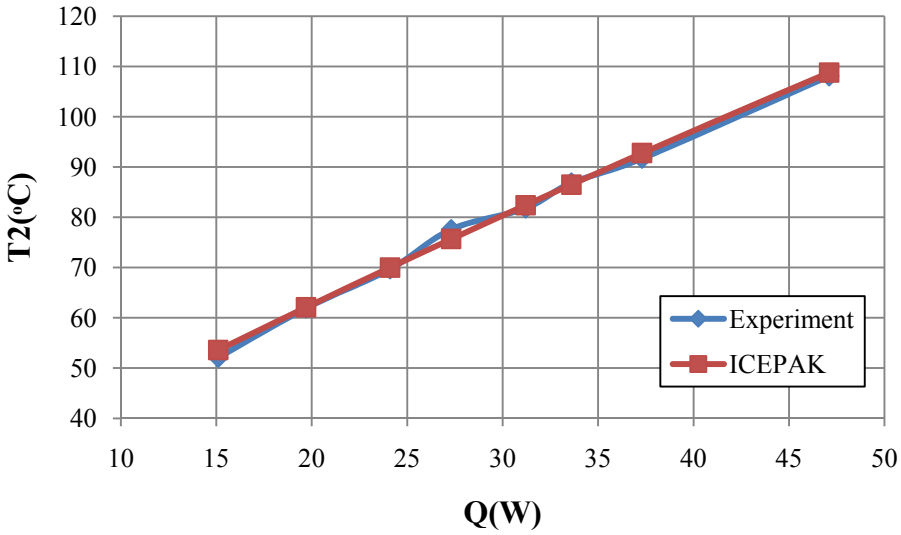

Figure 4.2.2.5 Variation of upper plate temperature (T_2) with power input to the bottom plate

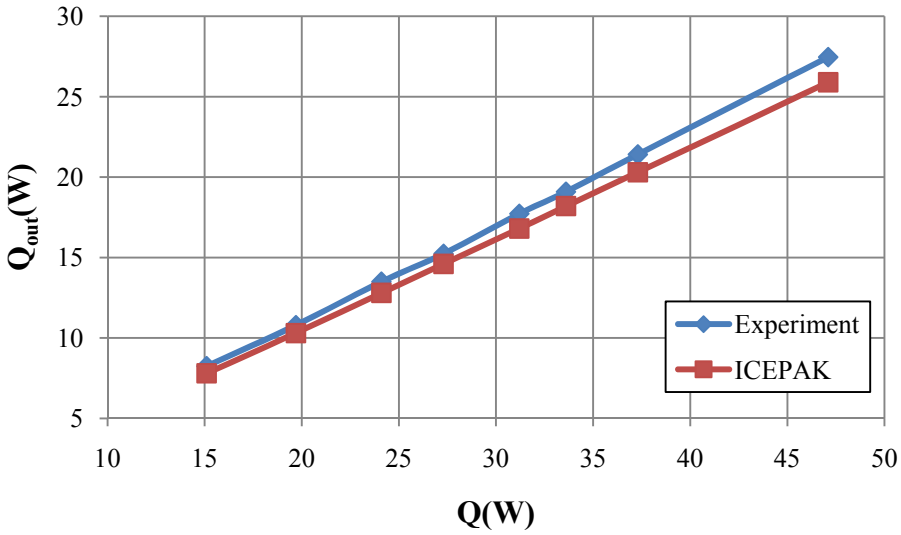

Figure 4.2.2.6 Variation of heat transfer rate from bottom plate to upper plate (Q_{out}) with power input to the bottom plate

It can be observed from the figures that ICEPAK results for the bottom and upper plate temperatures match very well with the experimental results. Although there is a slight difference in the results for heat transfer rate from the bottom plate to the upper plate, they are also very consistent. Therefore it can be concluded that present study model simulates the experiment well.

CHAPTER 5

RESULTS AND DISCUSSION

5.1 Case Study 1

The results obtained from analyses for Case Study 1 are given in this section. In order to compare the results with the experimental results presented in Ref. [1], the same 30 different fin configurations are investigated with 5 different power inputs. These results show the effect of different fin geometry parameters such as fin height H, fin length L, and fin spacing S on the rate of heat dissipation from the fin array under steady state conditions. The figures of only a few selected fin configurations are presented in each section in order to increase the readability of the Chapter. The rest of the plots are given in Appendix E.

5.1.1 Variation of Fin Performance with Fin Spacing, S

The average temperatures of fin arrays are plotted as a function of fin spacing S for fin height H = 25 mm and for fin lengths L = 250 mm and L = 340 respectively in Figure 5.1.1.1 and Figure 5.1.1.2, in order to observe the effect of fin spacing on the temperature of fin arrays. Each figure involves the results obtained for 5 different power inputs, Q_{in} = 25W, Q_{in} = 50W, Q_{in} = 75W, Q_{in} = 100W and Q_{in} = 125W. The rest of the plots for fin heights H =15 and H= 5 mm are given in Appendix E. The experimental results given in Ref. [1] are also plotted in the same figures in order to compare the results.

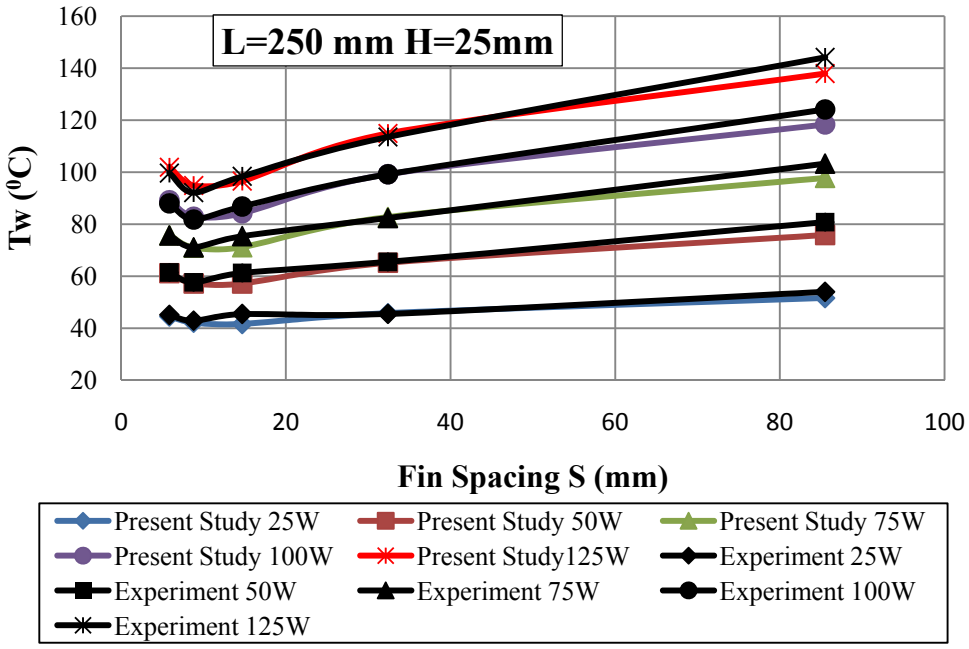

Figure 5.1.1.1 Variation of average fin temperature with fin spacing at fin length of L = 250 mm and at fin height of H = 25 mm

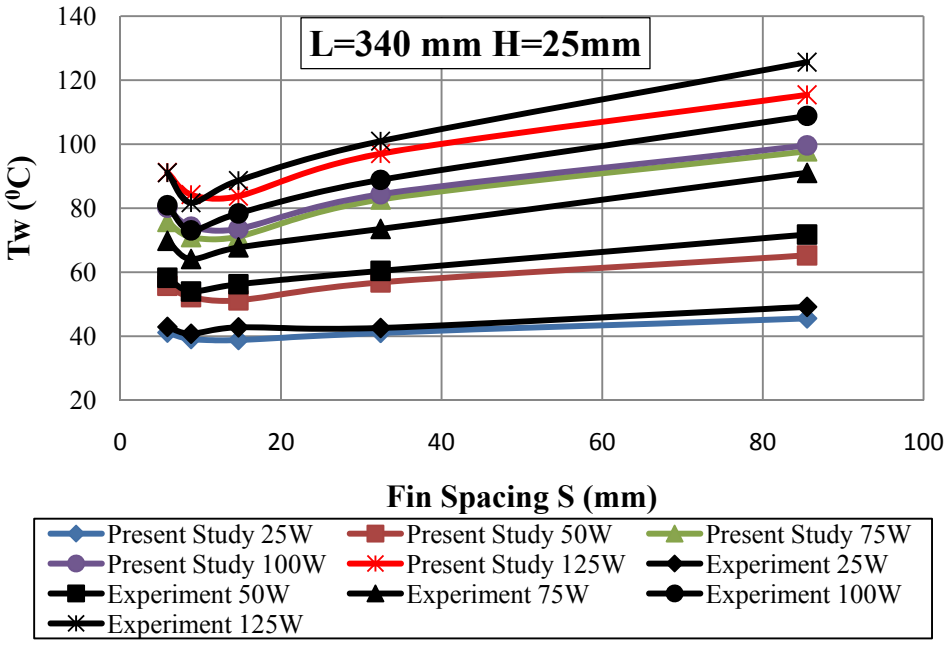

Figure 5.1.1.2 Variation of average fin temperature with fin spacing at fin length of L = 340 mm and at fin height of H = 25 mm

As it can be seen from Figure 5.1.1.1 and Figure 5.1.1.2 , the average temperatures of the fin arrays reached to minima for certain optimum fin spacing values. It can also be observed that when the fin spacing is increased the average temperatures of the fin arrays increase rapidly. Moreover if the fin spacing is decreased from the optimum value, average temperatures of the fin arrays again increase.

In both figures, it can be observed that the experimental results for the average temperatures of the fin arrays given in Ref. [1] are higher than the ICEPAK results. Since the exact details of the experiments are not given, it is impossible to model the experiment exactly. Furthermore the contact resistances are ignored in the analyses. Consequently, although there are some differences between the analyses results and the experiment results, both follow the same trend in figures.

The convection heat transfer rate from the fin arrays are plotted as a function of fin spacing S for fin height, H = 15 mm and for fin lengths L = 250 mm and L = 340 respectively in Figure 5.1.1.3 and Figure 5.1.1.4, in order to find the effect of fin spacing on the heat dissipation rate of fin arrays. Each figure involves the results obtained for 5 different power inputs, Q_{in} = 25W, Q_{in} = 50W, Q_{in} = 75W, Q_{in} = 100W and Q_{in} = 125W. The rest of the plots for fin heights H =25 and H= 5 mm are given in Appendix E. The experimental results given in Ref. [1] are also plotted in the same figures in order to compare the results.

Since ICEPAK only gives the total heat transfer rate and the radiation heat transfer rate, it is not possible to obtain the convection heat transfer rate from the fins directly. Therefore convection heat transfer rate is calculated by subtracting the radiation heat transfer rate from total heat transfer rate from the fin array for each case.

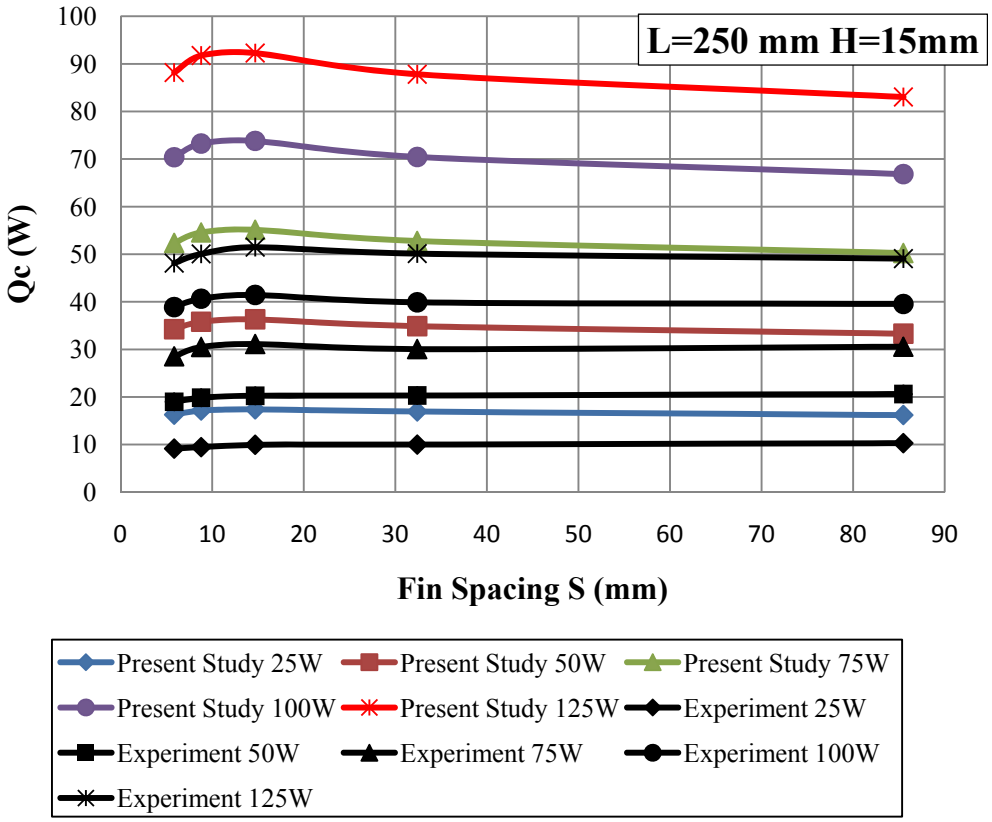

Figure 5.1.1.3 Variation of convection heat transfer with fin Spacing at fin length of L = 250 mm and at fin height of H = 15 mm

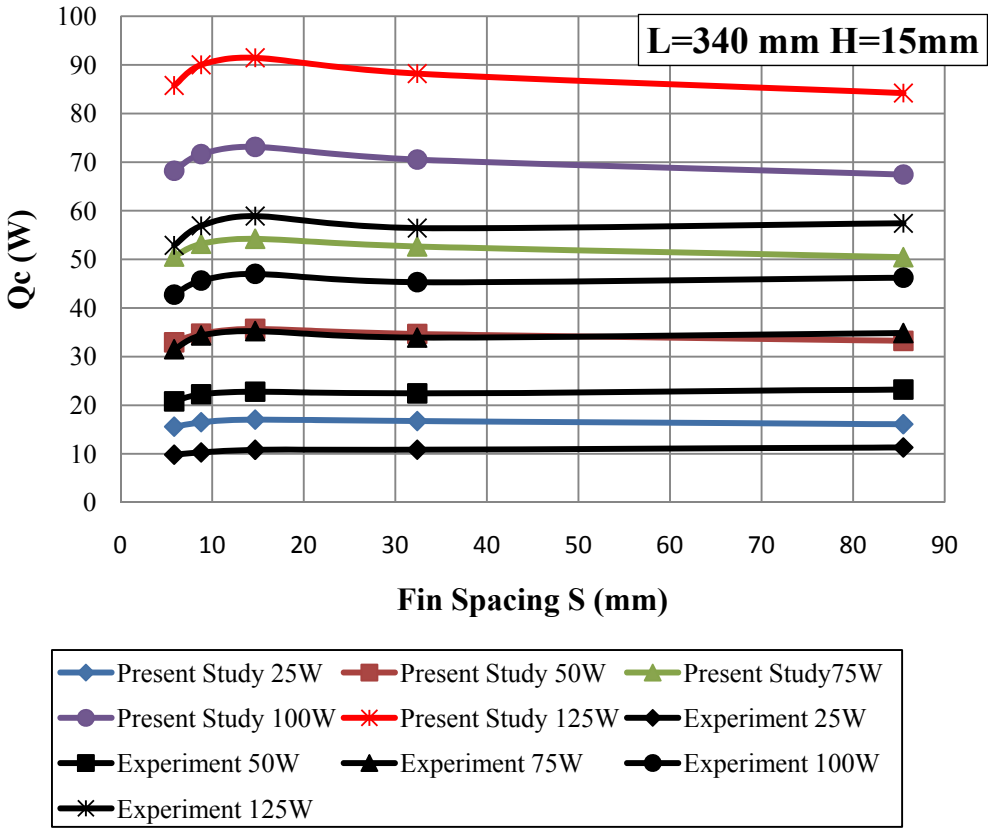

Figure 5.1.1.4 Variation of convection heat transfer with fin spacing at fin length of L = 340 mm and at fin height of H = 15 mm

In both of figures, once more, it can be observed that the experimental results for the convection heat transfer rate from fin the arrays given in Ref. [1] are much higher than the analyses results. This difference is more significant here for the convection heat transfer from fin array than for the average temperature of the fin arrays. Although the model used in present study is verified as explained in Chapter 3, it is still not possible to obtain the same results with the experimental ones. The mounting of the fin arrays on to the heater base plate may be one of the reasons behind the difference in the results. All of the details of the experimental setup are needed to build a very similar CFD model. Therefore with the given limited information in Ref. [1], it is not possible to

obtain exactly the same results. Moreover as it is stated before, the neglected contact resistance may also cause the difference in the results. The thermal contact resistance value is very hard to determine even with experiments.

Although there are significant differences between the experimental and analyses results, both cases show the same trends in the plots. As it can be observed from the Figure 5.1.1.3 and Figure 5.1.1.4, the convection heat transfer rates from the fin arrays reach to maxima for certain optimum fin spacing values. It can also be observed that when the fin spacing is increased from the optimum fin spacing value, the convection heat transfer rate from the fin array decreases. Moreover if the fin spacing is decreased from the optimum value, the convection heat transfer rate from the fin array again decreases.

5.1.2 Optimum Fin Spacing

Both from the experimental and the analyses results, it can be inferred that the optimum fin spacing for the maximum convection heat transfer rate from fins and minimum average temperature of the fin arrays is in the range S = 8.8 mm to S = 14.7 mm. Experiments performed in Ref. [1] do not include any data about the heat dissipation performance of fins for this fin spacing range, because it would be very hard to produce and experiment on every fin configuration that has fin spacing values in the range of 8.8 mm to 14.7 mm. However it is possible to create and analyze every possible fin configuration with CFD modeling. Therefore in order to obtain the missing data in the fin spacing range of 8.8 mm to 14.7 mm, more fin configurations which have fin spacing values of S = 9.64 mm , S = 10.62 mm, S = 11.75 and S = 13.09 mm are modeled in ICEPAK with number of fins N = 15, N = 14, N = 13 and N = 12 respectively.

The average temperatures of fin arrays in the range of S = 8.8 mm to S = 14.7 are plotted as a function of fin spacing S for power input, Q_{in} = 25W and for fin

length L = 340 in Figure 5.1.2.1 in order to find the optimum fin spacing value more precisely. Figure involves the results obtained for 3 fin heights H = 25 mm, H = 15 mm and H = 5 mm. The rest of the plots for power inputs Q_{in} = 75 W, Q_{in} = 125 W are given in Appendix E.

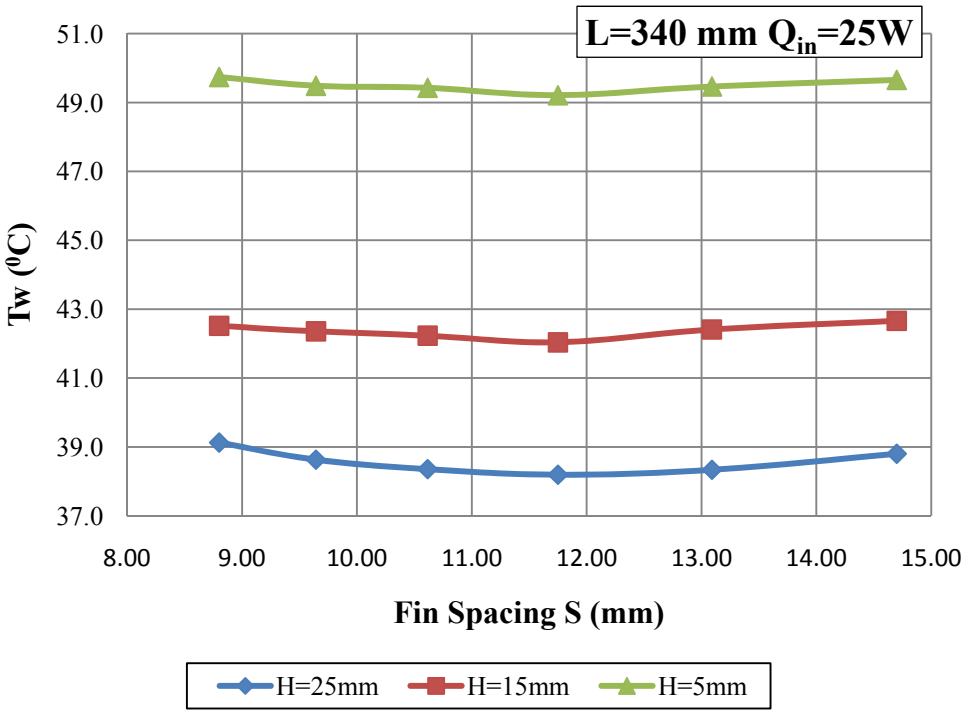

Figure 5.1.2.1 Variation of average fin temperature with fin spacing at fin length of L = 340 mm and at power input of Q_{in} = 25 W

The convection heat transfer rate from the fin arrays in the range of S = 8.8 mm to S = 14.7 are plotted as a function of the fin spacing S for power input, Q_{in} = 125W and for fin length L = 340 in Figure 5.1.2.2. The figure involves the results obtained for 3 different fin heights H = 25 mm, H = 15 mm and H= 5 mm. The rest of the plots for power inputs Q_{in} = 25 W, Q_{in} = 75 W are given in Appendix E.

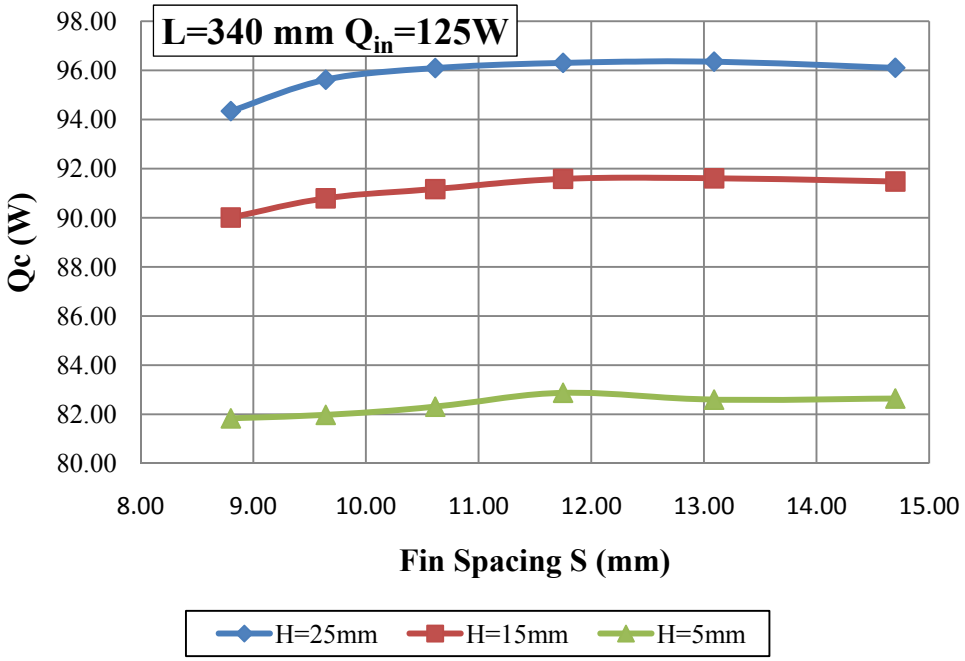

Figure 5.1.2.2 Variation of convection heat transfer rate with fin spacing at fin length of L = 340 mm and at power input of Q_{in} = 125 W

It can be inferred from the plots that there is indeed an optimum fin spacing where the fin average temperature reaches to minima and the convection heat transfer rate reaches to maxima. However it can also be observed that the optimum spacing value for the minimum fin average temperature and the optimum spacing value for the maximum convection heat transfer rate are different. In order to find these optimum fin spacing values, a polynomial curve is fitted to each data. A sample calculation is given below to find the optimum fin spacing value to maximize convection heat transfer rate the fin configuration with fin length L = 340 mm, fin height H = 25 mm and power input Q_{in} = 125 W.

The second order polynomial curve fit is found as:

$$Q_c(s) = -0.1303 \cdot s^2 + 3.2574 \cdot s + 75.574$$

Maximum value of Qc can be found taking the derivative of Qc and setting it equal to 0.

$$\frac{dQ_c}{ds} = -0.2606 \cdot s + 3.2574$$

$$\frac{dQ_c}{ds} = 0 \quad \rightarrow \quad -0.2606 \cdot s + 3.2574 = 0 \quad \rightarrow \quad s_{opt} \cong 12.5 \text{ mm}$$

The same procedure is followed and the optimum fin spacing values are found in a similar fashion. The optimum fin spacing values for minimizing the average fin temperature are given in Table 5.1.2.1.

Table 5.1.2.1 Optimum fin spacing values for minimizing average temperature of fin arrays

Q_{in} (W)	Optimum Fin Spacing, Sopt (mm)					
	H = 25 mm		H = 15 mm		H = 5 mm	
	L = 250 mm	L =340 mm	L = 250 mm	L =340 mm	L = 250 mm	L =340 mm
25	11.5	12.1	11.5	11.5	11.8	11.7
75	11.7	12	11.2	11.7	11.7	11.7
125	11.7	11.7	11.2	11.7	11.8	11.6

The optimum fin spacing values for maximizing the convection heat transfer rates from fin arrays are tabulated in Table 5.1.2.2.

Table 5.1.2.2 Optimum fin spacing values for maximizing convection heat transfer rate from fin arrays

Q_{in} (W)	Optimum Fin Spacing, Sopt (mm)					
	H = 25 mm		H = 15 mm		H = 5 mm	
	L = 250 mm	L =340 mm	L = 250 mm	L =340 mm	L = 250 mm	L =340 mm
25	12.2	12.7	12	12.4	11.9	12.1
75	11.9	12.5	11.9	12.5	11.8	12
125	11.6	12.5	11.9	12.4	11.8	12

The differences between these two tables are due to changing view factors with fin spacing and related changes in radiation heat losses. For comparison the optimum fin spacing values obtained in Ref. [1] are tabulated in Table 5.1.2.3.

Table 5.1.2.3 Optimum fin spacing values (from Ref. [1])

ΔT(K)	Optimum Fin Spacing, Sopt (mm)					
	H = 25 mm		H = 15 mm		H = 5 mm	
	L = 250 mm	L =340 mm	L = 250 mm	L =340 mm	L = 250 mm	L =340 mm
50	11	11.9	10.9	11.8	-	-
75	10.9	11.8	10.8	11.7	10.7	11.6
100	10.8	11.7	10.7	11.6	10.6	11.5
125	10.7	11.6	10.6	11.4	10.5	11.4
150	-	-	-	-	10.4	11.3

5.1.3 Variation of Fin Performance with Fin Height, H

The convection heat transfer rate from the fin arrays are plotted as a function of fin height, H for 3 different fin spacing S = 32.4 mm and for fin lengths L = 250 mm and L = 340 respectively in Figure 5.1.3.1 and Figure 5.1.3.2. Both figure involves the results obtained for 5 different power inputs, Q_{in} = 25 W, Q_{in} = 50W, Q_{in} = 75W, Q_{in} = 100W and Q_{in} = 125W. The figures for fin spacing S = 14.7 mm and S = 8.8 mm are given in Appendix E.

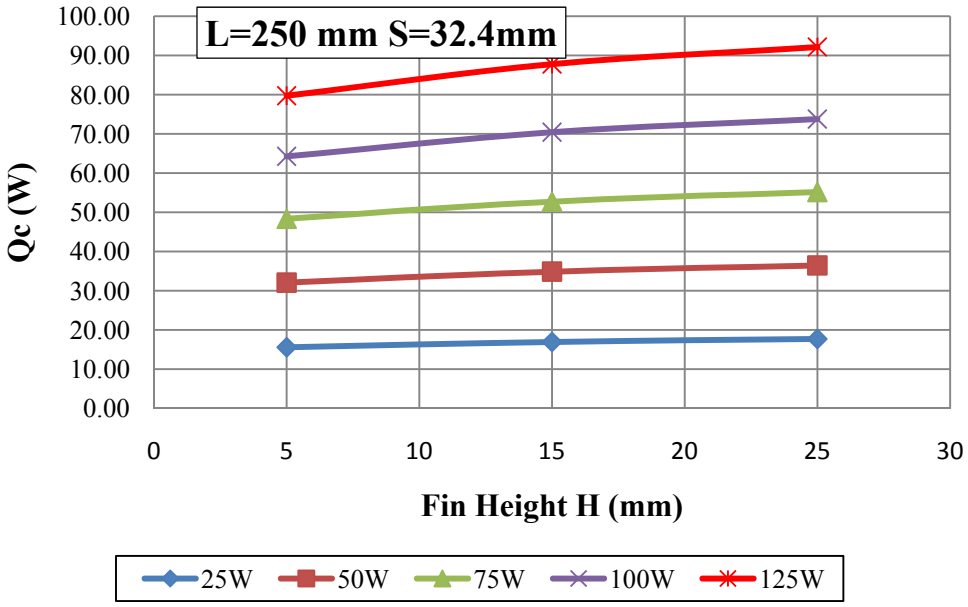

Figure 5.1.3.1 Variation of convection heat transfer with fin height at fin length of L = 250 mm and at fin spacing of S = 32.4 mm

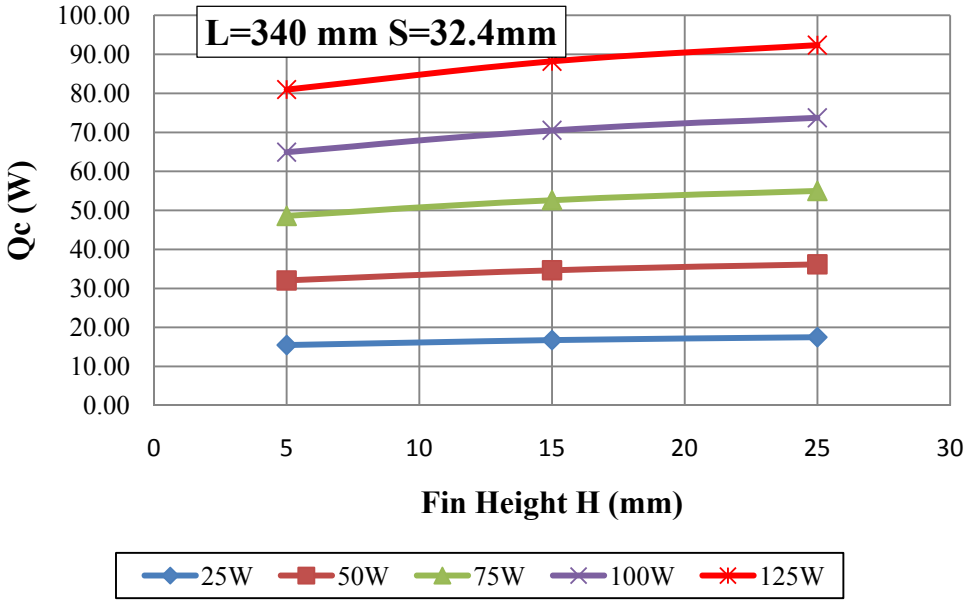

Figure 5.1.3.2 Variation of convection heat transfer with fin height at fin length of L = 340 mm and at fin spacing of S = 32.4 mm

It can be observed from the plots that for every power input, fin spacing and fin length combination, the convection heat transfer rate from the fin array increases with the increase in the fin height. With an increase in fin height, the total heat dissipation area also increases. Since the convection heat transfer rate directly related to the surface area in contact with air, increasing fin height increases the total heat dissipation.

5.2 Case Study 2

The results obtained from the analyses for Case Study 2 are given in this section. In order to compare the results with the experiment results presented in Ref. [2], the same 15 different fin configurations are investigated with 5 different power inputs. These results show the effect of fin spacing S on the rate of heat dissipation from the fin array under steady state conditions. Similar to Section 5.1, the figures of only a few selected fin configurations are presented in each sub-section in order to increase the readability of the Chapter. The rest of the plots are given in Appendix E.

5.2.1 Variation of Fin Performance with Fin Spacing, S

The average temperatures of the fin arrays are plotted as a function of fin spacing S for fin height H = 25 mm in Figure 5.2.1.1 in order to find the effect of fin spacing on the temperature of fin arrays. The figure involves the results obtained for 5 different power inputs, Q_{in} = 10 W, Q_{in} = 20W, Q_{in} = 30 W, Q_{in} = 40 W and Q_{in} = 50 W. The experimental results given in Ref. [2] are also plotted in the same figures in order to compare the results. The rest of the figures for fin heights H = 15 mm and H = 5 mm are given in Appendix E.

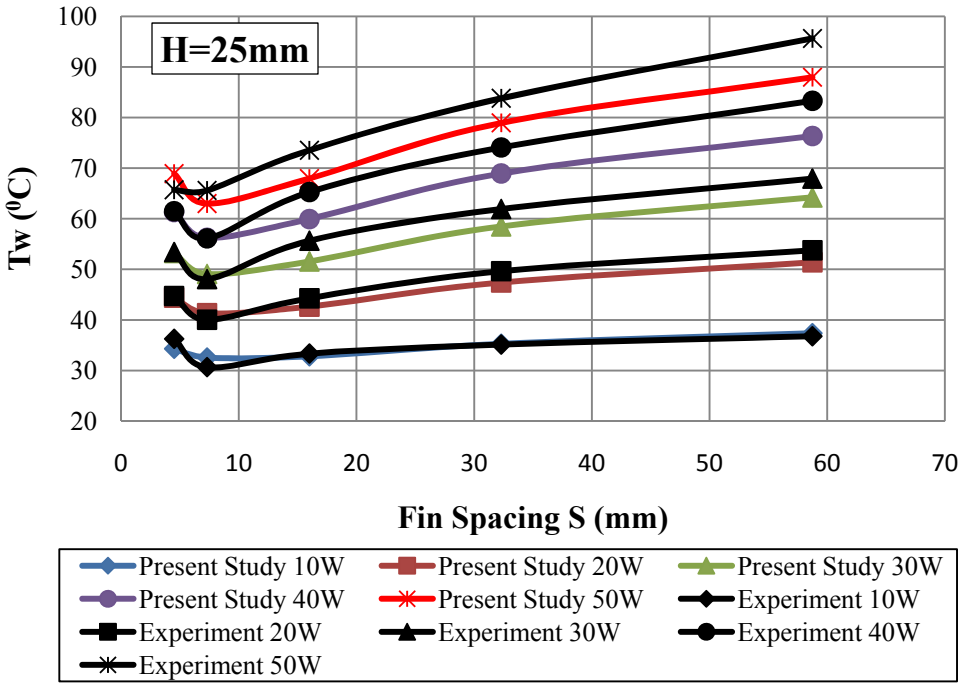

Figure 5.2.1.1 Variation of average fin temperature with fin spacing at fin height of H = 25 mm

As already encountered in Case Study 1; figures show that, the average temperatures of the fin arrays reach to minima for certain optimum fin spacing values. It can also be observed that the results found from analyses and experiment conducted in Ref. [2] show similar trends. However it can be noticed from the figure that average fin temperatures measured by experiment are higher than the ones obtained by ICEPAK. This difference is again due to lack of mounting details of the fin arrays to the heater bottom plate.

The convection heat transfer rates from the fin array are plotted as a function of fin spacing S for fin height H = 25 mm in Figure 5.2.1.2 in order to find the effect of fin spacing on the heat dissipation rate of fin arrays. The figure involves the results obtained for 5 different power inputs, Q_{in} = 10W, Q_{in} = 20W, Q_{in} = 30W, Q_{in} = 40W and Q_{in} = 50W. The experimental results are

again also plotted in the same figure comparison. The rest of the figures for fin heights H = 15 mm and H = 5 mm are given in Appendix E.

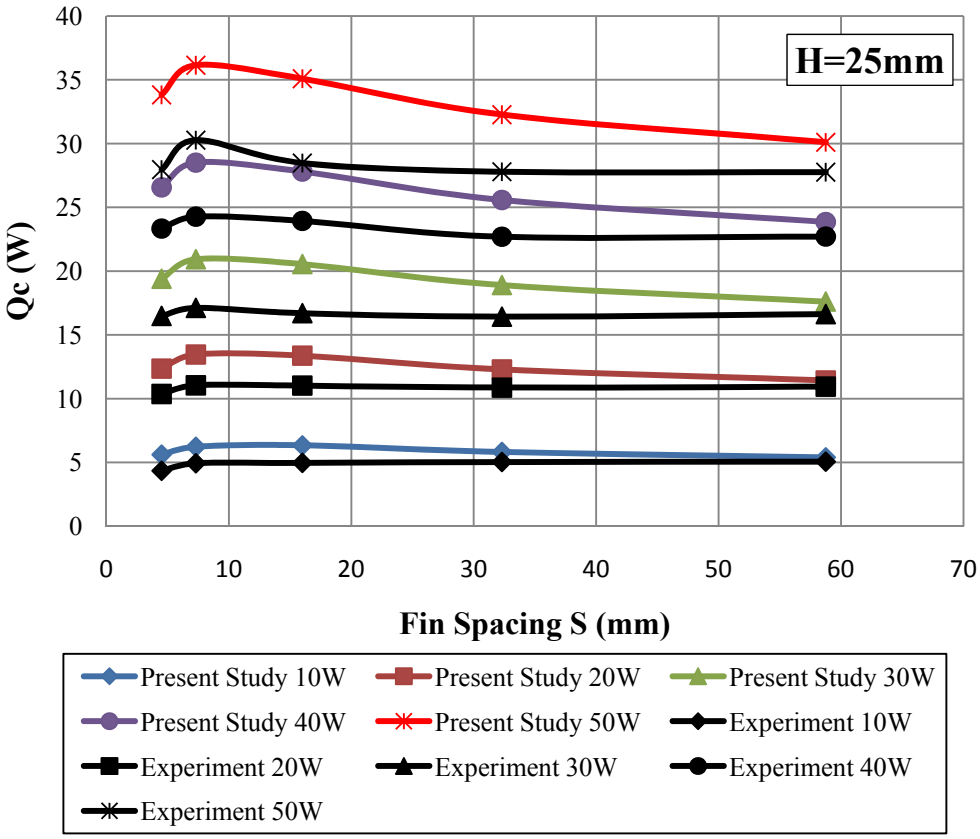

Figure 5.2.1.2 Variation of convection heat transfer with fin spacing at fin height of H = 25 mm

In a similar way for Case Study 1, it can be seen that the convection heat transfer rate from fin array reaches to maxima for certain optimum fin spacing values. If fin spacing is increased or decreased from this optimum value, the convection heat transfer rate from the fin array deceases.

Once more, it can also be observed from the graphs that the convection heat transfer results obtained from analyses are higher than the experimental results. Same reasons mentioned before for Case Study 1 are also valid here.

5.2.2 Optimum Fin Spacing

It can be inferred from both the experimental and analyses results that there is an optimum fin spacing value where while average temperature of the fin array reaches to a minimum and the convection heat transfer from fin array reaches to a maximum. According to the plots this optimum fin spacing value is between S = 4.5 mm and S = 16 mm. The information about the performance of the fin array for this fin spacing range was not sufficient in the experimental study. The reason is that in order to get the experimental data for these missing fin spacing values, many more fin arrays must be produced and experimented on making the whole experiment very hard and expensive. On the other hand it is possible to create and analyze every possible fin configuration with the help of ICEPAK easily and quickly. Therefore in order to find the optimum fin spacing value in the range of 4.5 mm to 16 mm, more fin configurations which have fin spacing values of S = 6.2 mm, S = 8.8 mm, S = 10 mm, S = 11.5 and S = 13.5 mm are modeled in ICEPAK with number of fins N = 16, N = 18, N = 20, N = 22 and N = 28 respectively.

The average temperatures of fin arrays in the range of S = 4.5 mm to S = 16 are plotted as a function of fin spacing S for power input, Q_{in} = 30 W, in Figure 5.2.2.1, in order to find the optimum fin spacing value more precisely. Each figure involves the results obtained for 3 different fin heights H = 25 mm, H = 15 mm and H = 5 mm. The figures for power inputs, Q_{in} = 40 W and Q_{in} = 50 W are given in Appendix E. Higher power inputs are selected for plots since it is easier to see the effect of fin spacing for high power inputs to the heater plate.

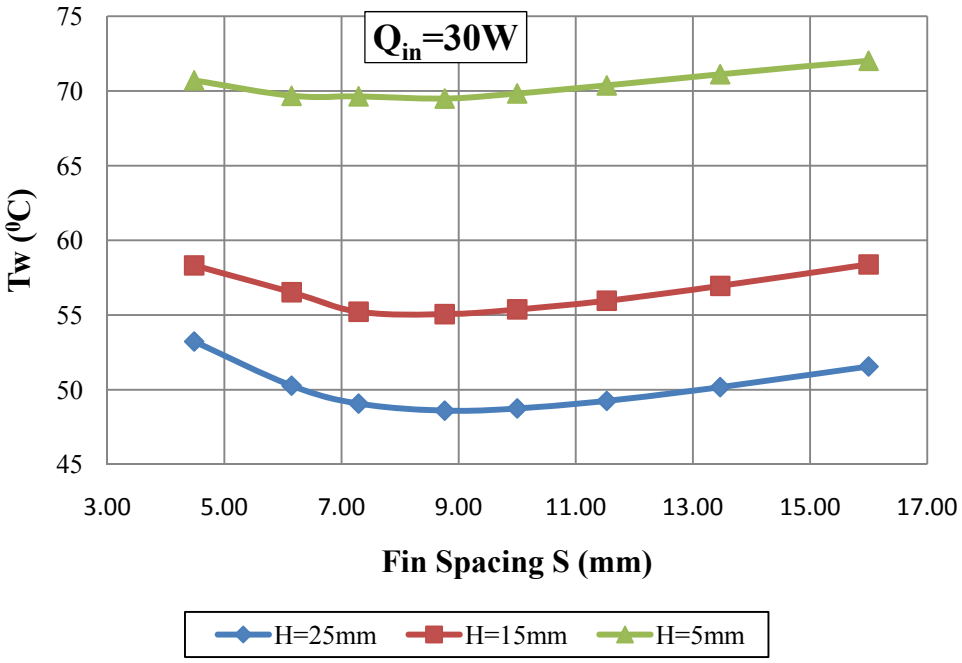

Figure 5.2.2.1 Variation of average fin temperature with fin spacing at power input of Q_{in} = 30 W

The convection heat transfer from the fin arrays in the range of S = 4.5 mm to S = 16 mm are plotted as a function of fin spacing S for power input, Q_{in} = 30W in. Each figure involves the results obtained for 3 different fin heights H = 25 mm, H = 15 mm and H= 5 mm. The figures for power inputs, Q_{in} = 40 W and Q_{in} = 50 W are again given in Appendix E.

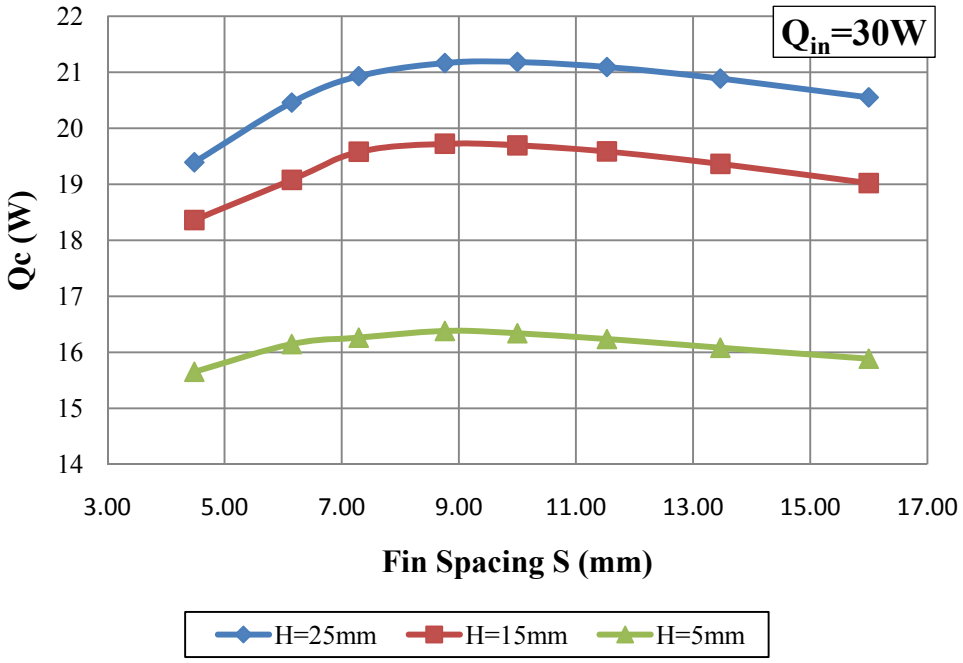

Figure 5.2.2.2 Variation of convection heat transfer with fin spacing at power input of Q_{in} = 30 W

It can be inferred from the figures that the optimum fin spacing value is around 9 mm. However it can also be observed that the optimum fin spacing value is different for minimizing the average fin temperature and for maximizing the convection heat transfer from fins. The more precise optimum fin spacing values are found using a similar polynomial curve fit method which is done for Case Study 1. The optimum fin spacing values which minimize the average temperature of fin arrays are tabulated in Table 5.2.2.1.

Table 5.2.2.1 Optimum fin spacing values for minimizing average temperature of fin arrays

Q_{in} (W)	Optimum Fin Spacing, Sopt (mm)		
	H = 25 mm	H = 15 mm	H = 5 mm
30	9.0	8.5	8.8
40	9.1	8.5	8.5
50	9.0	8.5	8.5

The optimum fin spacing values which maximize the convection heat transfer rate from fin arrays are tabulated in Table 5.2.2.2.

Table 5.2.2.2 Optimum fin spacing values for maximizing convection heat transfer from fin arrays

Q_{in} (W)	Optimum Fin Spacing, Sopt (mm)		
	H = 25 mm	H = 15 mm	H = 5 mm
30	9.2	9.1	9.0
40	9.1	9.0	8.9
50	9.0	8.8	8.9

For comparison the optimum fin spacing values obtained in Ref. [2] are tabulated in Table 5.2.2.3.

Table 5.2.2.3 Optimum fin spacing values (from Ref. [2])

$\Delta T(K)$	Optimum Fin Spacing, Sopt (mm)		
	H = 25 mm	H = 15 mm	H = 5 mm
30	7.3	7.8	-
40	6.8	7.5	6.8
50	6.1	7.2	6.3
50	6.5	6.6	6.5

CHAPTER 6

FLOW VISUALIZATION

One of the most useful advantages of CFD is its ability to visualize the flow easily. In this section the variation of temperature and velocity of the flow with different parameters investigated in the previous Chapter is presented by the help of CFD visualization. Since there are many different fin array configurations investigated in this study, it is not possible to show variation of flow speed and temperature for every fin configuration. Therefore only one fin configuration is selected to represent every visualization figure.

6.1 Variation of Flow Speed with Power Input

In order to show the variation of flow speed with power input to the heater base plate, the following fin configuration from the Case Study 1 is used:

- Fin length, L = 250 mm
- Fin height, H = 25 mm
- Fin spacing, S = 14.7 mm

Speed contours of the flow for three different power inputs to the heater base plate, Q_{in} = 25W, Q_{in} = 50 W and Q_{in} = 125 W are shown in Figure 6.1.1 to Figure 6.1.3 respectively. The speed scale is same for all the figures.

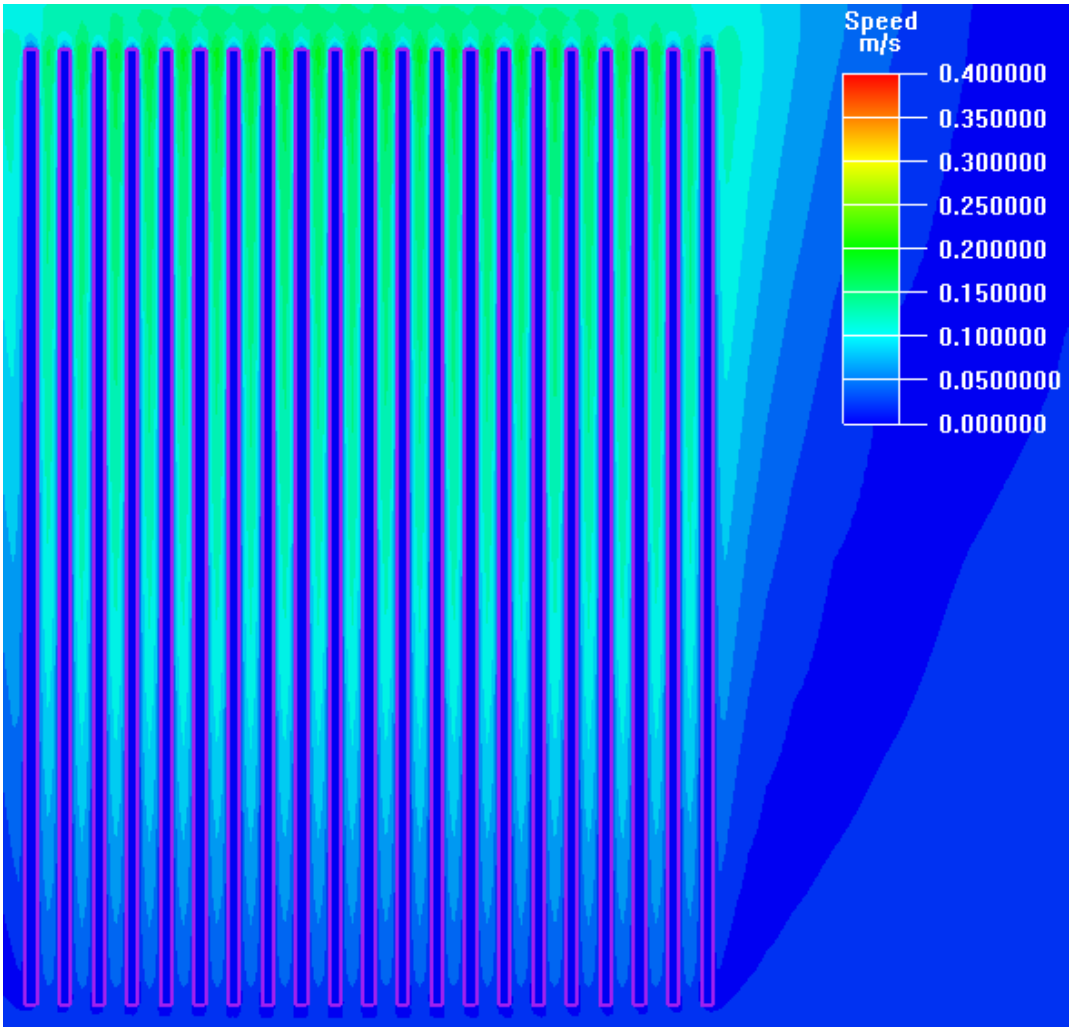

Figure 6.1.1 Speed contours for power input Q_{in} = 25 W

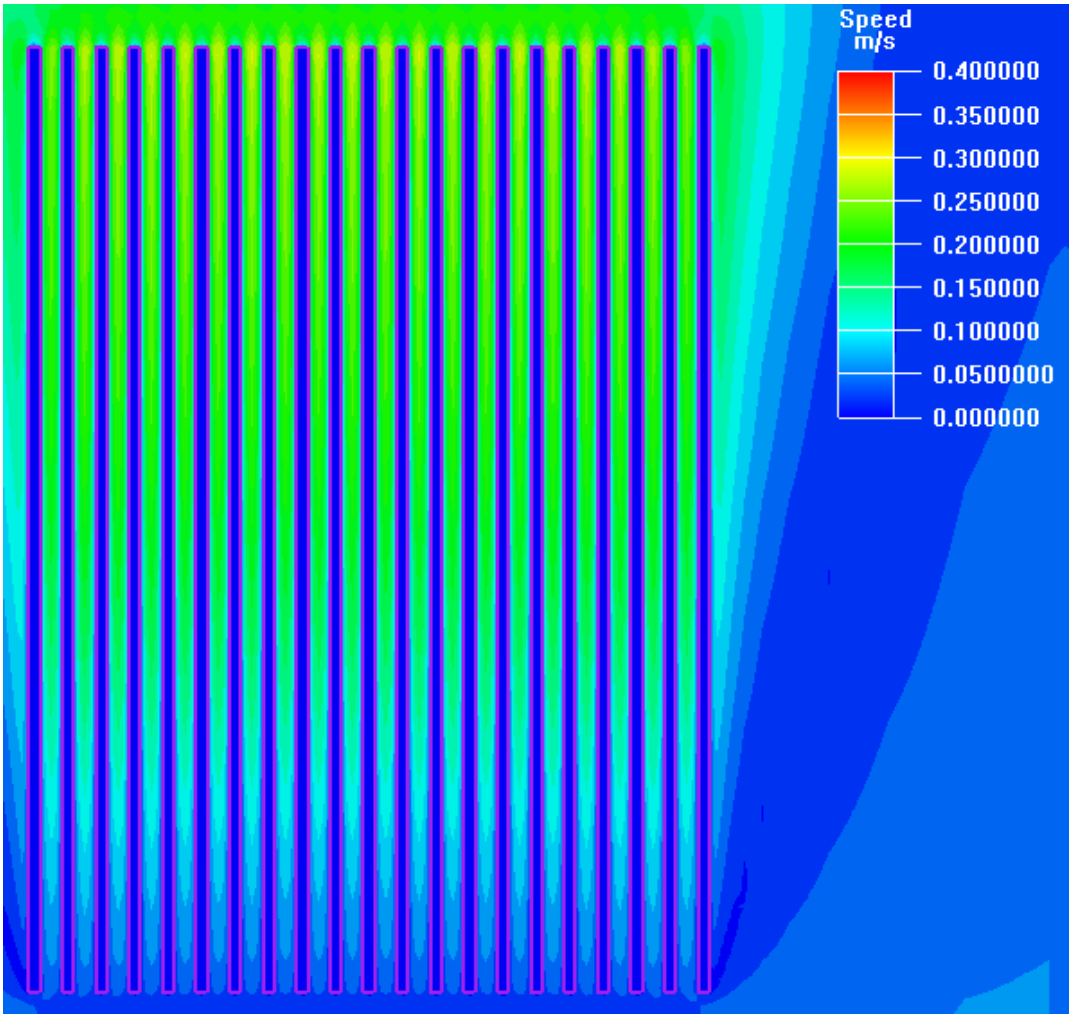

Figure 6.1.2 Speed contours for power input Q_{in} = 75 W

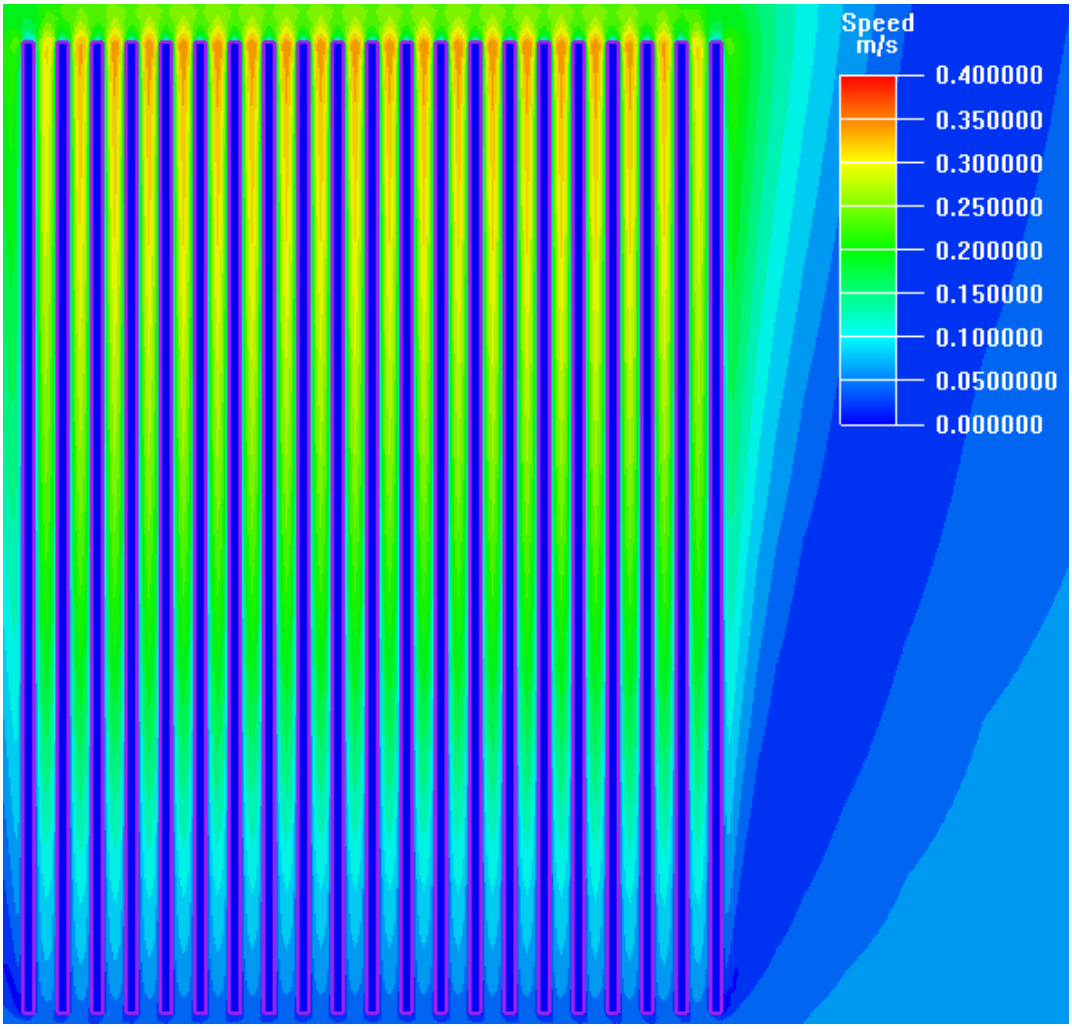

Figure 6.1.3 Speed contours for power input Q_{in} = 125 W

It can be seen from the figures that the speed of the flow increases with the power input to the plate. The maximum velocities are obtained as 0.25 m/s, 0.31 m/s and 0.36 m/s for heat inputs Q_{in} = 25 W, 75 W and 125 W respectively. This is an expected result because the higher power input causes higher air temperature near to the fins. Since in natural convection the air moves because of the difference in density, higher temperature will increase the difference of density in air. Thus the flow speed will be higher.

6.2 Variation of Flow Temperature with Fin Height

In order to show the variation of flow temperature with fin height, the following fin configuration from the Case Study 1 is used:

- Fin length, L = 340 mm
- Fin spacing, S = 13.1 mm
- Power input, Q_{in} = 25 W

Temperature contours of the flow for three different fin heights H = 25 mm, H = 15 mm and H = 5 mm are shown in Figure 6.2.1 to Figure 6.2.3 respectively. The temperature scale is same for all the figures.

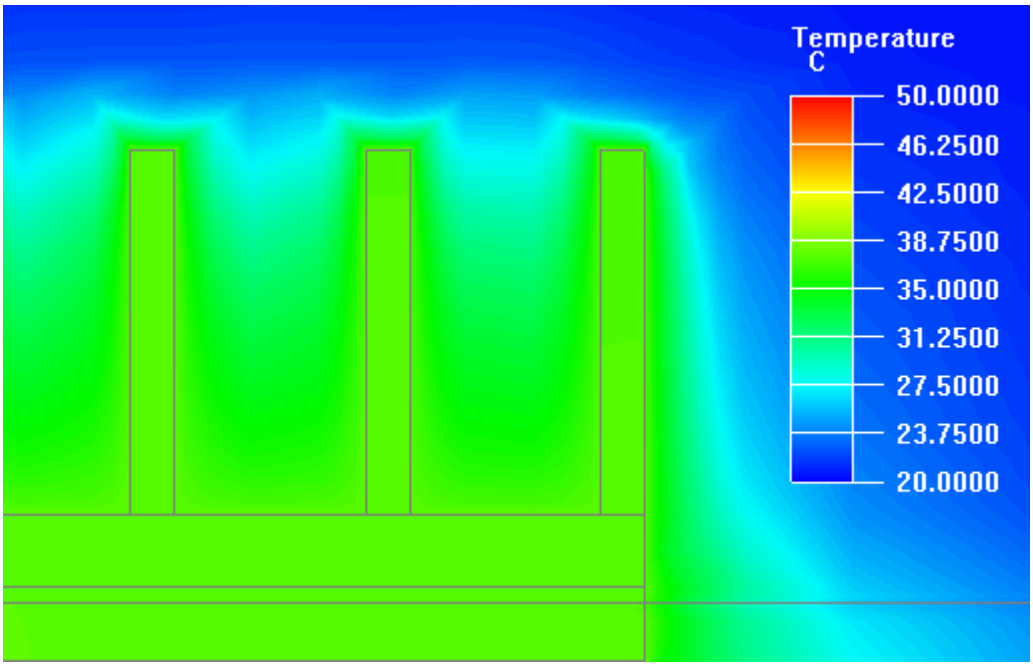

Figure 6.2.1 Temperature contours for fin height H = 25 mm

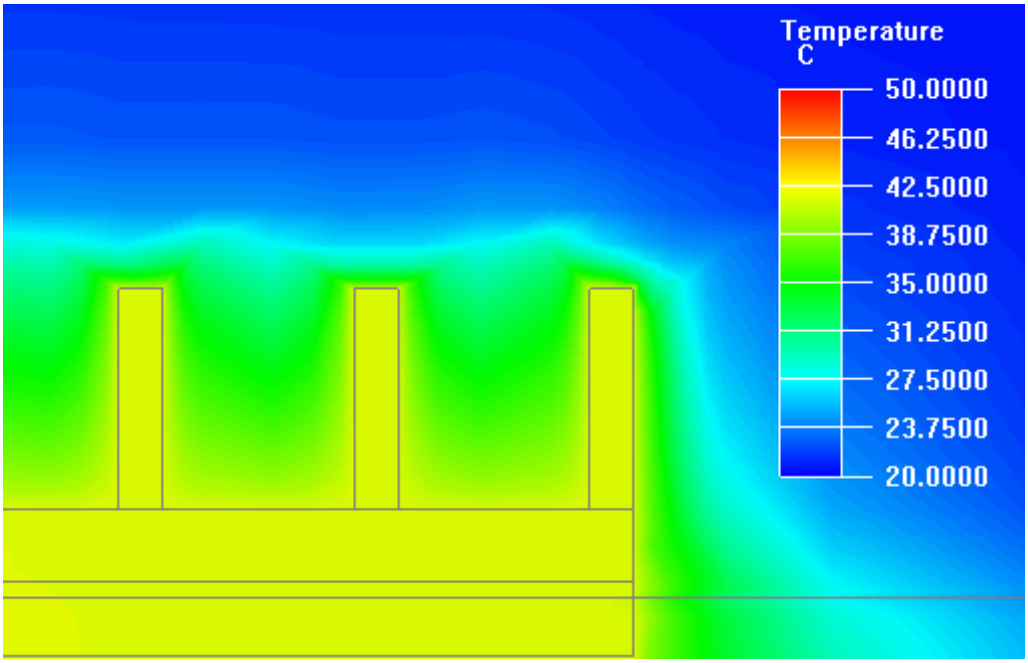

Figure 6.2.2 Temperature contours for fin height H = 15 mm

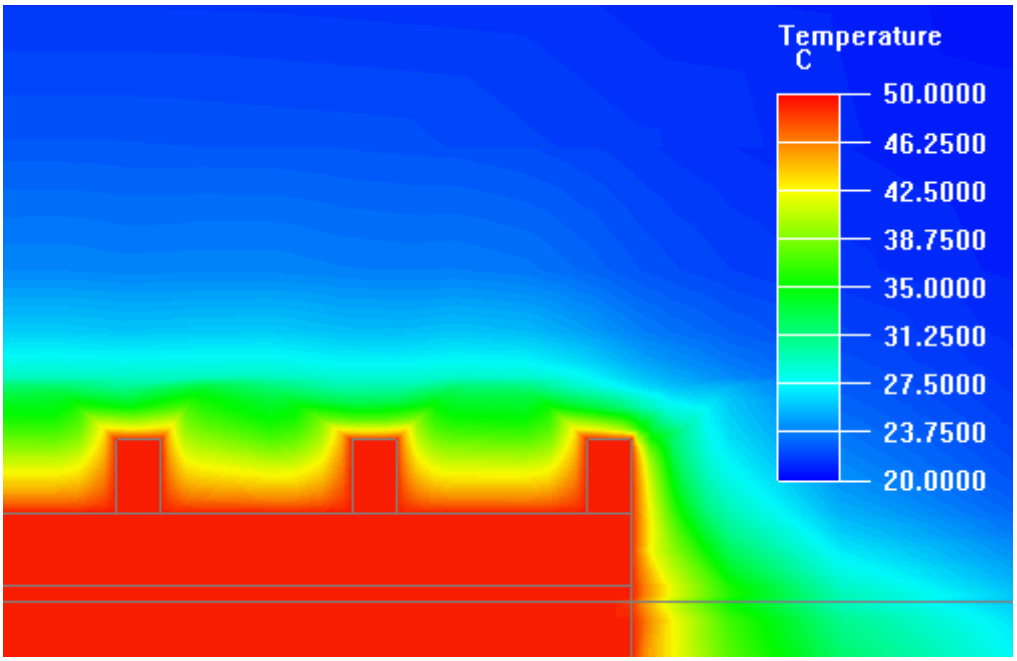

Figure 6.2.3 Temperature contours for fin height H = 5 mm

From the figures it can be observed that the fin configuration with the highest fin height that is H = 25 mm dissipates more heat energy to the air then the others even though the power input to the plates are same. Heat transfer from the fins to the air is directly proportional to the surface area of the fins. Besides an increase in fin height means an increase in surface area as well. Thus that is the reason why more heat is transferred to air for higher fin height values.

6.3 Variation of Flow Speed with Fin Spacing

The following fin configuration from the Case Study 2 is used in order to show the variation of flow speed with fin spacing:

- Fin length, L = 100 mm
- Fin height, H = 25 mm
- Power input, Q_{in} = 50 W

Speed contours of the flow for three different fin spacing values, S = 16 mm, S = 7.3 mm and S = 4.5 mm are shown in Figure 6.3.1 to Figure 6.3.3 respectively. The speed scale is same for all the figures.

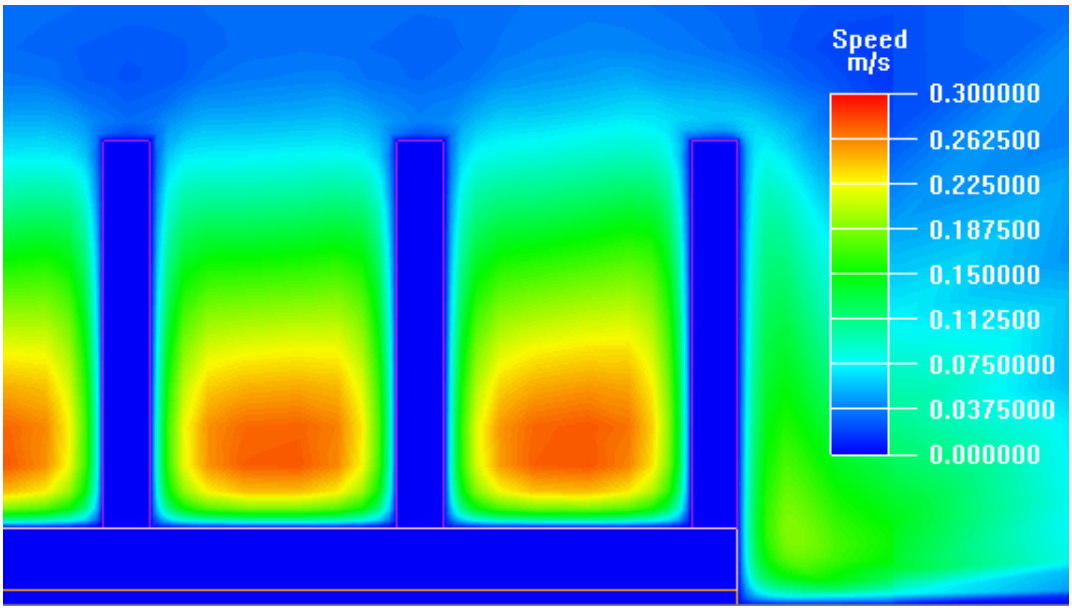

Figure 6.3.1 Speed contours for fin spacing S = 16 mm

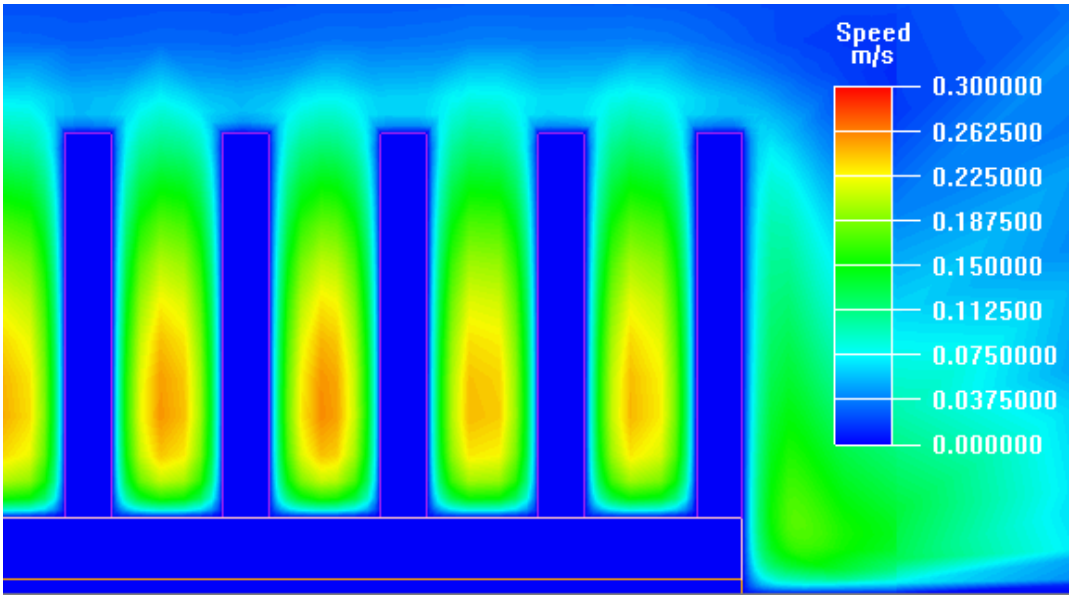

Figure 6.3.2 Speed contours for fin spacing S = 7.3 mm

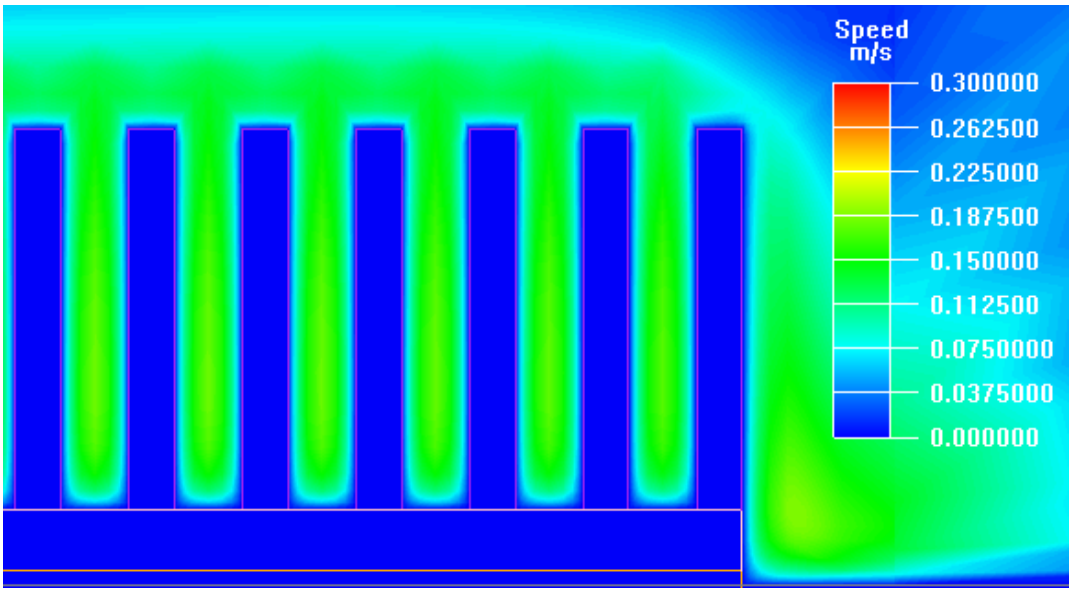

Figure 6.3.3 Speed contours for fin spacing S = 4.5 mm

It can be observed from the figures that the flow speed through fin channels decreases when fin spacing is increased. Boundary layers which are formed on the sides of fins begin to close the channel, thus decreasing the flow speed across the channel.

6.4 Variation of Flow Speed with Fin Height

In order to show the variation of flow speed with fin height, the following fin configuration from the Case Study 2 is used:

- Fin length, L = 100 mm
- Fin spacing, S = 10 mm
- Power input, Q_{in} = 50 W

Velocity vectors of the flow for three different fin height values, H = 25 mm, S = 15 mm and H = 5 mm are shown in Figure 6.4.1 to Figure 6.4.3 Figure 6.3.3 respectively. The velocity scale is kept same for all the figures.

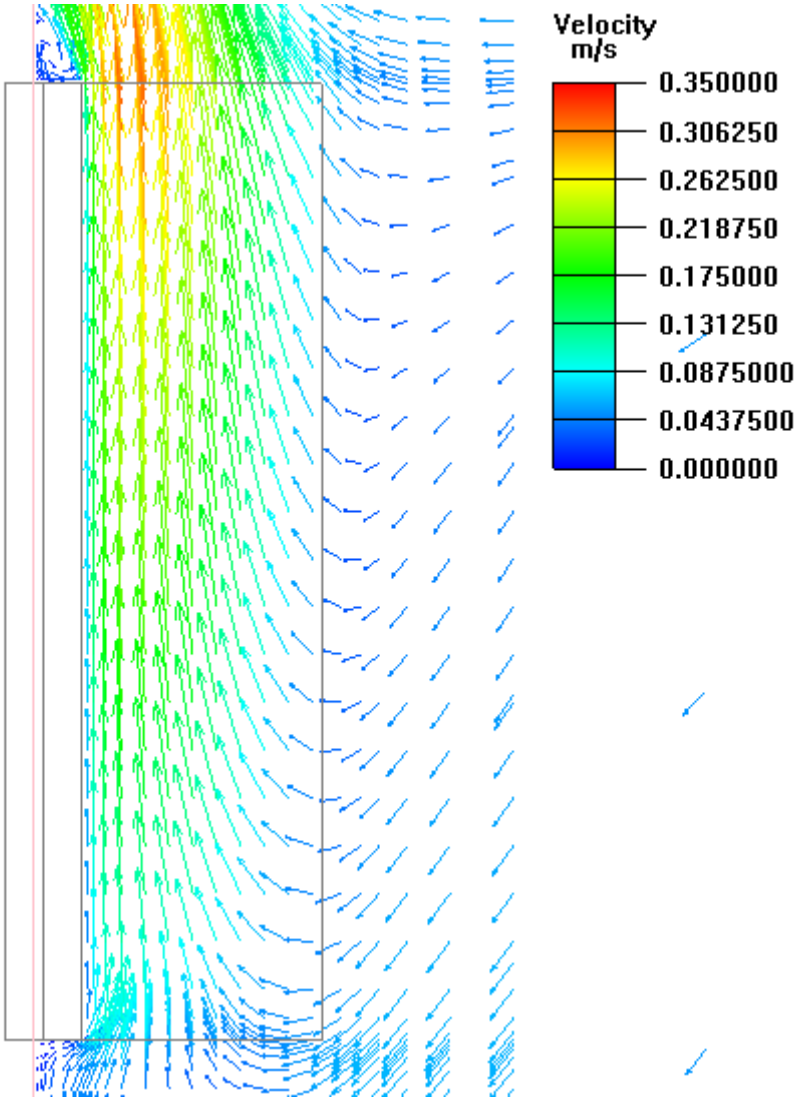

Figure 6.4.1 Velocity vectors for fin height H = 25 mm

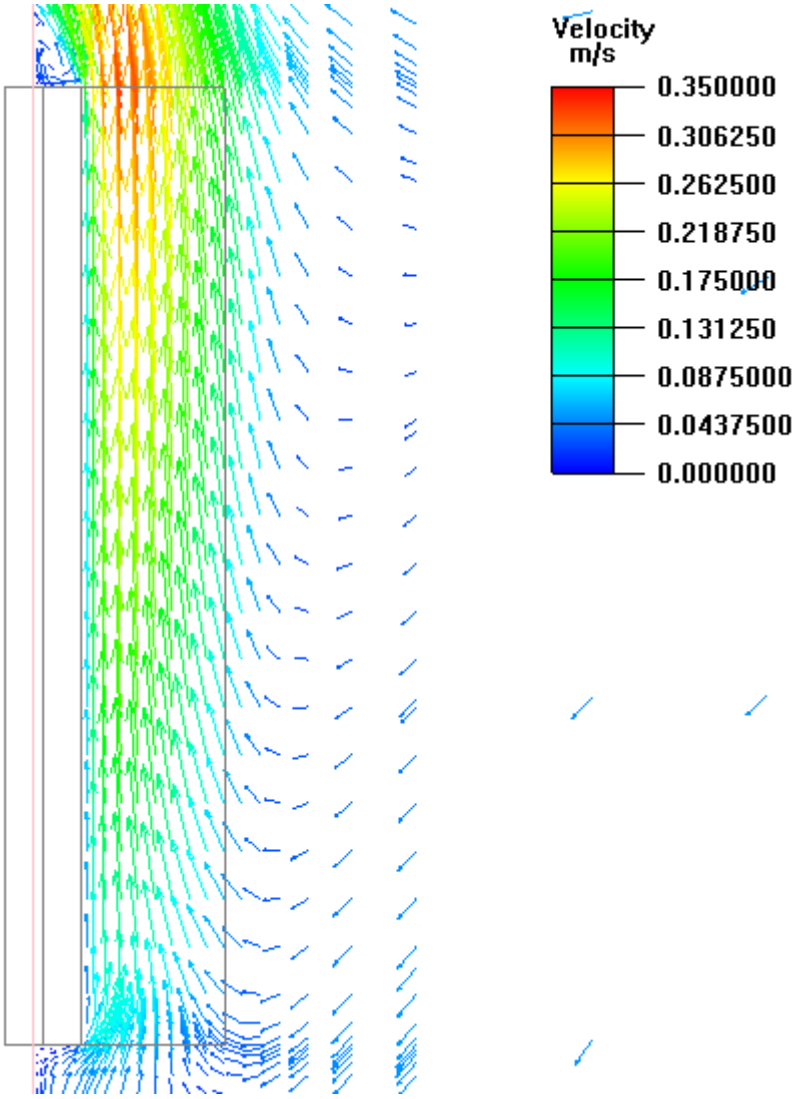

Figure 6.4.2 Velocity vectors for fin height H = 15 mm

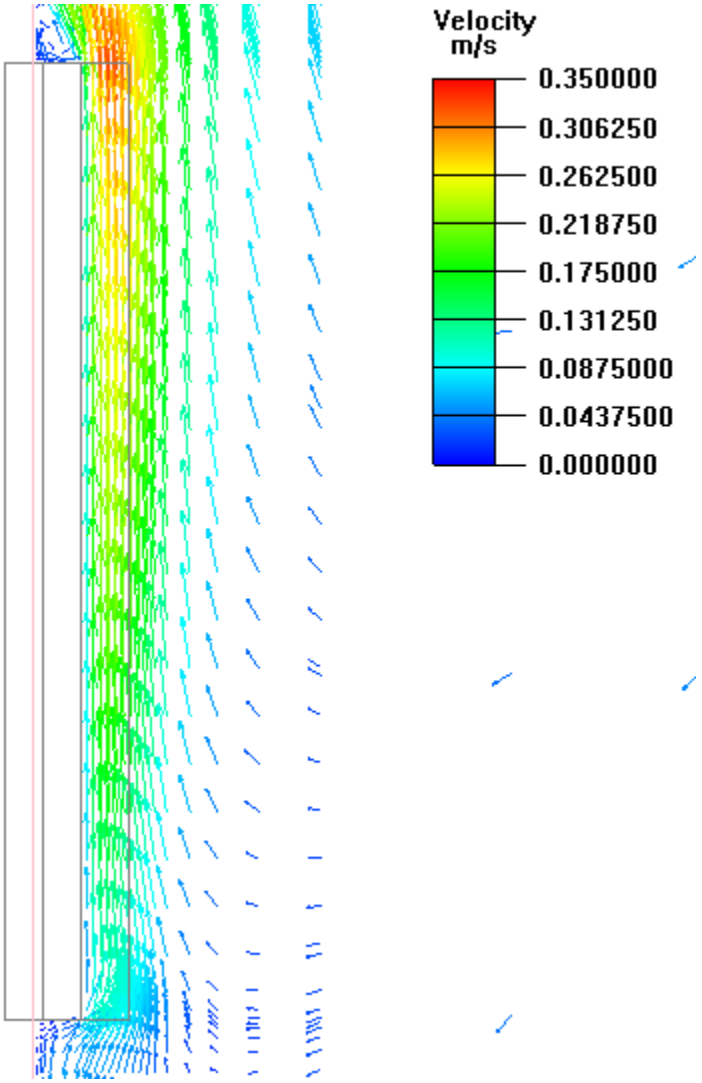

Figure 6.4.3 Velocity vectors for fin height H = 5 mm

From the figures it can be seen that for higher fin height values more air is entering the fin channels along the fin length. For low fin height values, air only enters the fin channel from the end of the fin.

CHAPTER 7

CORRELATION OF RESULTS

In Chapter 5, the results obtained from analyses and their comparison with the experimental data is presented. In this Chapter these results will be correlated. First the variation of the optimum fin spacing with Rayleigh number will be presented. After that a correlation of the maximum convection heat transfer rate from the fin arrays with Rayleigh number will be shown.

7.1 Correlation of Optimum Fin Spacing with Rayleigh Number

The optimum fin spacing values of both of the case studies from literature for minimizing the average temperature of the fin array and maximizing the convection heat transfer rate from fin arrays are given in Chapter 5. In order to find the correlation between the optimum fin spacing and Rayleigh number, the average temperature of the fin array is calculated for each optimum fin spacing value. All the flow properties are found using the film temperature which is the average of the fin array temperature and ambient temperature. Therefore by this method for every optimum fin spacing value, the corresponding Rayleigh number is calculated. In this study the optimum fin spacing values for maximizing the convection heat transfer from fins are chosen.

Yazicioğlu [1] suggested three different correlations between the optimum fin spacing and Rayleigh number. These correlations are as follows:

$$\frac{S_{opt}}{L} = 4.064 \times Ra_L^{-0.25} \tag{7.1.1}$$

$$\frac{S_{opt}}{L} = 3.899 \times Ra_L^{-0.25} \tag{7.1.2}$$

$$\frac{S_{opt}}{L} = 4.037 \times Ra_L^{-0.25} \tag{7.1.3}$$

The calculated values of Sopt/L from the simulation results with respect to Rayleigh number is plotted in Figure 7.1.1. A curve is fitted to the found data in order to obtain a similar relation with Eqs. (7.1.1), (7.1.2) and (7.1.3).

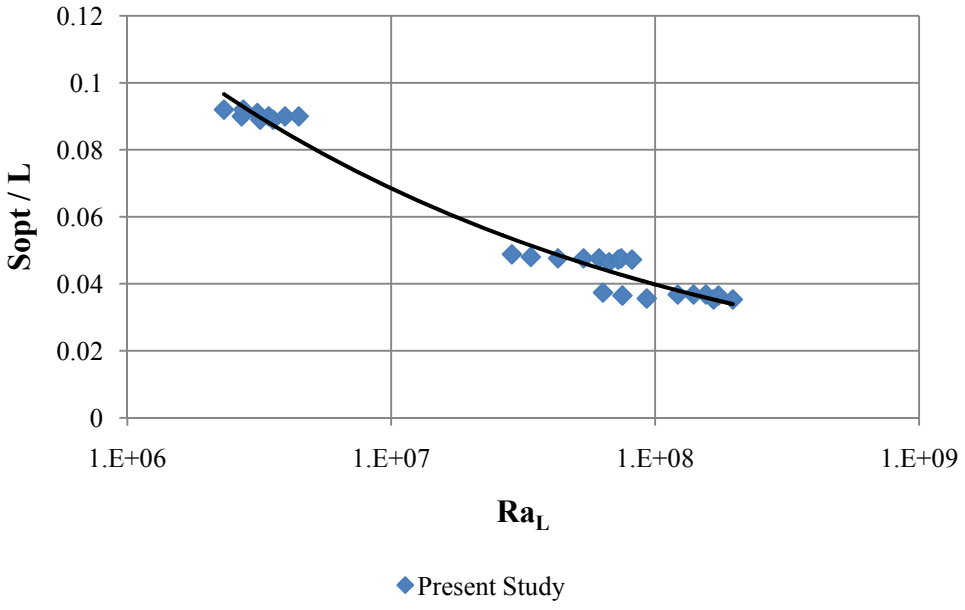

Figure 7.1.1 Variation of optimum fin spacing with Rayleigh number

The power curve fitted to the obtained data is obtained as:

$$\frac{S_{opt}}{L} = 3.0596 \times Ra_L^{-0.236} \qquad (7.1.4)$$

The correlations suggested in Ref. [1] and the one obtained from analyses are also plotted in Figure 7.1.2 for comparison purpose.

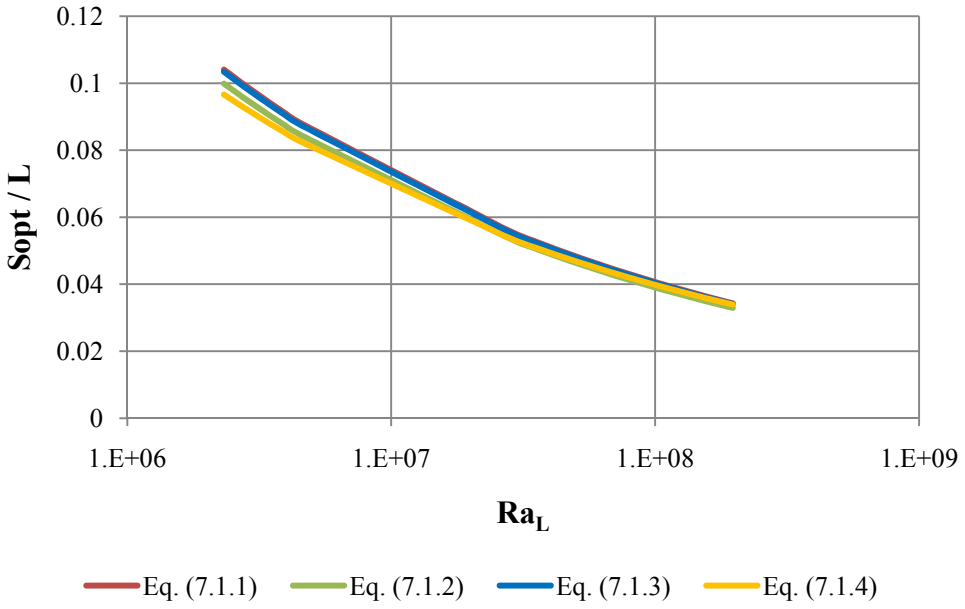

Figure 7.1.2 Comparison of correlations for optimum fin spacing with Rayleigh number

As it can be seen from Figure 7.1.2 that the correlation obtained from the analyses give close results with the correlations found in Ref. [1].

7.2 Correlation of Maximum Convection Heat Transfer Rate with Rayleigh Number

The variation of convection heat transfer rate from fin arrays are presented in Chapter 5. As it is stated before, the optimum fin spacing value gives the maximum convection heat transfer rate from fins. In order to obtain a measure of steady state maximum heat transfer rate from a rectangular fin on a vertical base in free convection heat transfer, a further correlation was suggested by Yazicioğlu in Ref. [3] and Ref. [4]. These correlations are as follows respectively:

$$Qc_{max} = (Qo)_c + 0.125 \times Ra_L^{1/2} kH\Delta T\left(\frac{W}{L}\right) \tag{7.2.1}$$

$$Qc_{max} = (Qo)_c + 0.2116 \times Ra_L^{1/2} kH\Delta T\left(\frac{W}{L}\right) \tag{7.2.2}$$

where

Qc_{max} is maximum convection heat transfer rate from fin array.

$(Qo)_c$ is convection heat transfer rate from vertical flat plate.

Since for the optimum fin spacing the convection heat transfer rate from fins reaches to a maximum; Qc_{max} is calculated for every optimum fin spacing value obtained for every fin configuration investigated with ICEPAK. It is also possible to find the average temperatures of the fin array for the optimum fin spacing value. Furthermore these average fin array temperatures can be used in order to find $(Qo)_c$ from the analyses performed for the vertical flat plates. The results obtained from analyses are shown in Figure 7.2.1 with a power curve fit to get a correlation similar to Equation (7.2.1) and Equation (7.2.2). The results consist of the both case studies investigated in the present study.

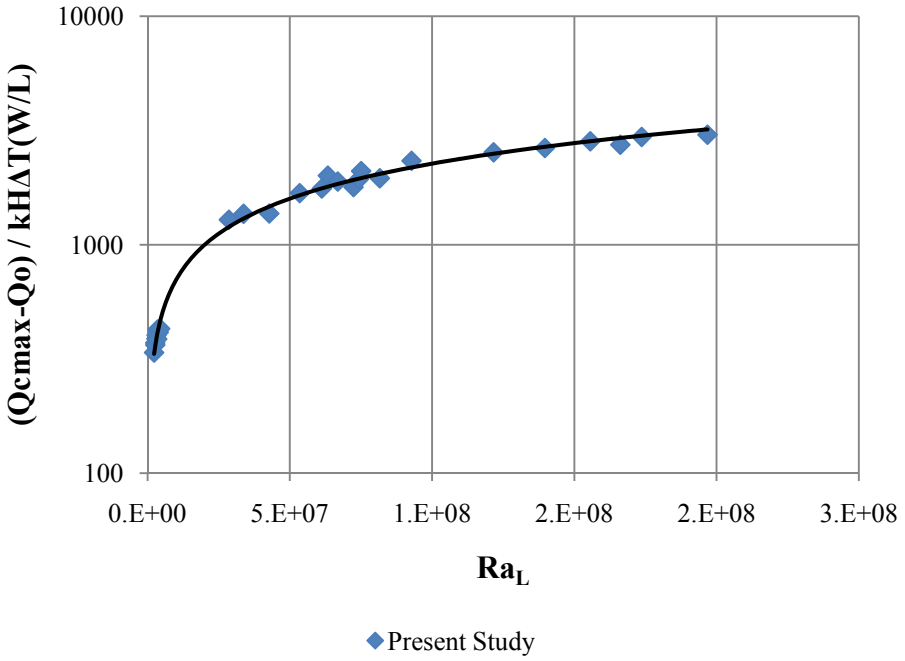

Figure 7.2.1 Variation of maximum heat transfer rate with Rayleigh number

By assuming the same form with the experimental correlation, the power curve fitted to the acquired data is obtained as:

$$Qc_{max} = (Qo)_c + 0.1898 \times Ra_L^{0.51} kH\Delta T\left(\frac{W}{L}\right) \qquad (7.2.3)$$

The comparison of the results obtained from analyses with experimental results from Ref. [1] and Ref. [2] is plotted in Figure 7.2.2 The Eqs. (7.2.1), (7.2.2) and (7.2.3) are also shown on the same plot for comparison.

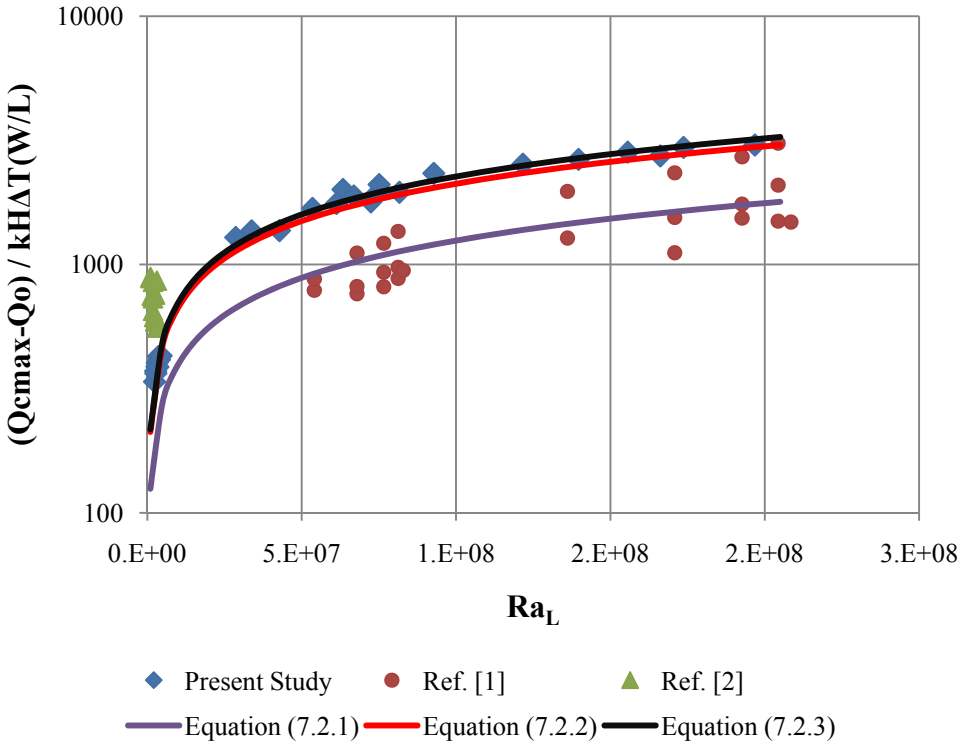

Figure 7.2.2 Comparison of analyses results with experimental data

It can be observed from the graph that the experimental results are scattered on the plot while present study results show a stable trend. Even though the x-axis of the graph is in logarithmic scale, there are very large differences between the experimental results. This shows that experimental results are not very consistent. Also it can be seen from the graph that the correlation found from analyses results (Equation 7.2.3) is very similar to the Equation (7.2.2) suggested in Ref. [4].

CHAPTER 8

CONCLUSIONS

In this study steady state natural convection heat transfer from vertically placed fin arrays are investigated with the help of a commercially used CFD program ICEPAK. The main objective of this study is to show the advantages of CFD solutions to natural convection from finned heat sinks by simulating cases from literature. For this purpose two experimental studies done on vertical heat sinks are chosen and investigated in this study.

Before analyzing the selected two cases, the models are verified. In order to do so, natural convection from vertical flat plate and natural convection from two parallel vertical flats are analyzed for both cases. The results are compared with theoretical correlations and experiment results from literature.

After verification of the models the effects of geometric parameters on the performance of heat dissipation from fin arrays are examined. For this purpose, 30 different fin array configurations for first case selected from literature and 15 different fin array configurations for the second case selected from literature are modeled and analyzed by the help of ICEPAK. The results of analyzes and their comparison with literature is given in Chapter 5. These results are correlated and also compared with literature in Chapter 7.

It is found that convection heat transfer rate depends on fin height and fin length as predicted. For a given fin spacing, the convection heat transfer rate from fins increases with fin height. This trend is observed for every fin

configuration. On the other hand it is seen that average temperature of fins reaches to minimum value for a specified fin spacing value. Furthermore for a specified fin spacing value, convection heat transfer rate reaches to its maximum value.

These optimum fin spacing values are found in literature by conducting limited experiments. In order to find the exact optimum fin spacing value, many fin set-ups must be produced and worked on. Not only this is very hard, it is also expensive and time consuming. However with the help of CFD, it is possible to create every possible fin model easily without any significant time and money consumption. In experiments selected from literature, only 5 different fin spacing values were investigated. In order to find the exact optimum fin spacing values, more fin configurations are modeled and analyzed.

Although these specified fin spacing values for maximizing heat dissipation from fins and minimizing the average temperature of fins are not exactly the same value, they are very close. Besides, although it is observed that this optimum fin spacing value is different for various fin heights and fin lengths, this difference is not very significant. Therefore it can be assumed that there is one optimum fin spacing value for vertical fin arrays and this value is found as approximately 10 mm.

The results obtained from the analyses follow a trend similar to the results of the experiments. Still it is noticed that results for the convection heat transfer rate from fin arrays are significantly different. Although all the models are verified first, it is still not possible to model an exact simulation of the experiments. The exact details of the experiment components are not given in literature and consequently some educational guesses are made in order to create the models similar to experiments as much as possible. However since the mounting details of the fin arrays to the base plate are not known, the contact resistance between these two components is not taken into account.

In the light of the results obtained from analyses two useful correlations are obtained. Both correlations are compared with other correlations and experimental data in literature. The first correlation is suggested for variation of optimum fin spacing with Rayleigh number and it is as follows:

$$\frac{S_{opt}}{L} = 3.0596 \cdot Ra_L^{-0.236} \tag{7.1}$$

The second correlation is suggested for variation for maximum convection heat transfer from fin with Rayleigh number and it is as follows:

$$Qc_{\max} = \left(Qo\right)_c + 0.1898 \cdot Ra_L^{0.51} kH\Delta T\left(\frac{W}{L}\right) \tag{7.2}$$

The present study does not investigate roughness effects on the solution and fin height optimization. Furthermore these subjects are suggested for future work. Besides since current study also does not contain contact resistances, a future work can also be done by implementing the contact resistances.

REFERENCES

[1] Yazicioğlu B., "Performance of Rectangular Fins on a Vertical Base in Free Convection Heat Transfer", M.S. Thesis in Mechanical Engineering, Middle East Technical University , Ankara (2005).

[2] Güvenc A., "An Experimental Investigation on Performance of Rectangular Fins on a Vertical Base in Free Convection Heat Transfer", M.S. Thesis in Mechanical Engineering, Middle East Technical University , Ankara (1999).

[3] Yazicioğlu B., Yüncü H., "Optimum Fin Spacing of Rectangular Fins on a Vertical Base in Free Convection Heat Transfer", Heat Mass Transfer 44, 11-21, (2007).

[4] Yazicioğlu B., Yüncü H., "A Correlation for Optimum Fin Spacing of Vertically-Based Rectangular Fin Arrays Subjected to Natural Convection Heat Transfer", Journal of Thermal Science and Technology 29, 11 99-105, (2009).

[5] Starner K.E. and McManus H.N., "An Experimental Investigation of Free Convection Heat Trasnfer from Rectangular Fin Arrays", Journal of Heat Transfer, 273-278, (1963).

[6] Leung C.W. and Probert S.D., "Thermal Effectiveness of Short Protrusion Rectangular, Heat Exchanger Fins", Applied Energy, 1-8, (1989).

[7] Leung C.W., Prober S.D. and Shilston M.J. "Heat Exchanger: Optimal Separation for Vertical Rectangular Fins Protruding from a Vertical Rectangular Base", Applied Energy, 77-85, (1985).

[8] Jones C.D. and Smith L.F., "Optimum Arrangement of Rectangular Fins on Horizontal Surfaces for Free Convection Heat Transfer", Journal of Heat Transfer, 6-10, (1970).

[9] Fitzroy N.D., "Optimum Spacing of Fins Cooled by Free Convection", Journal of Heat Transfer, 462-463, (1971).

[10] Yüncü H. and Anbar G., "An Experimental Investigation on Performance of Rectangular Fins on a Horizontal Base in Free Convection Heat Transfer", Heat and Mass Transfer 33, 507-514, (1998).

[11] Yüncü H. and Mobedi M., "A Three Dimensional Numerical Study on Natural Convection Heat Transfer from Short Horizontal Rectangular Fin Array", Heat and Mass Transfer 39, 267-275, (2003).

[12] Harahap F., Lesmana H., Dirgayasa A.S., "Measurements of Heat Dissipation from Miniaturized Vertical Rectangular Fin Arrays under Dominant Natural Convection Conditions", Heat and Mass Transfer 42, 1025-1036, (2006).

[13] Vollaro A.D.L., Grignaffini S., Gugliermetti F., "Optimum Design of Vertical Rectangular Fin Arrays", International Journal of Thermal Sciences 38, 525-259, (1999).

[14] Dialameh L., Yaghoubi M., Abouali O., "Natural Convection from an Array of Horizontal Rectangular Thick Fins with Short Length", Applied Thermal Engineering 28, 2371-2379, (2008).

[15] Kundu B., Das P.K., "Performance and Optimum Design Analysis of Convective Fin Arrays Attached to Flat and Curved Primary Surfaces", International Journal of Refrigeration, 1-14, (2008).

[16] Leung C.W., Probert S.D., "Heat-Exchanger Performance: Influence of Gap Width between Consecutive Vertical Rectangular Fin Arrays", Applied Energy 56, 1-8, (1997).

[17] Mobedi M., Sunden B., "Natural Convection Heat Transfer from a Thermal Heat Source Located in a Vertical Plate Fin", International Communications in Heat and Mass Transfer 33, 943-950, (2006).

[18] Nada S.A., "Natural Convection Heat Transfer in Horizontal and Vertical Closed Narrow Enclosures with Heated Rectangular Finned Base Plate", International Journal of Heat and Mass Transfer 50, 667-679, (2007).

[19] Yalcin H.G., Baskaya S., Sivrioglu M., "Numerical Analysis of Natural Convection Heat Transfer from Rectangular Shrouded Fin Arrays on a Horizontal Surface", International Communications in Heat and Mass Transfer 35, 299-311, (2008).

[20] Incropera F.P., DeWitt D.P., Fundamentals of Heat and Mass Transfer, John Wiley & Sons, New York, (1990).

[21] Mcadams W.H., Heat Transmission, McGraw-Hill, New York, (1954).

[22] ICEPAK User's Guide 4.3, Fluent Inc., 2006.

APPENDIX A

VERIFICATION OF COMPUTATIONAL DOMAIN SIZE

For all the analyses of the fin arrays a sufficiently large domain size is chosen as stated in Chapter 3 in order to decrease the total mesh number while still trying to satisfy the large room condition. In this section the effect of this domain size on the results are investigated. For this purpose two different fin configurations are selected among first case study and modeled in a very large domain. The dimension of this domain is chosen as 3000 x 3000 x 3000 mm to satisfy the large room condition. The selected fin array configurations from first case study are given below:

The first fin array configuration:

- Fin Length, L = 250 mm
- Fin Height, H = 15 mm
- Number of Fins = 16
- Power Input to Fins = 100 W

The second fin array configuration:

- Fin Length, L = 340 mm
- Fin Height, H = 25 mm
- Number of Fins, N = 11
- Power Input to Fins = 75 W

The 3D view and the mesh structure of the model for large domain size are given in Figure A.1.

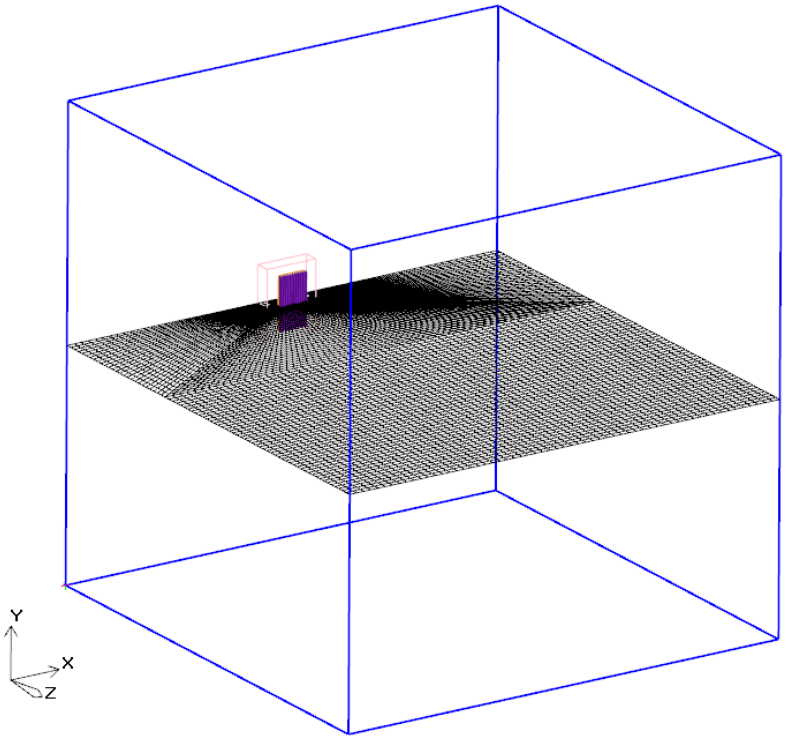

Figure A.1 3D view and mesh structure of the model with large domain

Same basic parameters, solution settings and mesh size control parameters explained in Chapter 3 are used in this section too. The average temperature of the fin arrays and convection heat transfer rate from fins are obtained for each fin configuration mentioned above and compared with the results obtained for normal domain size. The comparison of the results is given in Table A.1.

Table A.1 Comparison of results for different domain sizes

	Fin Configuration 1		Fin Configuration 2	
	Tw(^{o}C)	Qc (W)	Tw(^{o}C)	Qc (W)
Normal Domain Size	97.5	73.3	62.7	56.8
Large Domain Size	93.4	75.6	58.3	59.4

It can be seen from the Table A.1 that the difference between large domain size and normal domain size is not very significant. Consequently smaller domain size is used in all the analyses done throughout this study in order to decrease the mesh size and computational time.

APPENDIX B

CONVERGENCE CRITERIA

It is very important to check the convergence of the solution in CFD problems in order to have precise results. As already stated in chapter the following convergence options are selected in the ICEPAK for all the analyses done:

- Number of iterations is selected as 250.
- Residual for continuity is selected as 0.0001.
- Residual for energy is selected as 1E-9.

Apart from the convergence of the governing transport equations, the stability and convergence of the results are also checked. For instance the temperature points on the fin arrays are checked to observe whether the values converge to a single value or not.

The convergence plot of the residuals for the fin array configuration where fin length L = 250 mm, fin height H = 25 mm and fin spacing S = 14.7 is shown in Figure B.1. The convergence of the six temperature reading points for the same fin configuration is shown in Figure B.2. The jumps in the plot are because of the power input change to the base plate. Therefore every graph after a jump should be counted as an individual run.

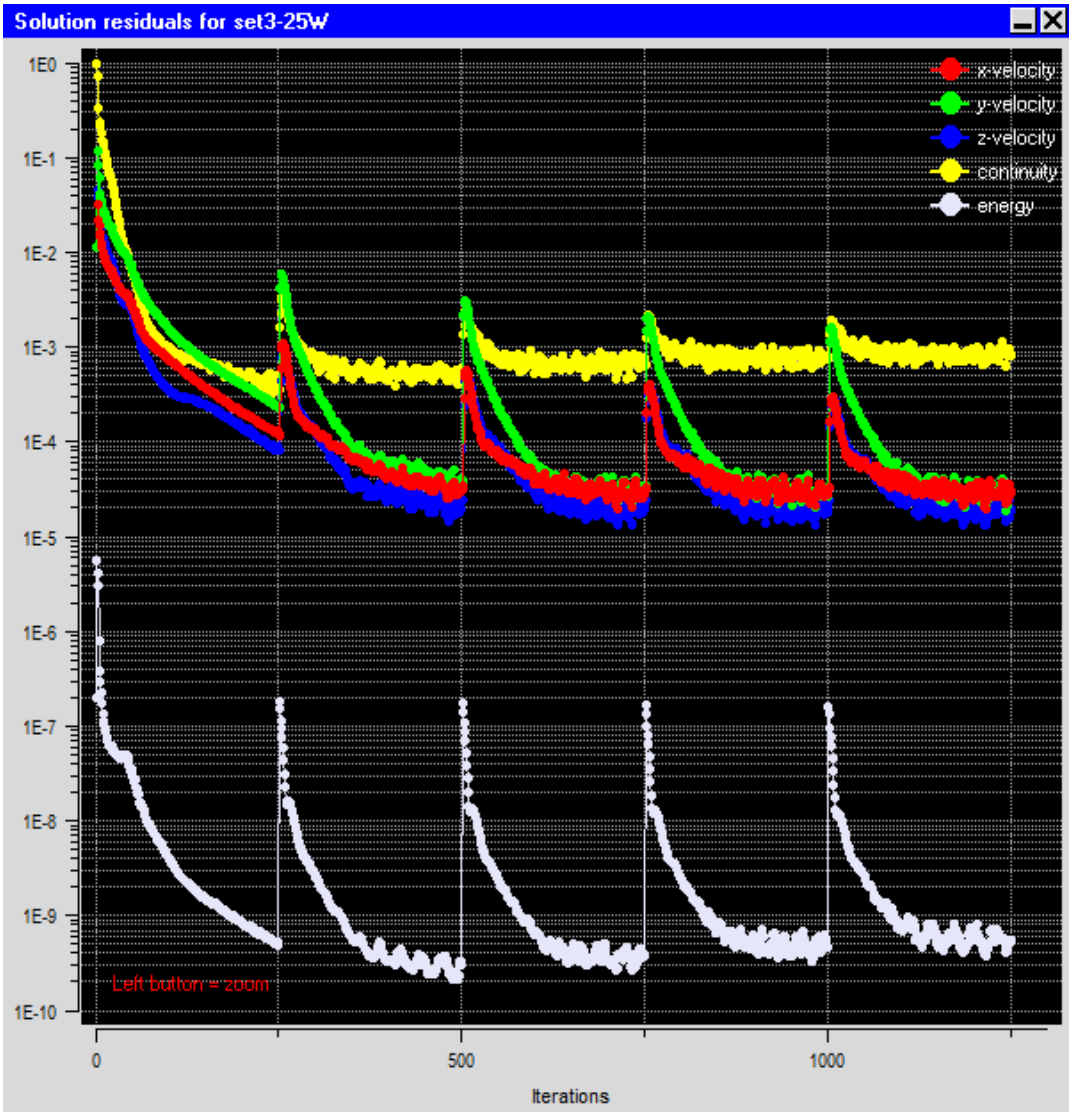

Figure B.1 Solution residuals for the fin array configuration with fin length L=250 mm, fin height H=25 mm and fin spacing S=14.7 mm

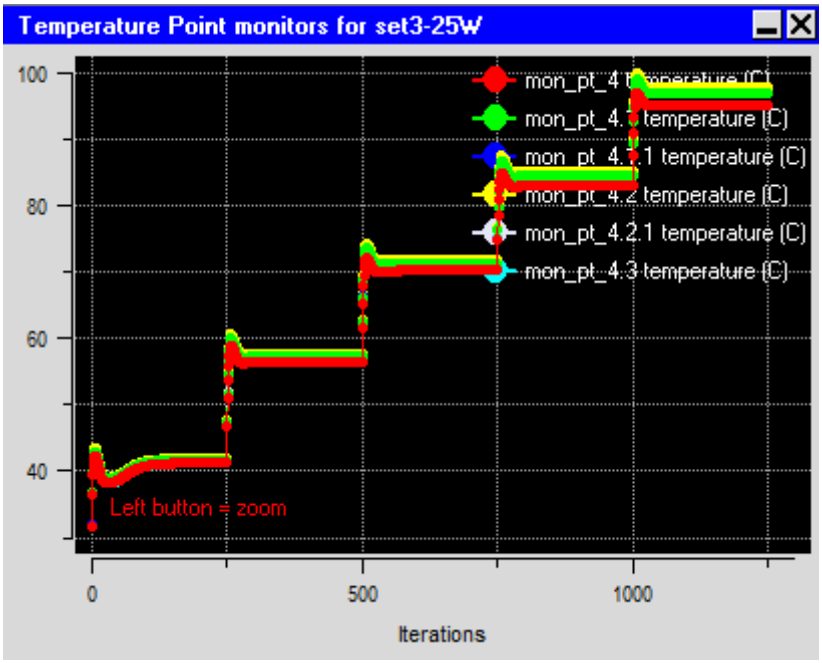

Figure B.2 Six temperature readings for the fin array configuration with fin length L=250 mm, fin height H=25 mm and fin spacing S=14.7 mm

The convergence plot of the residuals for the fin array configuration where fin length L = 340 mm, fin height H = 5 mm and fin spacing S = 32.4 is shown in Figure B.3. The convergence of the six temperature reading points for the same fin configuration is shown in Figure B.4. Once again the jumps in the plot are because of the power input change to the base plate.

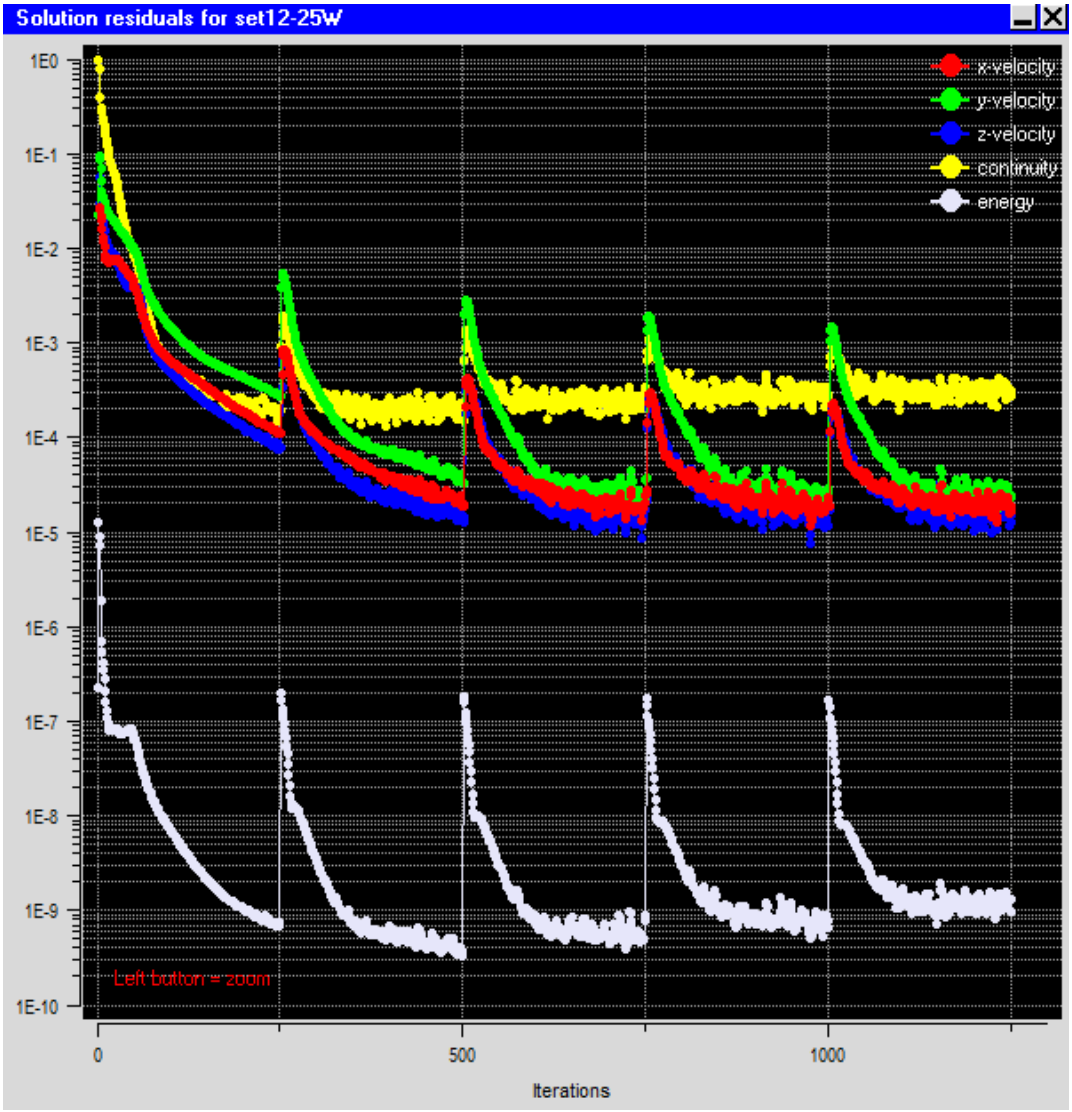

Figure B.3 Solution residuals for the fin array configuration with fin length L=340 mm, fin height H=5 mm and fin spacing S=32.4 mm

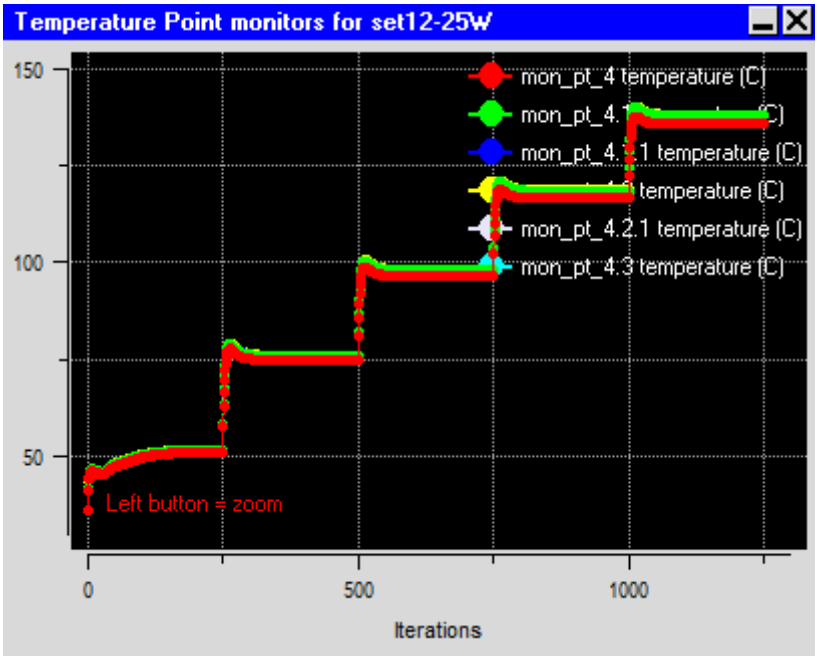

Figure B.4 Six temperature readings for the fin array configuration with fin length L=340 mm, fin height H=5 mm and fin spacing S=32.4 mm

The number of iterations for each run is selected as 250 and it can be inferred from the figures that this amount of iterations are sufficient for results to converge.

APPENDIX C

COMPARISON OF FIRST AND SECOND ORDER SOLUTION PARAMETERS

The effect of selection of first or second order solution parameters on results are analyzed by using two fin configurations from first cases study explained in Appendix A and Appendix B. These two fin configurations are given below again.

Fin Configuration 1:

- Fin Length, L = 250 mm
- Fin Height, H = 15mm
- Number of Fins = 16
- Power Input to Fins = 100W

Fin Configuration Case 2:

- Fin Length, L = 340 mm
- Fin Height, H = 25mm
- Number of Fins, N = 11
- Power Input to Fins = 75 W

For first order solution the following discretization schemes are selected:

- Standard discretization scheme for pressure
- First order discretization scheme for temperature
- First order discretization scheme for momentum

For second order solution the following discretization schemes are selected:

- Second order discretization scheme for pressure
- Second order discretization scheme for temperature
- Second order discretization scheme for momentum

Average temperature of the fin array (Tw) and convection heat transfer from the fin array (Qc) are obtained using the above fin configurations and discretization schemes. Results are shown in Table C.1.

Table C.1 Comparison of first and second order discretization schemes

	First Order		Second Order	
	Tw (^{o}C)	Qc (W)	Tw(^{o}C)	Qc(W)
Fin Configuration 1	97.46	73.25	98.5	72.89
Fin Configuration 2	62.74	56.89	63.18	56.65

As it can be inferred from the Table C.1, first and second order discretization schemes gives very close results. Therefore in order to shorten the computation time first order discretization schemes are used throughout all of the analyses.

APPENDIX D

MESH SIZE CONTROL

In order to find the necessary mesh size and amount, once more the two different fin configurations used in Appendix A, Appendix B and Appendix C are analyzed with different mesh sizes. Three different mesh sizes are used to analyze each configuration. The results obtained from three different mesh amounts are compared with each other.

D.1 Fin Configuration 1

The first fin configuration is as follows:

- Fin Length, L = 250 mm
- Fin Height, H = 15mm
- Number of Fins = 16
- Power Input to Fins = 100W

Mesh Size A

The following mesh control properties are used for this mesh size:

- Max X size = 27 mm
- Max Y size = 75 mm
- Max Z size = 20 mm
- Mesh parameter is set to normal.
- Min elements in gap = 3
- Min elements on edge = 2
- Max size ratio = 2

- No object parameters are used.

When this mesh control properties are used, the total mesh number is 53856. The view of the mesh structure is given in Figure D.1.1.

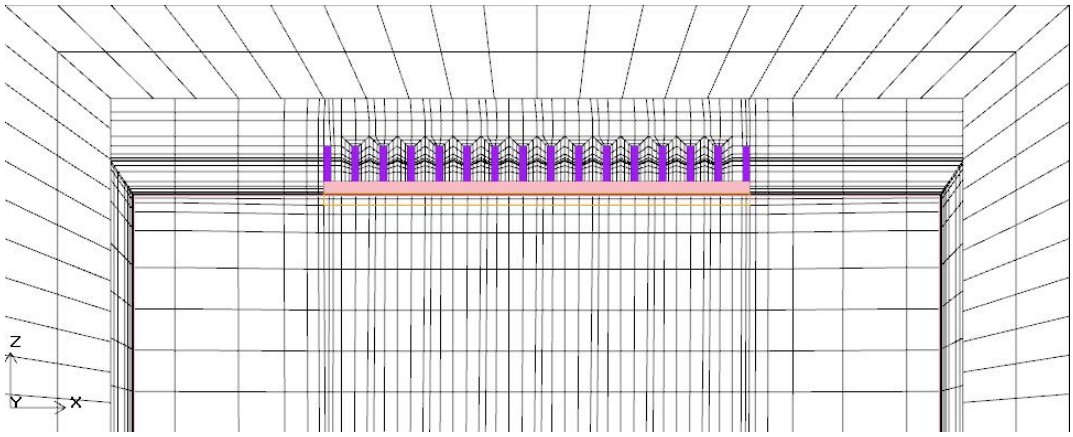

Figure D.1.1 Mesh structure for fin configuration 1, mesh size A

Mesh Size B

The following mesh control properties are used for this mesh size:

- Max X size = 27 mm
- Max Y size = 75 mm
- Max Z size = 20 mm
- Mesh parameter is set to normal.
- Min elements in gap = 3
- Min elements on edge = 2
- Max size ratio = 2
- Object parameters for fin arrays are used as follows:
    - Pins X element count = 2

- Pins Y element count = 60
- Pins Z element count = 10
- Base element height = 0.5 mm
- Pins element height = 0.5 mm
- Base element ratio = 1.5
- Pins element ratio = 1.5

As a result total mesh amount for this mesh size is 615265. The view of the mesh structure is given in Figure D.1.2.

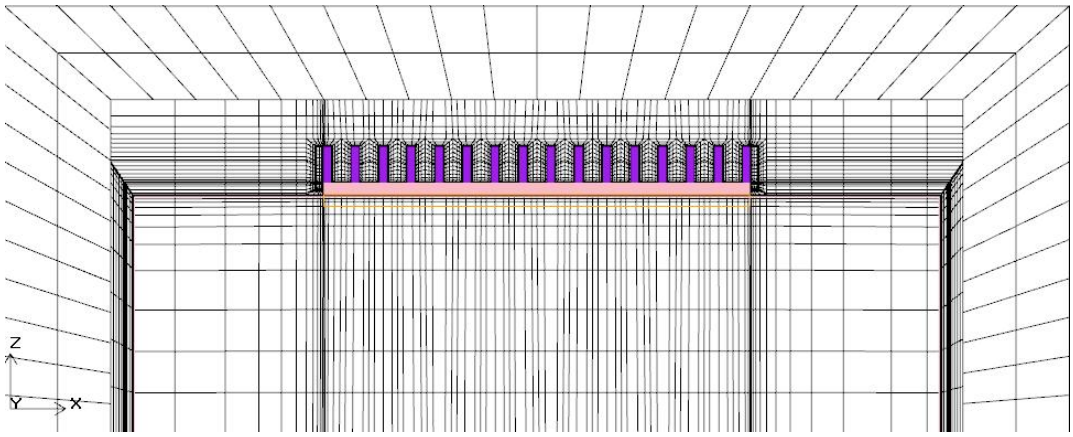

Figure D.1.2 Mesh structure for fin configuration 1, mesh size B

Mesh Size C

The following mesh control properties are used for this mesh size:

- Max X size = 27 mm
- Max Y size = 75 mm
- Max Z size = 20 mm
- Mesh parameter is set to normal.
- Min elements in gap = 3

- Min elements on edge = 2
- Max size ratio = 2
- Object parameters for fin arrays are used as follows:
    - Pins X element count = 4
    - Pins Y element count = 80
    - Pins Z element count = 20
    - Base element height = 0.5 mm
    - Pins element height = 0.5 mm
    - Base element ratio = 1.2
    - Pins element ratio = 1.2

Total number of mesh amount with these mesh control parameters is 1752114. The view of the mesh structure is given in Figure D.1.3.

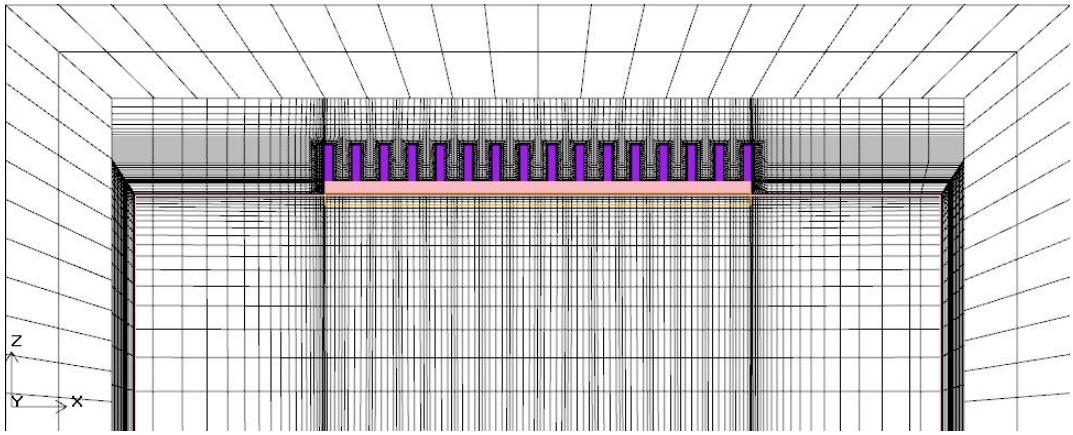

Figure D.1.3 Mesh structure for fin configuration 1, mesh size C

Comparison

The results obtained from three different mesh size controls for the first fin configuration are given in Table D.1.1.

Table D.1.1 Comparison of three mesh amounts for fin configuration 1

Fin Configuration 1	Mesh Amount	Computational Time	Tw(^{o}C)	Qc (W)
Mesh A	53856	5 mins	94.94	76.32
Mesh B	615265	25 mins	97.46	73.25
Mesh C	1752114	105 mins	97.88	73.65

D.2 Fin Configuration 2

The second fin configuration is as follows:

- Fin Length, L = 340 mm
- Fin Height, H = 25mm
- Number of Fins, N = 11
- Power Input to Fins = 75 W

Mesh Size A

The following mesh control properties are used for this mesh size:

- Max X size = 27 mm
- Max Y size = 75 mm
- Max Z size = 20 mm
- Mesh parameter is set to normal.
- Min elements in gap = 3
- Min elements on edge = 2
- Max size ratio = 2
- No object parameters are used.

When this mesh control properties are used, the total mesh number is 65140. The view of the mesh structure is given in Figure D.2.1.

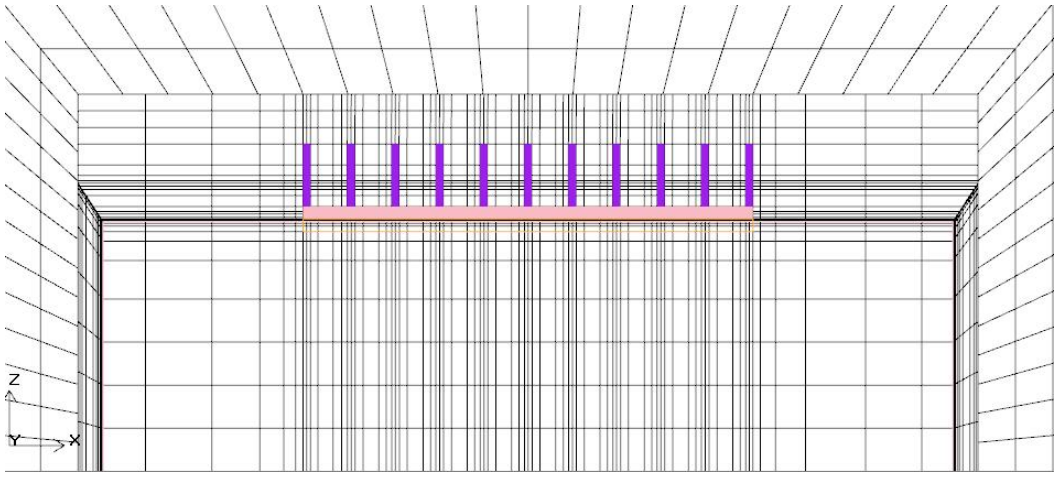

Figure D.2.1 Mesh structure for fin configuration 2, mesh size A

Mesh Size B

The following mesh control properties are used for this mesh size:

- Max X size = 27 mm
- Max Y size = 75 mm
- Max Z size = 20 mm
- Mesh parameter is set to normal.
- Min elements in gap = 3
- Min elements on edge = 2
- Max size ratio = 2
- Object parameters for fin arrays are used as follows:
    - Pins X element count = 2
    - Pins Y element count = 60
    - Pins Z element count = 10

- Base element height = 0.5 mm
- Pins element height = 0.5 mm
- Base element ratio = 1.5
- Pins element ratio = 1.5

As a result total mesh amount for this mesh size is 573498. The view of the mesh structure is given in Figure D.2.2.

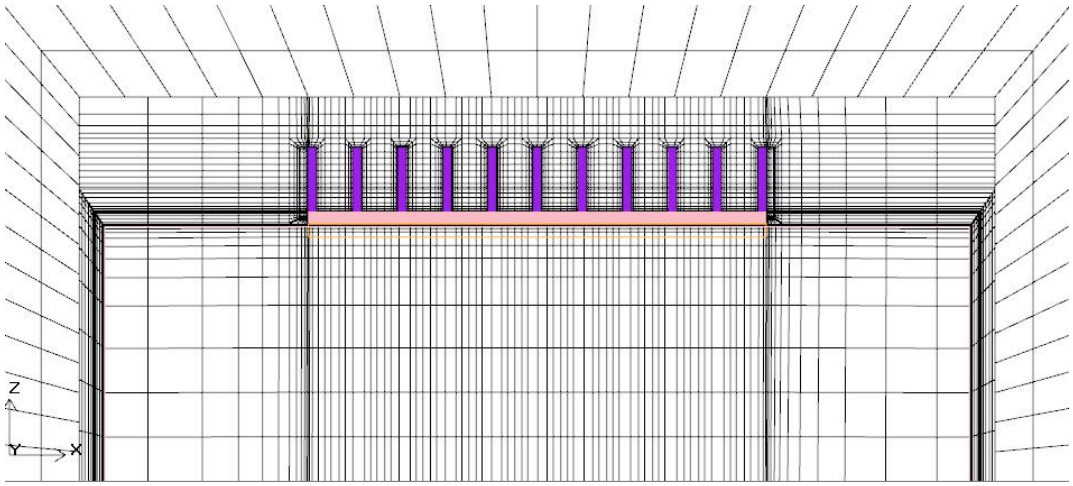

Figure D.2.2 Mesh structure for fin configuration 2, mesh size B

Mesh Size C

The following mesh control properties are used for this mesh size:

- Max X size = 27 mm
- Max Y size = 75 mm
- Max Z size = 20 mm
- Mesh parameter is set to normal.
- Min elements in gap = 3

- Min elements on edge = 2
- Max size ratio = 2
- Object parameters for fin arrays are used as follows:
    - Pins X element count = 4
    - Pins Y element count = 80
    - Pins Z element count = 20
    - Base element height = 0.5 mm
    - Pins element height = 0.5 mm
    - Base element ratio = 1.2
    - Pins element ratio = 1.2

Total number of mesh amount with these mesh control parameters is 1957464. The view of the mesh structure is given in Figure D.2.3.

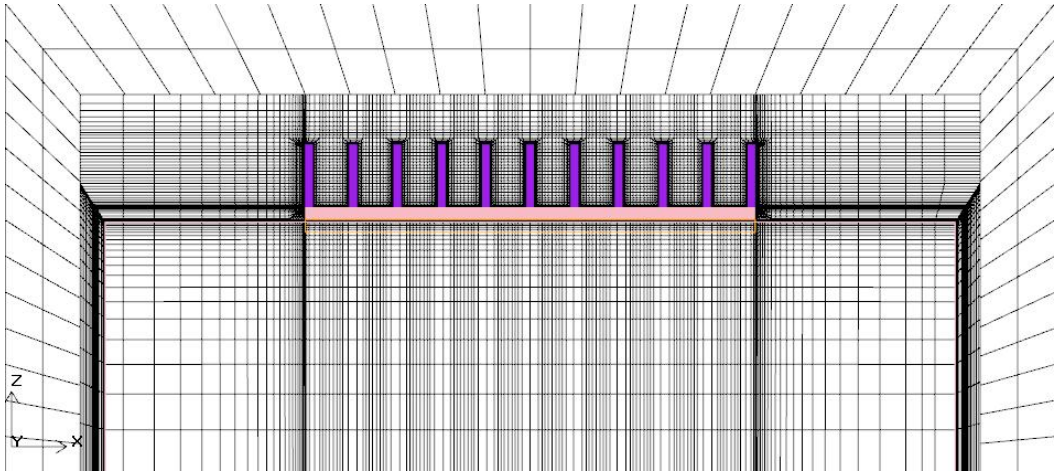

Figure D.2.3 Mesh structure for fin configuration 2, mesh size C

Comparison

The results obtained from three different mesh size controls for second fin configuration are given in Table D.2.1.

Table D.2.1 Comparison of different mesh amounts for fin configuration 2

Fin Configuration 2	Mesh Amount	Computational Time	Tw(^{o}C)	Qc (W)
Mesh A	65140	6 mins	65.23	53.45
Mesh B	573498	25 mins	62.74	56.89
Mesh C	1957464	135 mins	62.48	56.87

As it can be seen from the Table D.1.1 and table D.2.1 while mesh size B and mesh size C gives similar results, mesh size A gives different results. Since mesh size B gives as accurate results as mesh size C and still has lower computational time, it is taken as optimum mesh size. Therefore parameters for mesh size B is used for all of the fin array configurations investigated in this study.

APPENDIX E

GRAPHS

The figures which are not given in Chapter 5 are presented in this section.

E.1 Case Study 1

E.1.1 Variation of Fin Temperature with Fin Spacing

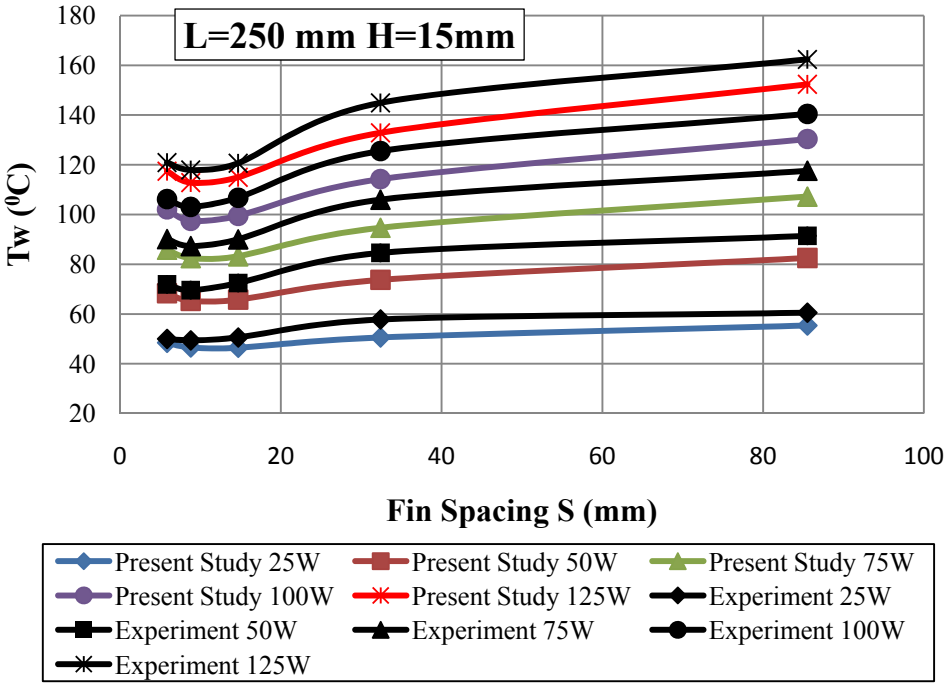

Figure E.1.1.1 Variation of average fin temperature with fin spacing at fin length of L = 250 mm and at fin height of H = 15 mm

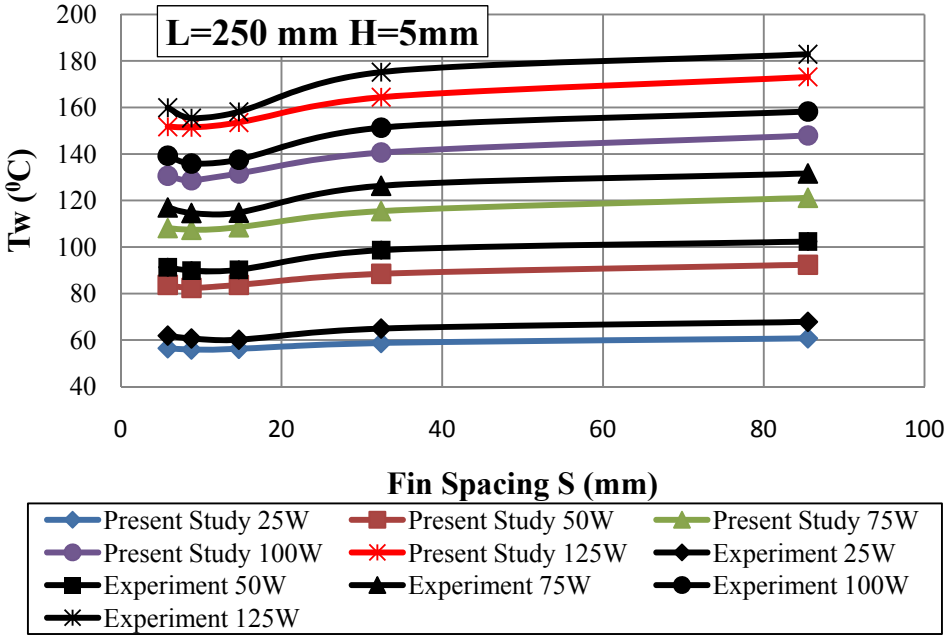

Figure E.1.1.2 Variation of average fin temperature with fin spacing at fin length of L = 250 mm and at fin height of H = 5 mm

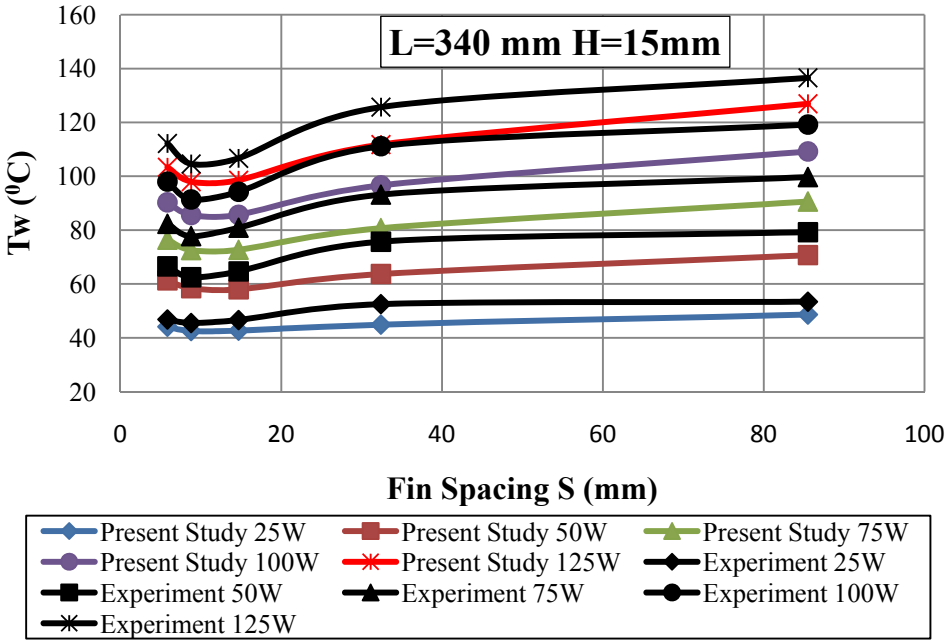

Figure E.1.1.3 Variation of average fin temperature with fin spacing at fin length of L = 340 mm and at fin height of H = 15 mm

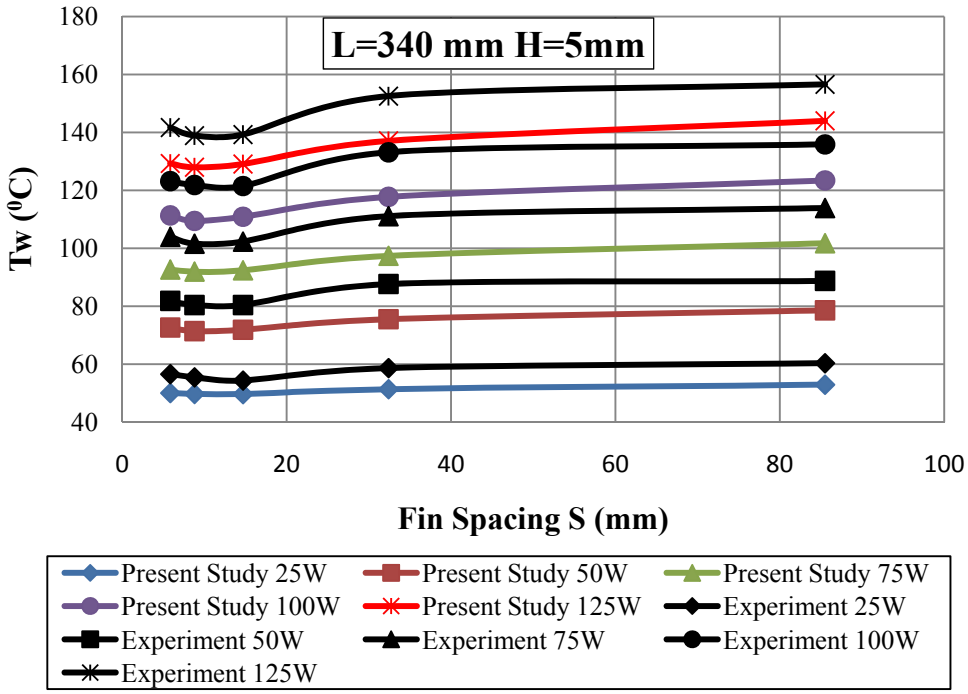

Figure E.1.1.4 Variation of average fin temperature with fin spacing at fin length of L = 340 mm and at fin height of H = 5 mm

E.1.2 Variation of Convection Heat Transfer Rate with Fin Spacing

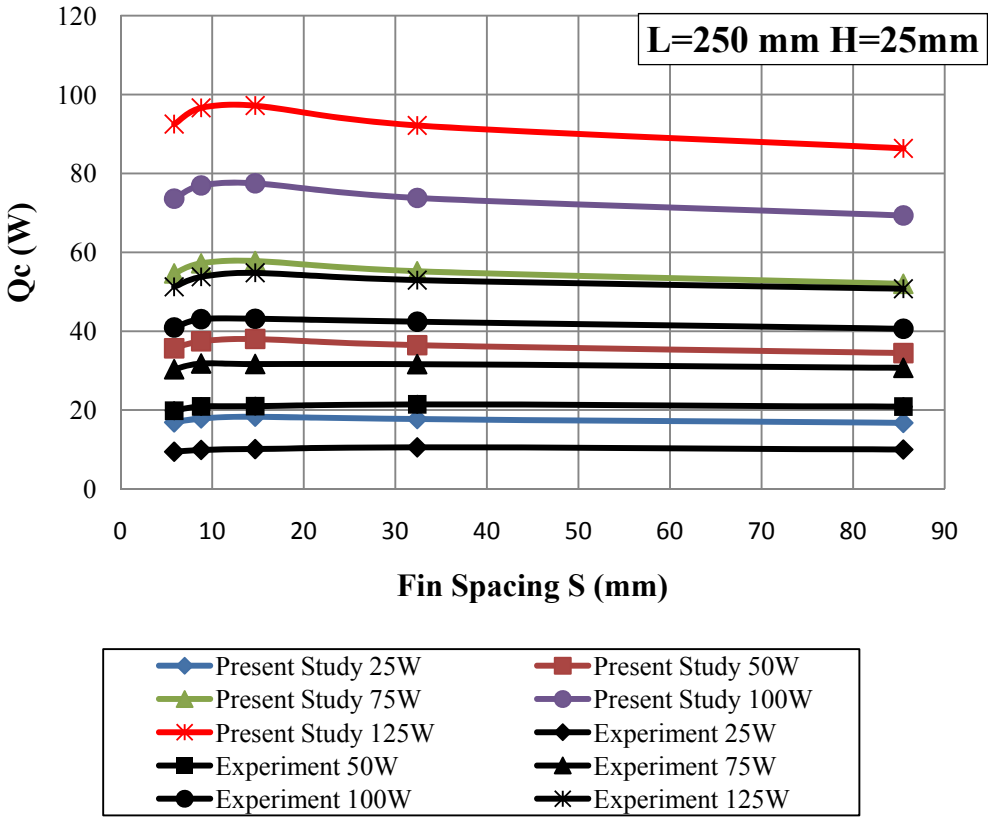

Figure E.1.2.1 Variation of convection heat transfer with fin spacing at fin length of L = 250 mm and at fin height of H = 25 mm

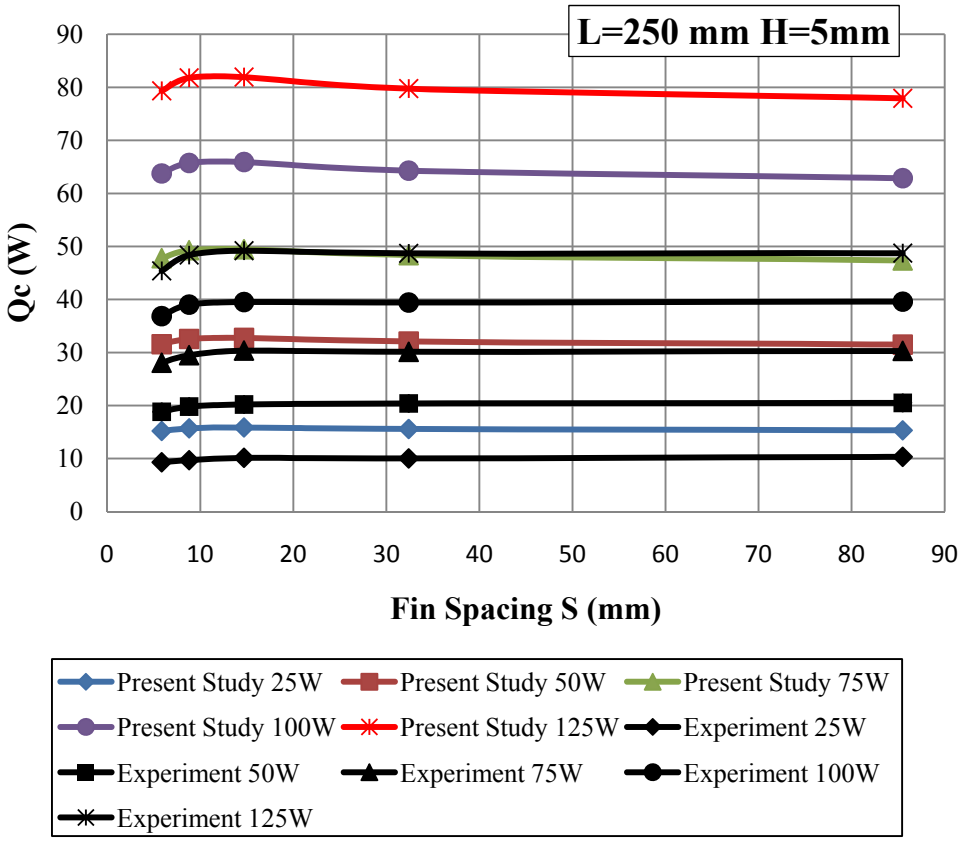

Figure E.1.2.2 Variation of convection heat transfer with fin spacing at fin length of L = 250 mm and at fin height of H = 5 mm

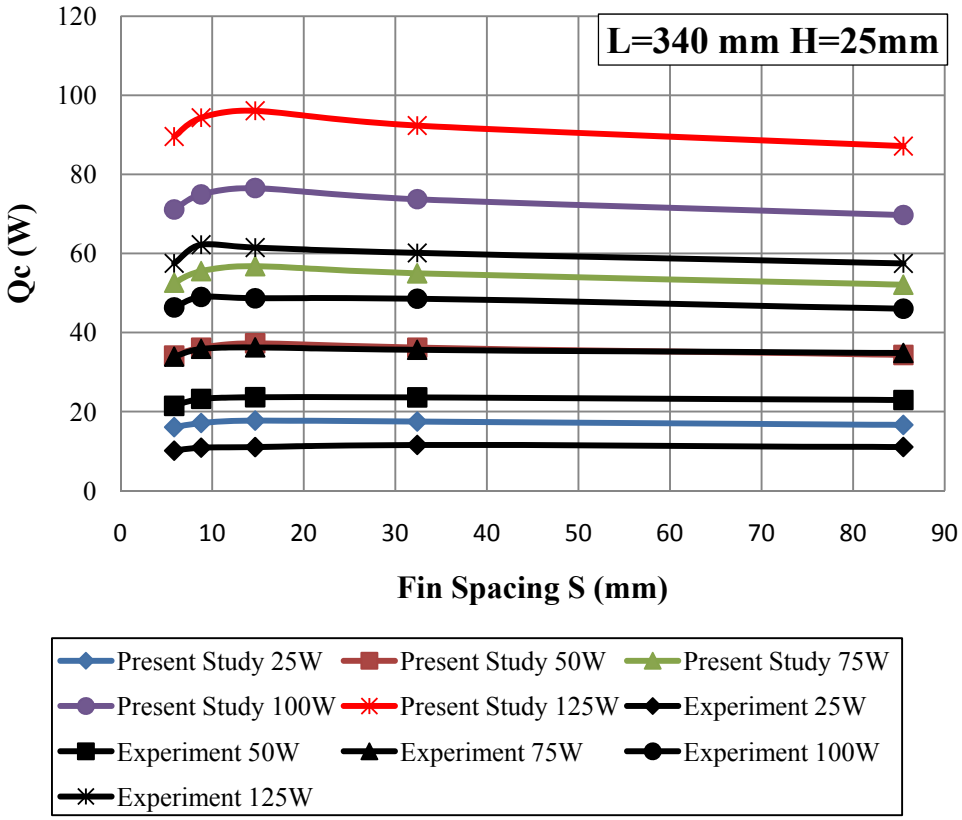

Figure E.1.2.3 Variation of convection heat transfer with fin spacing at fin length of L = 340 mm and at fin height of H = 25 mm

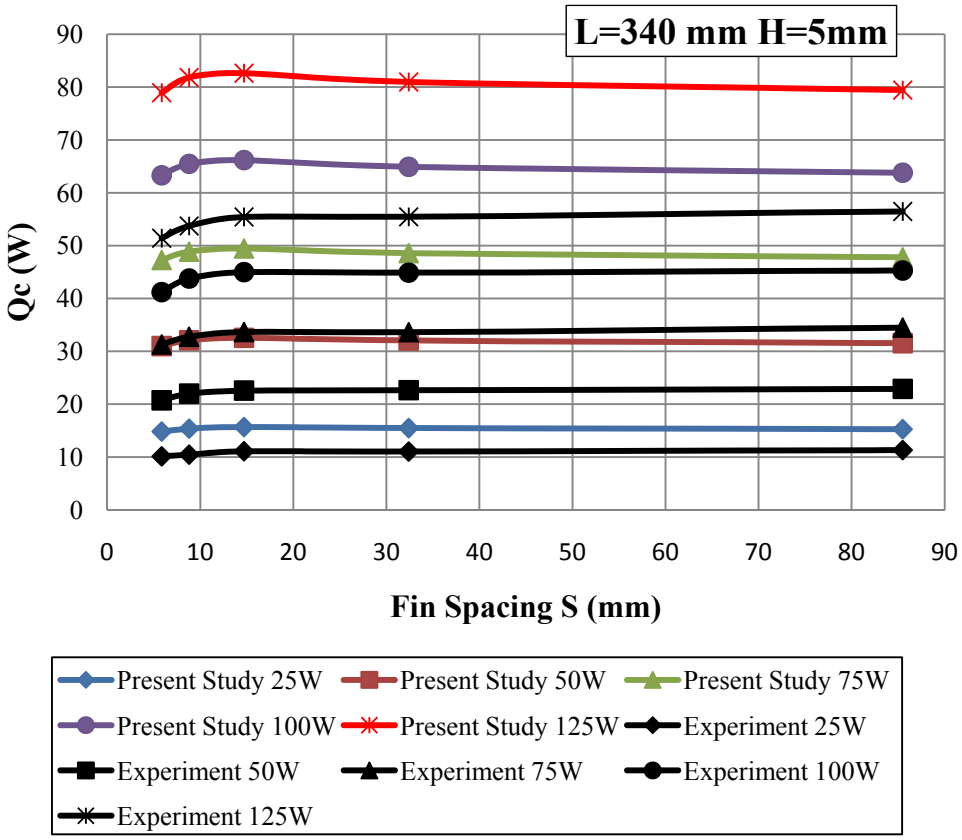

Figure E.1.2.4 Variation of convection heat transfer with fin spacing at fin length of L = 340 mm and at fin height of H = 5 mm

E.1.3 Optimum Fin Spacing for Minimum Fin Temperature

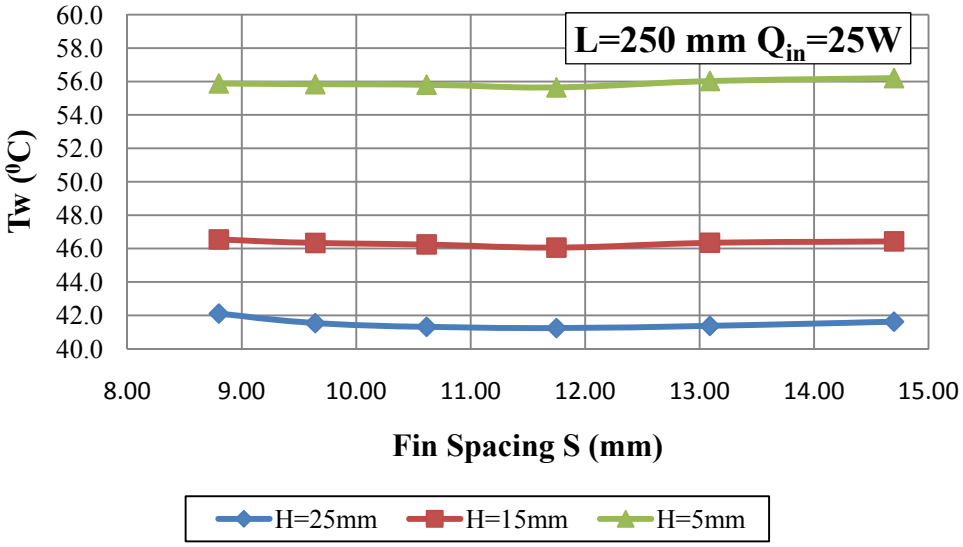

Figure E.1.3.1 Variation of average fin temperature with fin spacing at fin length of L = 250 mm and at power input of Q_{in} = 25 W

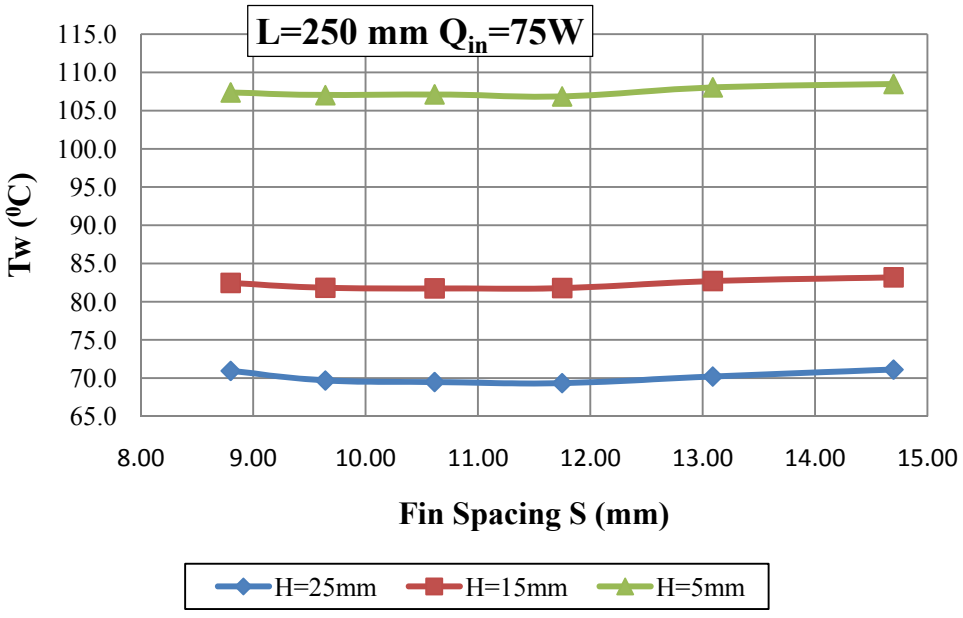

Figure E.1.3.2 Variation of average fin temperature with fin spacing at fin length of L = 250 mm and at power input of Q_{in} = 75 W

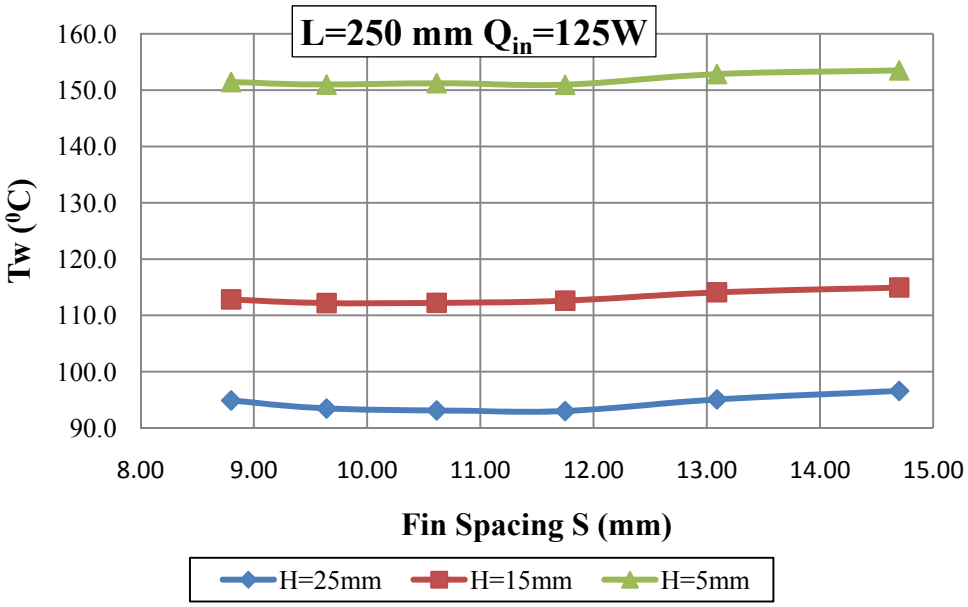

Figure E.1.3.3 Variation of average fin temperature with fin spacing at fin length of L = 250 mm and at power input of Q_{in} = 125 W

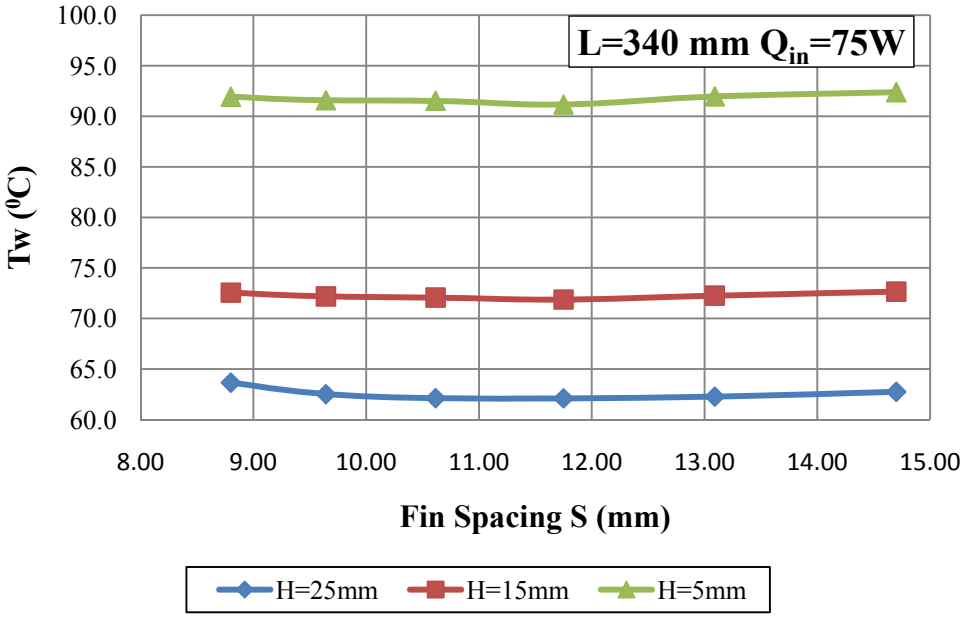

Figure E.1.3.4 Variation of average fin temperature with fin spacing at fin length of L = 340 mm and at power input of Q_{in} = 75 W

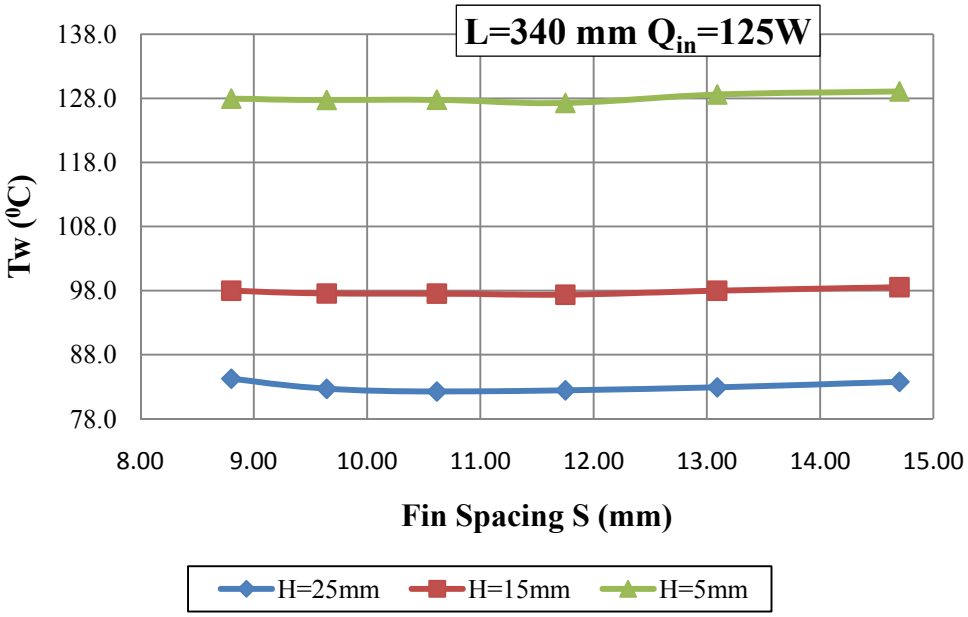

Figure E.1.3.5 Variation of average fin temperature with fin spacing at fin length of L = 340 mm and at power input of Q_{in} = 125 W

E.1.4 Optimum Fin Spacing for Maximum Convection Heat Transfer Rate

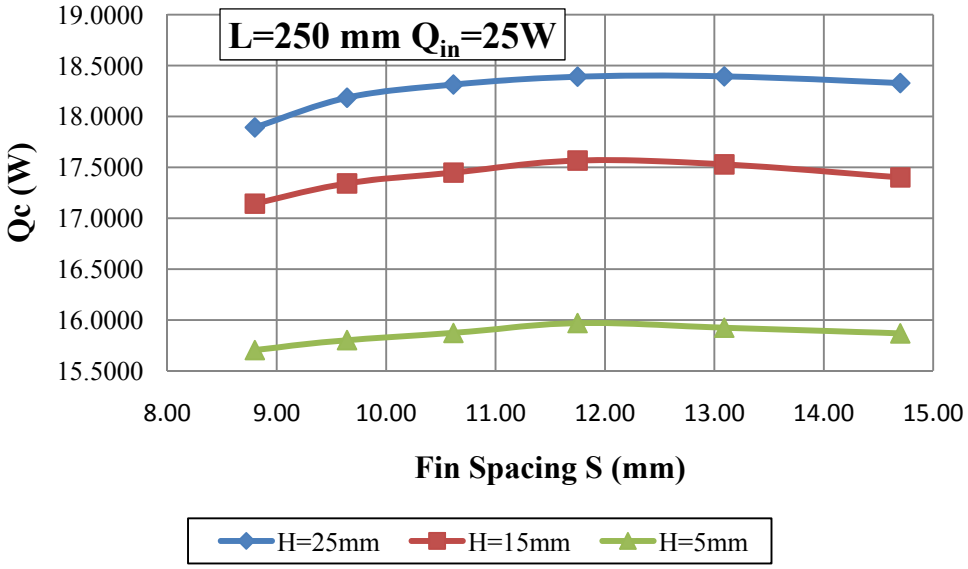

Figure E.1.4.1 Variation of convection heat transfer with fin spacing at fin length of L = 250 mm and at power input of Q_{in} = 25 W

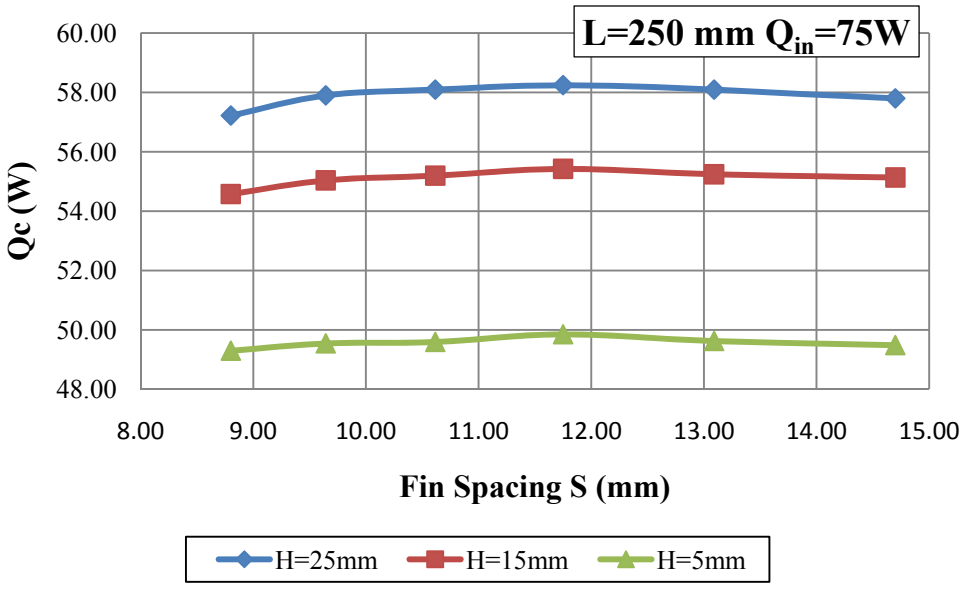

Figure E.1.4.2 Variation of convection heat transfer with fin spacing at fin length of L = 250 mm and at power input of Q_{in} = 75 W

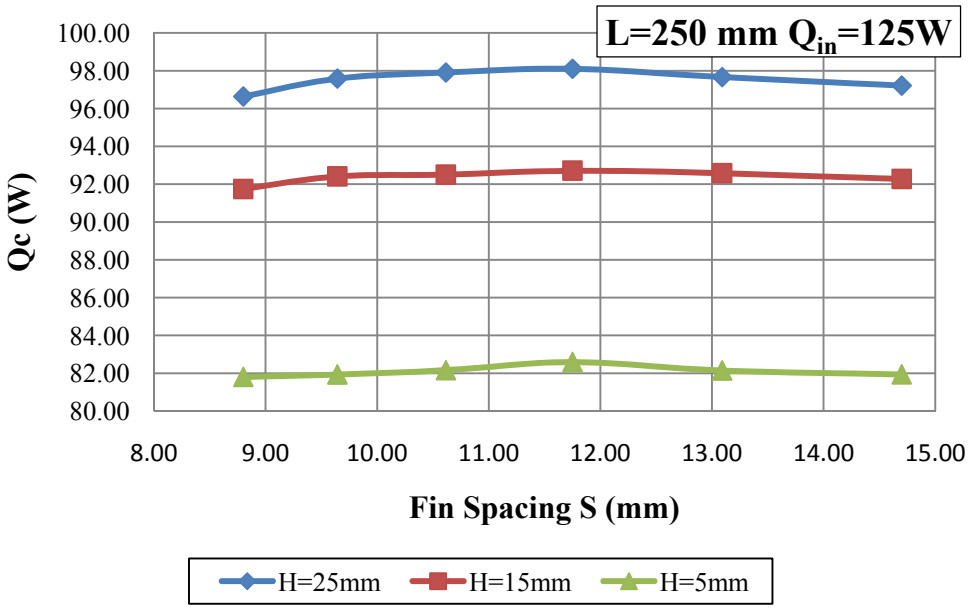

Figure E.1.4.3 Variation of convection heat transfer with fin spacing at fin length of L = 250 mm and at power input of Q_{in} = 125 W

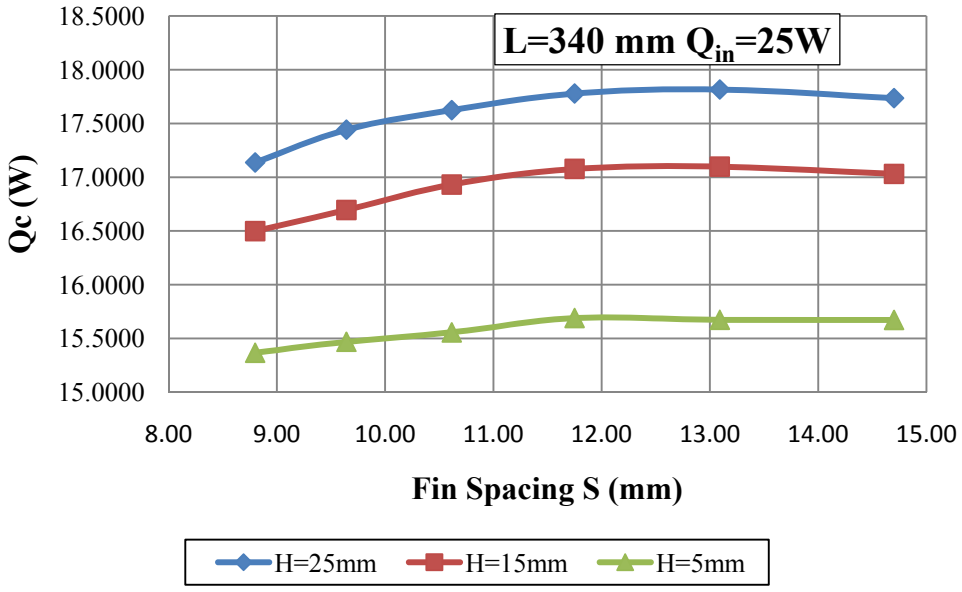

Figure E.1.4.4 Variation of convection heat transfer with fin spacing at fin length of L = 340 mm and at power input of Q_{in} = 25 W

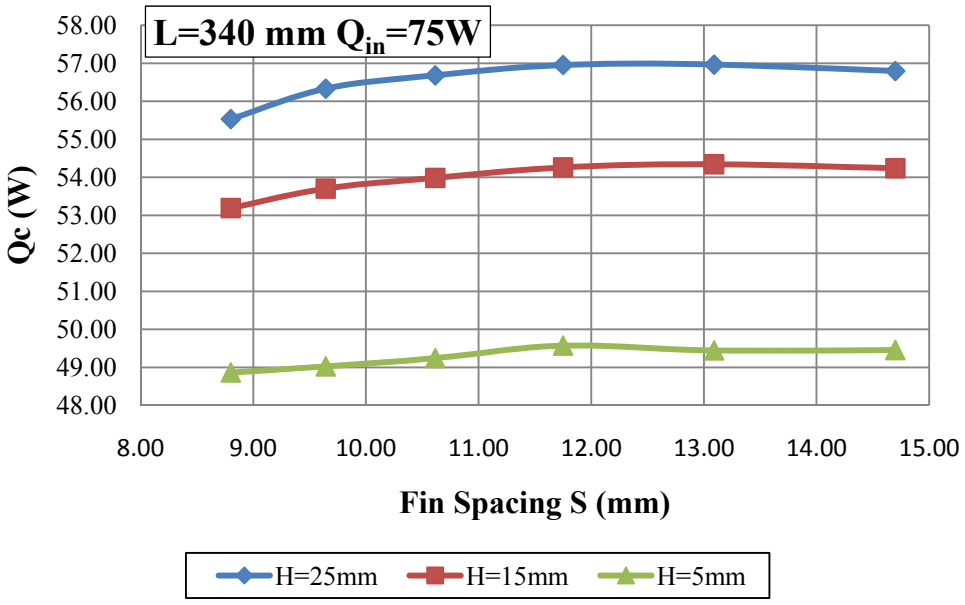

Figure E.1.4.5 Variation of convection heat transfer with fin spacing at fin length of L = 340 mm and at power input of Q_{in} = 75 W

E.1.5 Variation of Convection Heat Transfer Rate with Fin Height

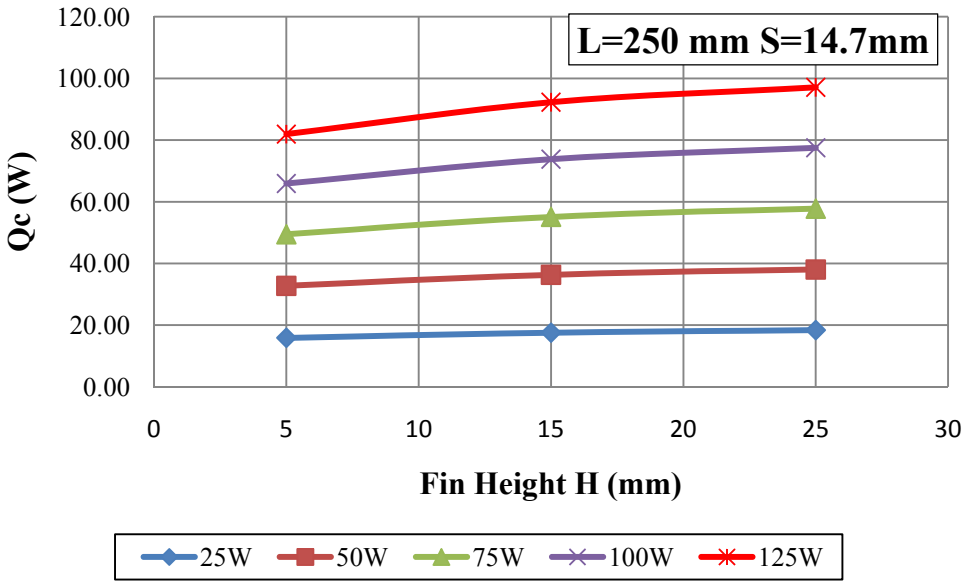

Figure E.1.5.1 Variation of convection heat transfer with fin height at fin length of L = 250 mm and at fin spacing of S = 14.7 mm

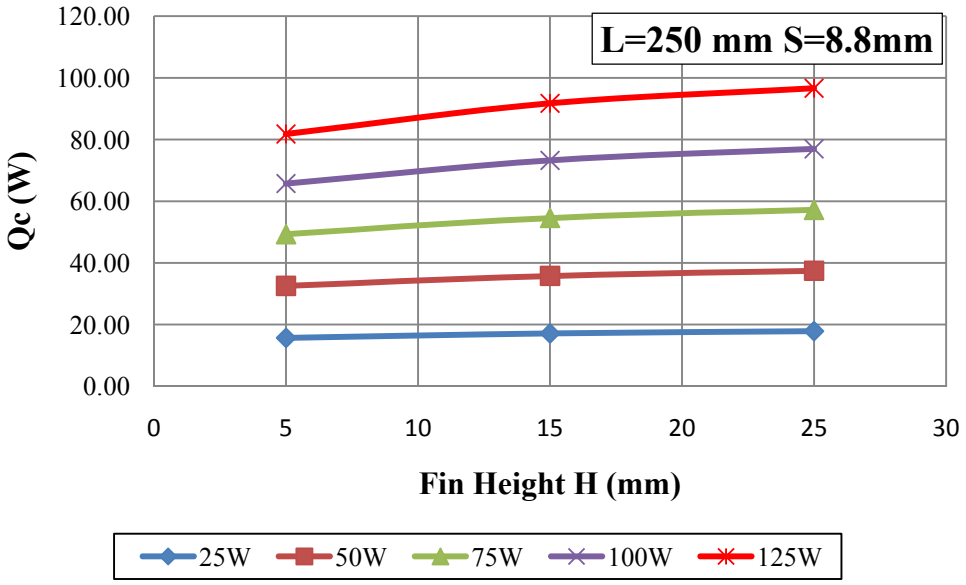

Figure E.1.5.2 Variation of convection heat transfer with fin height at fin length of L = 250 mm and at fin spacing of S = 8.8 mm

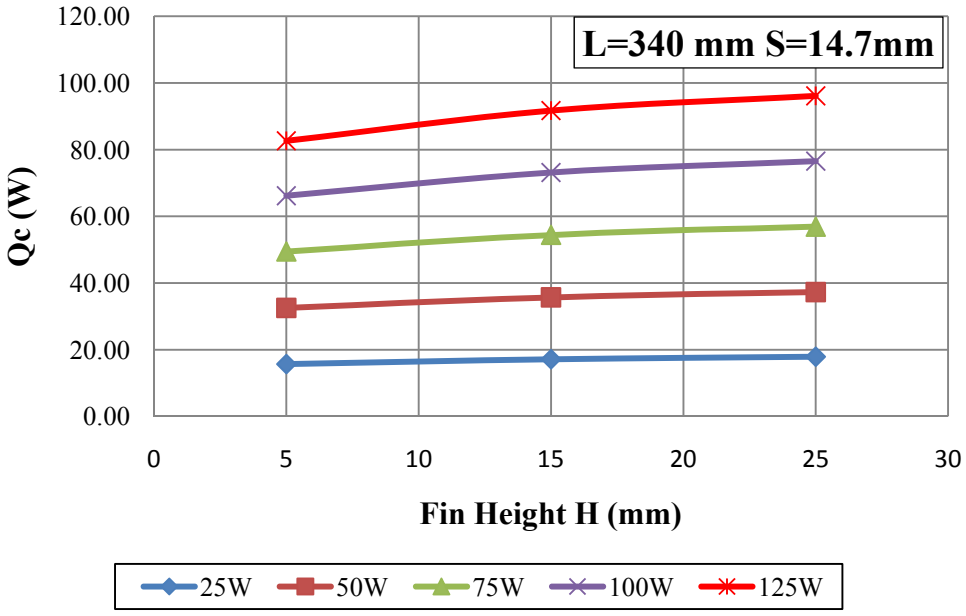

Figure E.1.5.3 Variation of convection heat transfer with fin height at fin length of L = 340 mm and at fin spacing of S = 14.7 mm

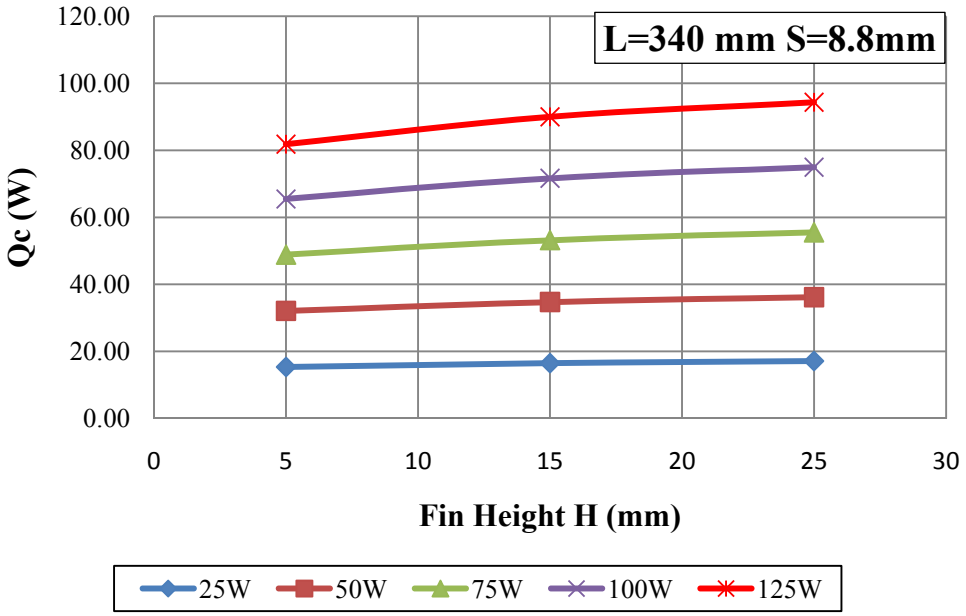

Figure E.1.5.4 Variation of convection heat transfer with fin height at fin length of L = 340 mm and at fin spacing of S = 8.8 mm

E.2 Case Study 2

E.2.1 Variation of Fin Temperature with Fin Spacing

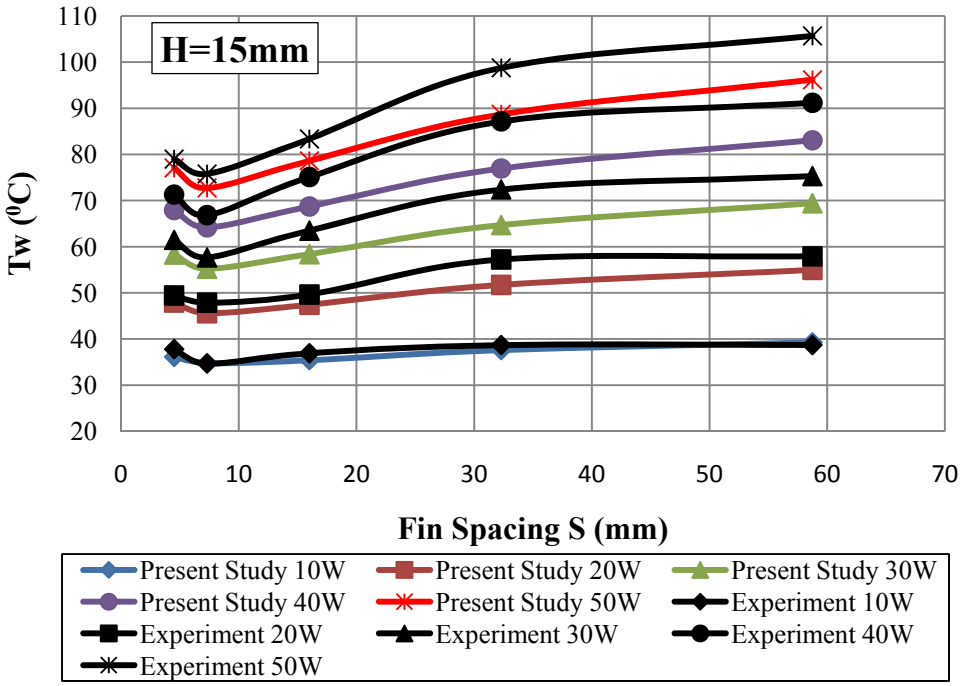

Figure E.2.1.1 Variation of average fin temperature with fin spacing at fin height of H = 15 mm

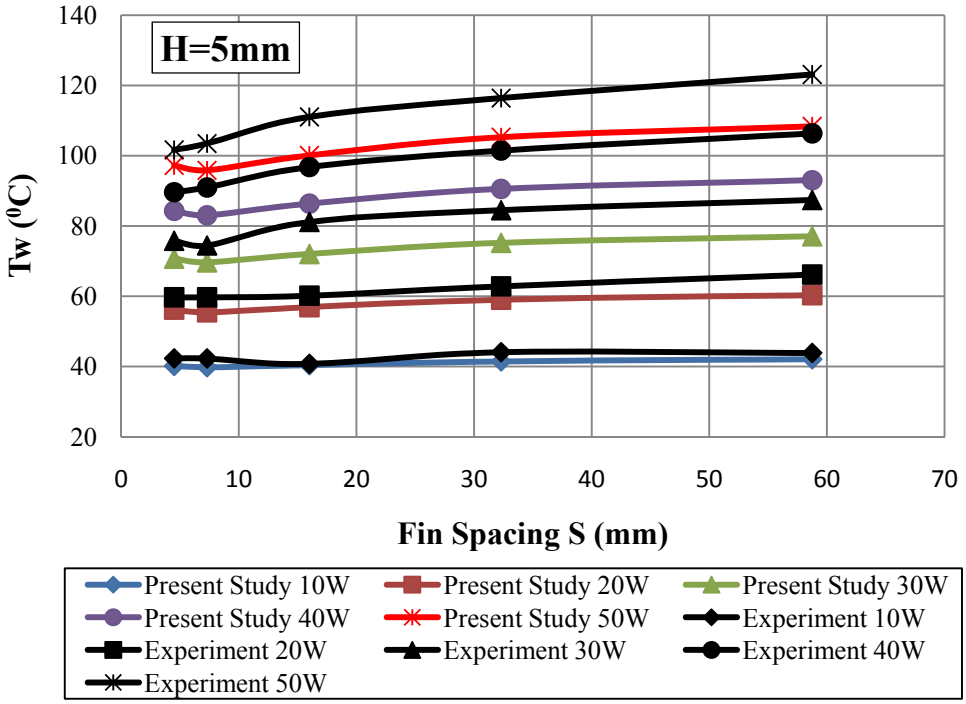

Figure E.2.1.2 Variation of average fin temperature with fin spacing at fin height of H = 5 mm

E.2.2 Variation of Convection Heat Transfer with Fin Spacing

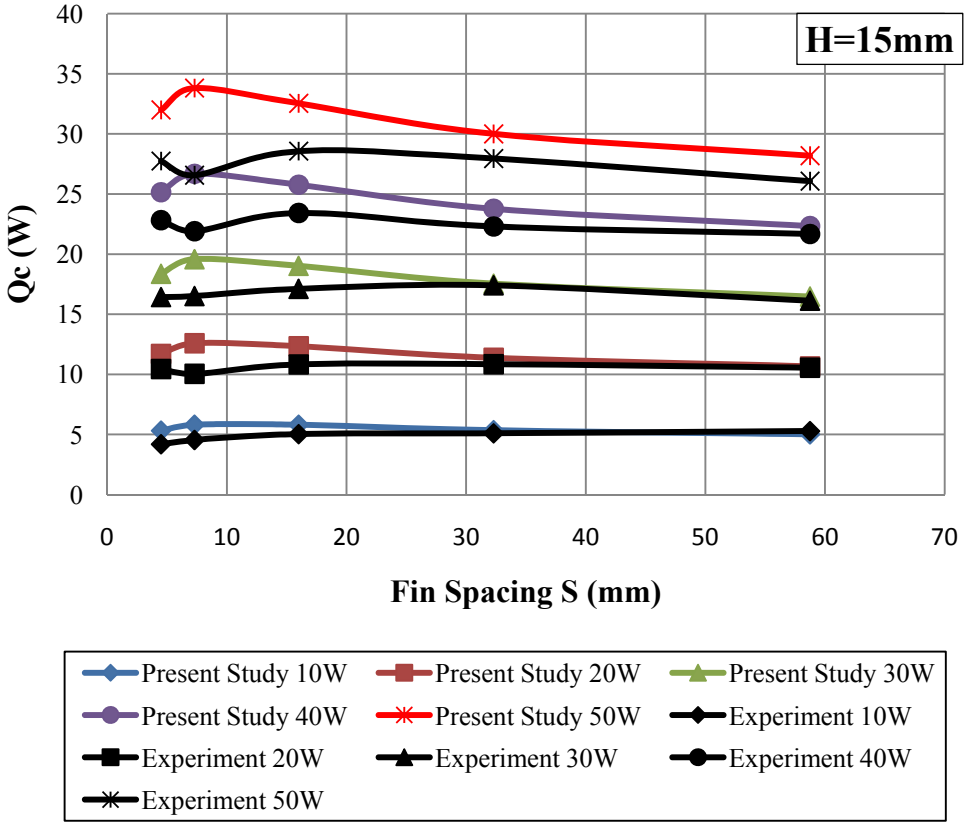

Figure E.2.2.1 Variation of convection heat transfer with fin spacing at fin height of H = 15 mm

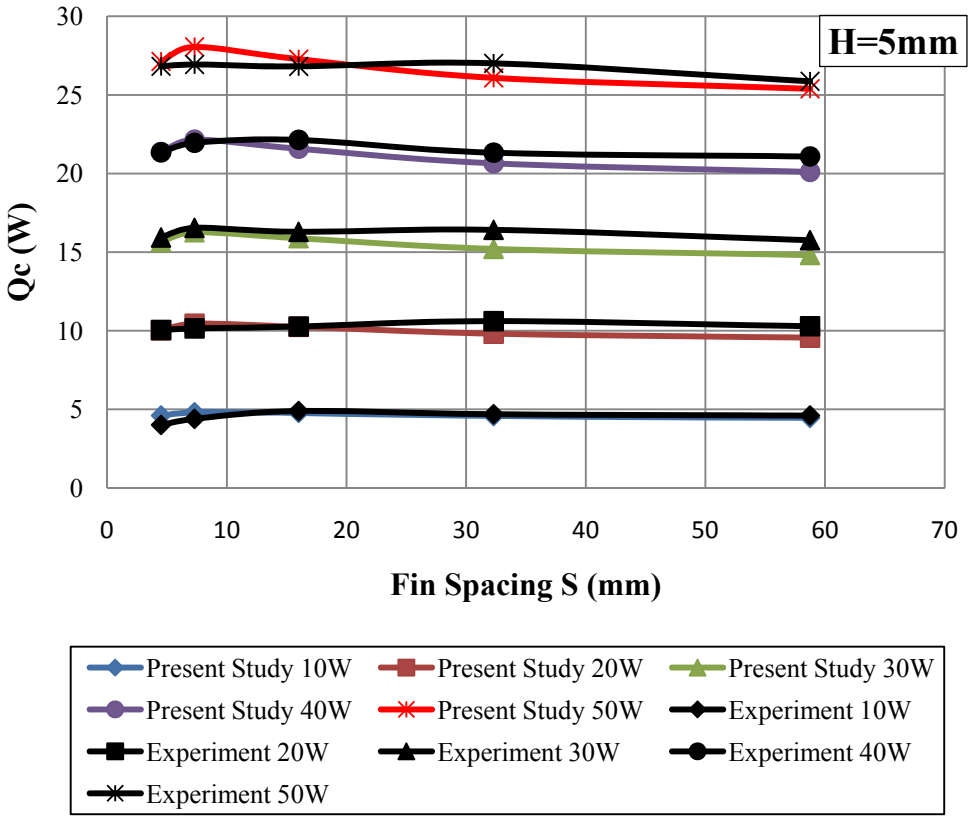

Figure E.2.2.2 Variation of convection heat transfer with fin spacing at fin height of H = 5 mm

E.2.3 Optimum Fin Spacing for Minimum Fin Temperature

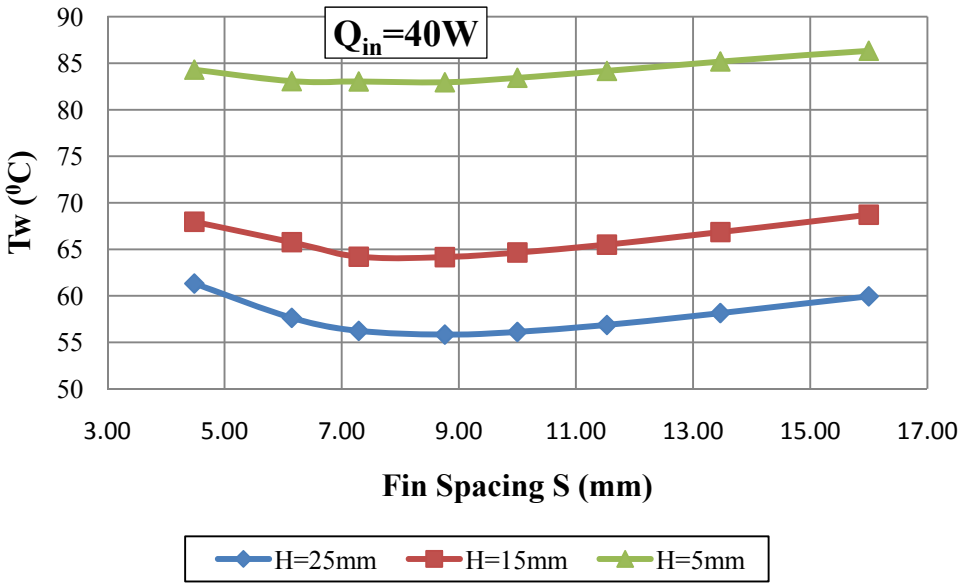

Figure E.2.3.1 Variation of average fin temperature with fin spacing at power input of Q_{in} = 40 W

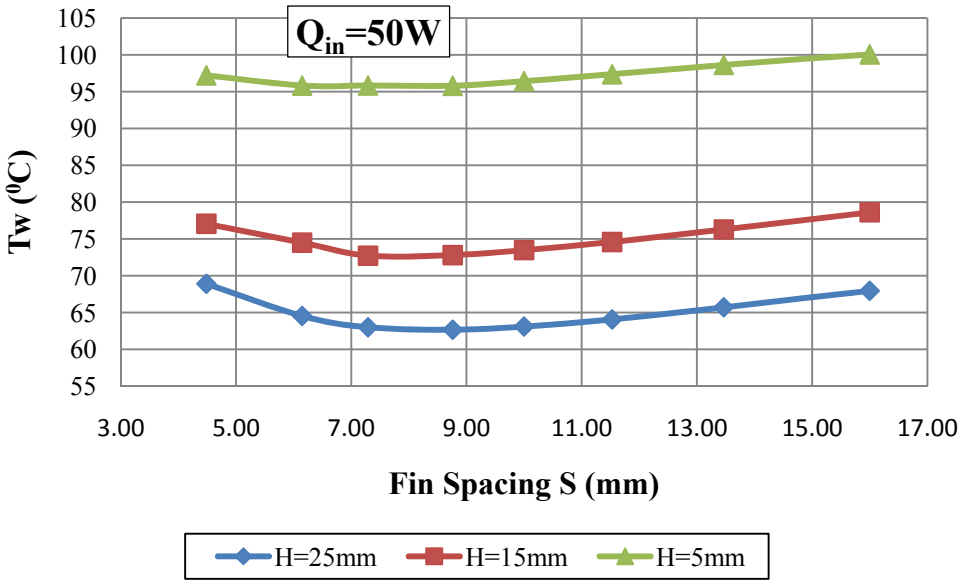

Figure E.2.3.2 Variation of average fin temperature with fin spacing at power input of Q_{in} = 50 W

E.2.4 Optimum Fin Spacing for Maximum Convection Heat Transfer Rate

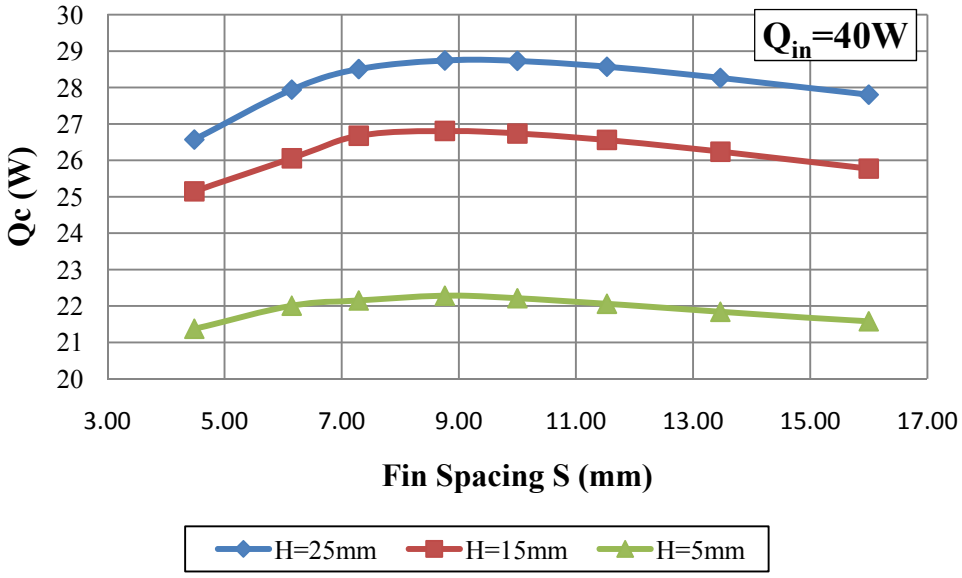

Figure E.2.4.1 Variation of convection heat transfer with fin spacing at power input of Q_{in} = 40 W

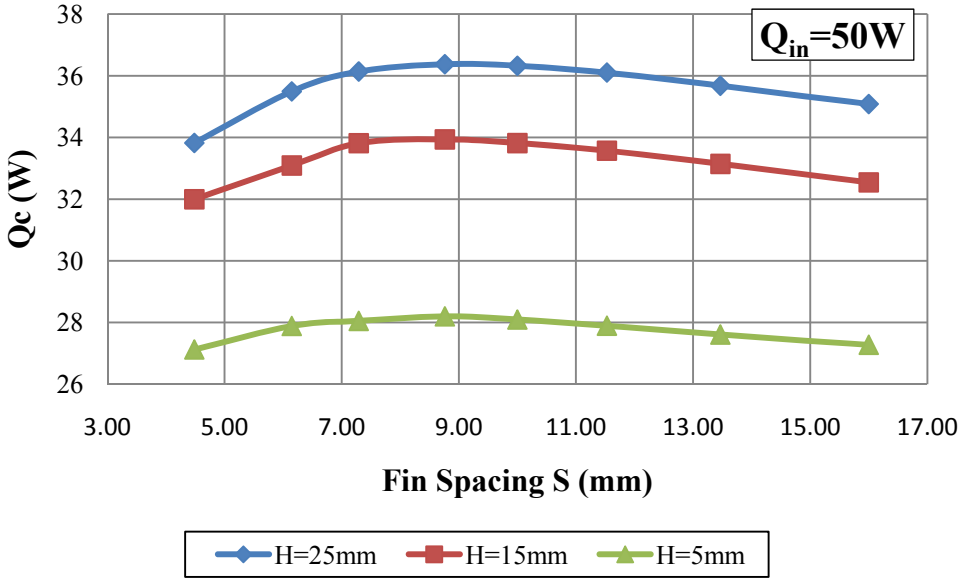

Figure E.2.4.2 Variation of convection heat transfer with fin spacing at power input of Q_{in} = 50 W